DISCOVERY AND BIOCHEMICAL EVALUATION OF CHEMICAL PROBES FOR THE STUDY OF JUMONJI-C DOMAIN CONTAINING HISTONE DEMETHYLASES AND ANTIBIOTIC RESISTANCE MACHINERY IN MRSA

by

JESSICA DANIELLE PODOLL

B.S., Cornell University, 2010

A thesis submitted to the

Faculty of the Graduate School of the

University of Colorado in partial fulfillment

of the requirement for the degree of

Doctor of Philosophy

Department of Chemistry and Biochemistry

2015

This thesis entitled:

Discovery and Biochemical Evaluation of Chemical Probes for the Study of Jumonji-C Domain Containing Histone Demethylases and Antibiotic Resistance Machinery in MRSA written by Jessica Danielle Podoll

has been approved for the Department of Chemistry and Biochemistry

_____

Xiang Wang

_____

Amy Palmer

Date_____

The final copy of this thesis has been examined by the signatories, and we Find that both the content and the form meet acceptable presentation standards Of scholarly work in the above mentioned discipline.

ABSTRACT

Podoll, Jessica Danielle (Ph.D., Biochemistry)

Discovery and Biochemical Evaluation of Chemical Probes for the Study of Jumonji-C Domain Containing Histone Demethylases and Antibiotic Resistance Machinery in MRSA

Thesis directed by Assistant Professor Xiang Wang

Part I:

Histone demethylases (HDMs) are vital epigenetic regulators that have been implicated in multiple disease states including cancers. Demethylation catalyzed by jumonji-C domain-containing HDMs (JHDMs) is coupled to decarboxylation of α-ketoglutarate (α-KG). Based on this mechanism, we developed a bivalent inhibitor by linking together mimics of the primary substrate (methyllysine) and the cofactor (α-KG) called methylstat. Methylstat is a pan-JHDM inhibitor that is also active in cells.

Using methylstat as a starting point, a fluorescent analog, methylstat^{fluor}, was developed and used as a tracer in fluorescence polarization (FP) - based binding and competition assays to determine quantitatively the binding affinities of JHDM inhibitors and native substrates. The FP assay was miniaturized and adapted for high-throughput screening in order to facilitate future discovery of class-specific JHDM inhibitors.

Part II:

Antibiotic resistance is an urgent global health concern. In the United States alone, antibiotic resistant bacteria caused over 2,000,000 illnesses and 23,000 deaths last year. Resistance-modifying agents (RMAs) offer an approach to address antibiotic resistance. These restore antibiotic sensitivity by targeting resistance conferring genes. Recently, we have used a natural-product-like library of indole alkaloids to discover novel RMAs for a variety of antibiotics.

One compound in particular, known as Of1, showed a dramatic potentiating effect in combination with β-lactam antibiotics in Methicillin-resistant *Staphylococcus aureus* (MRSA). Of1 is capable of re-sensitizing multiple MRSA strains to a variety of β-lactam antibiotics, but possesses no antibiotic activity on its own and has no super-sensitizing effect in non-resistant strains of *S. aureus*.

Investigations of the mode of action of Of1 revealed that it exerts its effects independently of β-lactamase inhibition. We further discovered that Of1 is capable of reducing transcription of the inducible β-lactam resistance determinants, β-lactamase and PBP2a. Finally, we found that Of1 stabilizes the binding interaction between the β-lactamase repressor protein, BlaI, and the β-lactamase DNA promoter region. We hypothesize that through this stabilizing action, Of1 reduces transcription of the active resistance determinants, β-lactamase and PBP2a. This discovery would represent an entirely novel mechanism and drug target for combating β-lactam resistance.

DEDICATION

To Alexander Sol Eldredge. (1991-2013)

ACKNOWLEDGEMENTS

I could write an entire second dissertation acknowledging everyone who made my journey toward my PhD possible. I cannot express my gratitude to my advisors, mentors, friends, and family in just a couple pages. Everyone who has touched my life has played a significant role and contributed a necessary piece of Jessica's PhD puzzle. Firstly, I am grateful to my advisor, Xiang Wang, for welcoming me into his lab and creating an environment in which I have been able to flourish as a scientist. Xiang's guidance, support and innovation made this work possible, and enabled my scientific accomplishments. I would also like to acknowledge my committee: Amy Palmer, Shelley Copley, James Goodrich, and Corrrella Detweiler for their advice and continued support as I finish my degree. I acknowledge my funding sources: The Graduate School Summer Fellowship (13'), The Joseph Addison Sewall Graduate Fellowship (14'), as well as financial support through the Leadership in Biotechnology Training Grant (GM008732). Furthermore, I acknowledge Dr. Xuelai Luo, who was my first laboratory supervisor in the Wang lab. Xuelai was extremely patient with me as an inexperienced scientist and taught me many valuable techniques. Dr. Wei Wang was also instrumental during the cloning stages of my project and has been an excellent resource for molecular biology techniques. I would also like to acknowledge Dr. Le Chang, Dr. Wenqing Xu, Laura Marholz and Patrick Barbour for each of their contributions to my project through synthesis of compounds and analogs, biological assays, or proofreading anything and everything. Furthermore I would like to acknowledge Shane Walls, who was involved in some of the most important phases of my project as an undergraduate researcher and, I am proud to mention, has now joined the Wang lab to continue as a graduate student.

On a personal note, I owe many thanks to my wonderful friends and family that I am so fortunate to have as a part of my life. In particular, I must mention Danielle Pfaff who has been an incredible friend and support throughout my time as a graduate student; from Muay Thai and ski-trips, to intensive orals prep and even acting as the unofficial ‘editor-in-chief’ of this dissertation! I cannot give enough thanks to my loving parents, Mindy Harris Podoll and Richard Podoll. Throughout my entire life, my parents’ unwavering love and support has enabled me to become the person that I am today. No matter what, I have always been able to count on my parents to share excitement in my accomplishments, help me when I get too stressed, or just to have fun skiing, golfing or traveling the world. To say, my brother, Joshua Podoll, has played an integral role in my life is an understatement. Josh has been my best friend and confidant from birth. Even though Josh now resides half way across the country, he is only a phone call away for me and always has time to talk (or listen to me talk) about anything and everything. Last, but certainly not least, I am eternally grateful for my loving fiancé, Geoffrey Vernon, whom I will be marrying immediately after I graduate! Geoff’s support throughout this time has enabled me to reach this stage and finish my PhD. Geoff never let me doubt myself, or what I am able to accomplish. Even though Geoff and I have weathered both our graduate careers together, we have never had a lack of fun or fuzzy animals in our lives; as well as a mental connection that boarders on eerie, but makes us the world’s best Charades team.

If you have read this acknowledgement section in its entirety, please know that it is not comprehensive, because that would require a lot more paper. Thank you for reading! I hope you enjoy reading this dissertation as much as I enjoyed writing it.

CONTENTS

TABLES

FIGURES

Chapter 1 : Efforts to develop jumonji C domain-containing histone demethylase inhibitors and associated biophysical assays

1.1 Introduction and Background

1.1.1 Histone Demethylases are Epigenetic Regulators.

In eukaryotic cells, DNA organization takes the form of chromatin. Chromatin is a nucleoprotein complex made up of a condensed DNA structure involving 146 DNA base pairs wound around a core of proteins known as the nucleosome (Figure 1.1).[1,2] The nucleosome is made up of an octamer of proteins, known as histones. Within the octamer ensemble, there are pairs of four histone proteins: H2A, H2B, H3, and H4. Although the core of these proteins is highly structured, their N-terminus is comprised of an unstructured tail, which is flexible and subject to a differential chromatin state, where covalent posttranslational modifications occur to specific amino acids (Figure 1.1).[3] Although the pattern of histone modifications can be heritable, the modifications themselves are dynamic in nature and can be altered to affect changes in gene expression in response to external stimuli; termed “epigenetics”.[4] Thusly, it was hypothesized that these histone proteins served another function over and above their role in organizing and scaffolding the DNA: and with this observation, a hypothesis known as the “Histone Code” was born.[5]

The Histone Code is comprised of patterns of histone modifications in a region of DNA, and the manner in which they interact with their environment. These provide a language that is decoded by the cellular machinery to reveal patterns of gene expression that are cell-type specific or a response to some extracellular stimulus. In

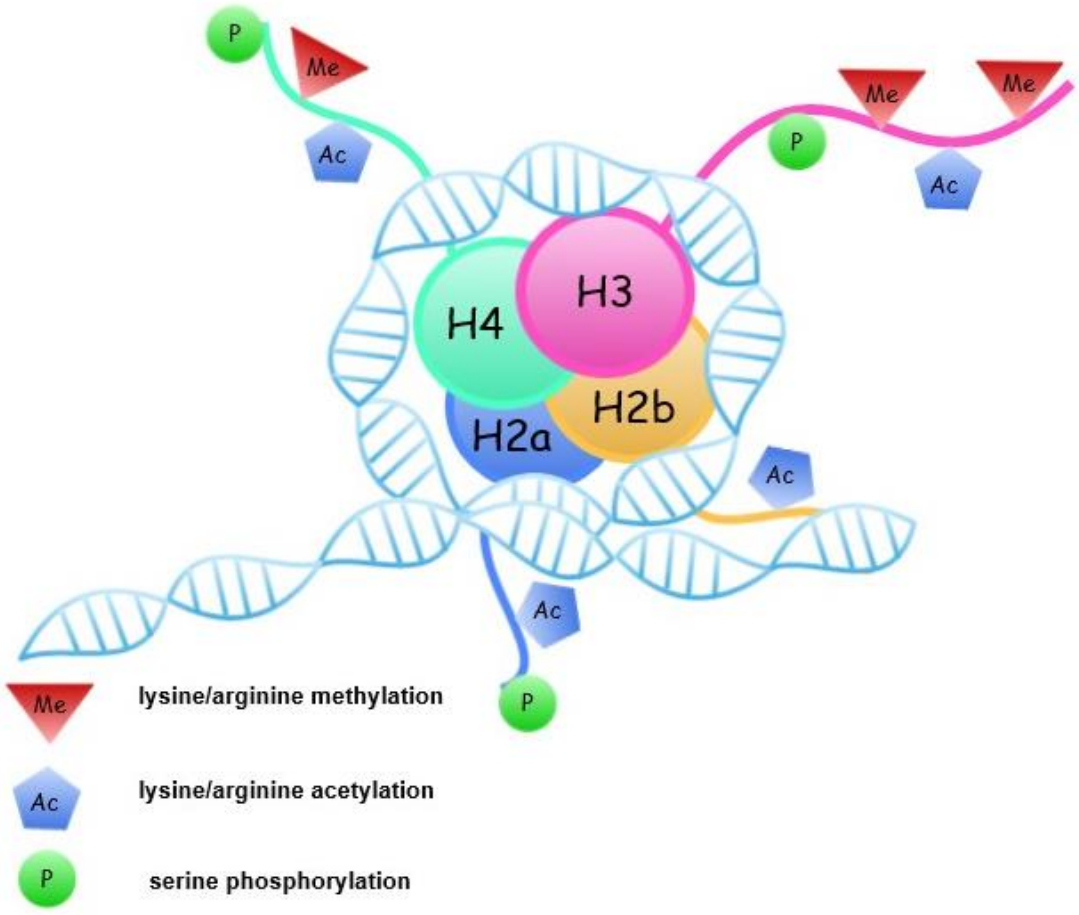

Figure 1.1: Model of the nucleosome with representative N-terminal histone modifications.

DNA is wound around the octamer of histones forming the individual unit of chromatin: the nucleosome. Post-translational modifications (e.g. methylation, acetylation, phosphorylation, etc.) of H2a, H2b, H3, and H4 N-terminal tails comprise the 'Histone Code' which serves to direct gene expression by effects of DNA packing and recruitment of effector proteins known as epigenetics.

particular, the modifications of histone H3 tails via methylation is governed by a suite of proteins called histone methyltransferases (HMTs, writers) and histone demethylases (HDMs, erasers).[6] These elements of regulatory control play a vital role in transcriptional activation or repression of many genes essential for development and differentiation; dis-regulation of histone modifications due to over activation or silencing of HMTs and HDMs can lead to many severe disease states. [7–10] For example, histone methyl writers and erasers can contribute to regulatory feedback loops that either silence transcription via di- and tri-methylation of Lysine 27 in histone H3 (H3K27me2/me3) or activate transcription by concurrently demethylating H3K27 and trimethylating Lys4 in histone H3 (H3K4me3).[11] Additionally, specific histone-modifying events are entirely dependent on orthogonal chemical modifications occurring first (e.g. acetylation, phosphorylation, etc.). For example, in order for H3K4 methylation to take place, H2B mono-ubiqutination must first be present.[12] This and other examples demonstrate the finely tuned, complex and dynamic nature of the Histone Code, as well as the degree of crosstalk therein.[13,14] However, the intricate molecular mechanisms that comprise this network and enable the specificity of this epigenetic regulation remain largely unknown.

Although the dynamic nature of many histone modifications has been widely accepted, enzymatic removal of histone lysine methylation was only verified fairly recently. It was hypothesized that histone lysine methylation was removed by either complete turnover of the protein following cell division, or by proteolysis of the histone tail containing the modification.[15,16] This hypothesis was largely due to the known chemical stability of lysine methylation. In 2004, the first HDM was discovered, known

as LSD1, a discovery that changed the known landscape of epigenetics.[17] Following the initial discovery of an HDM, the field opened up to investigate the many nuances of histone methylation dynamics and its downstream effects. Soon thereafter, another, mechanistically distinct, family of HDMs was discovered: Jumonji C (JmjC) domain-containing HDMs (JHDMs)[18]. These two HDM families are currently the only enzyme

Table 1.1: Representative histone demethylases organized by mechanism class and substrate specificity[a]

HDM Name	Mechanism Class	Histone Substrate(s)
LSD1	FAD dependent	H3K4me(1/2), H3K9me(1/2)
LSD2		H3K9me(1/2)
JMJD1(A, B, C)	α-KG dependent (jmjC domain)	H3K9me(1/2)
JMJD2(A, B, C)		H3K9me(2/3), H3K36me(2/3)
JMJD2D		H3K9me3
JMJD3		H3K27me(2/3)
UTX		H3K27me(2/3)
JMJD5		H3K36me2
JHDM1A		H3K36me(1/2)
JHDM1B		H3K36me(1/2), H3K4me3
JHDM1D		H3K9me(1/2), H3K27me(1/2)

[a]This table is not a comprehensive list of HDMs, but an illustration of the difference in number of enzymes within each class and their substrate specificities

classes known to demethylate histone proteins. LSD1 is a flavin adenine dinucleotide (FAD)-dependent HDM, while JHDMs require α-ketoglutarate (α-KG) coordinated in the enzyme active site for catalysis. There are far more known JHDMs than FAD-dependent HDMs (of which there are only two known). Furthermore, JHDM substrate specificity includes lysines at all methylation states, whereas FAD-dependent HDMs only act on mono-and di-methylated lysine substrates (Table 1.1).[17,19–21]

Selective JHDM activity has been observed as an important contributor in essential cellular activities including cellular differentiation (including myogenesis and spermatogenesis), and aberrant activity of JHDMs is a hallmark of multiple cancers as well as X-linked mental retardation.[9,22–24] Investigations of JHDMs will thus give crucial insight into their roles in developmental and disease biology. Furthermore, the demonstrated role of JHDMs in disease states illustrates these epigenetic regulators as potential drug targets. The development of chemical probes with which to study these HDMs represents an invaluable contribution to the epigenetic community.

1.1.2 Determination of the JHDM active site structure yielded valuable mechanistic insight.

The first JHDM (JHDM1A) was discovered based on the observation that the FAD-dependent LSD1 mechanism of demethylation is incapable of demethylating tri-methylated lysine substrates since the mechanism proceeds via the oxidation of a basic amine species to form an imine intermediate (Figure 1.2a).

Since tri-methyllysine modifications are a known element of the histone code, it became clear that another mechanism must be at play in order for tri-methyllysine demethylation to occur[18] Since the mechanism of demethylation proceeds via

hydroxylation of the methyl-group, it became clear that an enzyme capable of direct hydroxylation would be required to demethylate a tri-methyl substrate. JHDMs were identified as the HDM, since the JmjC domain is capable of directly hydroxylating a methyl-group by coupling the hydroxylation to decarboxylation of α-KG. Shortly after the discovery of JHDMs, the first crystal structure of a JHDM active site, that of JMJD2A, was solved in 2007 giving valuable insight into its catalytic mechanism and the orientation of its substrate and cofactors in its catalytic core.[25] The conserved catalytic JmjC domain has structural features characteristic of α-KG/Fe(II) dependent dioxygenases (Figure 1.3, PDB ID: 2Q8E). [19,20,26–28] The mechanism of JHDM driven demethylation involves direct hydroxylation of the methylated lysine. The methylated lysine substrate forms into a transitional hydroxy-methylated lysine, which subsequently collapses into formaldehyde and the final demethylated lysine product (Figure 1.2b). [15,18–20,29,30] The discovery of the JHDMs provided the missing puzzle piece required for a complete understanding of the mechanisms by which histone lysine residues are demethylated, a vastly important element of the histone code. Furthermore, the study of JHDMs became a field of its own. Although JHDMs are prevalent and vital epigenetic regulators, they remain difficult to study in a biochemical and cellular context. The dearth of tools with which to study JHDMs inspired efforts to develop chemical probes capable of delivering vital information about the downstream effects of JHDMs.

1.1.3 Methylstat: a bivalent, small-molecule inhibitor of JHDMs.[a]

[a] The initial biochemical and cellular evaluation of methylstat was carried out by Dr. Xuelai Luo, synthesis of methylstat was carried out by Dr. Yongxiang Liu

Following the initial discovery of HDMs, an effort ensued to characterize classes and types of HDMs, as well as their roles in cellular processes and disease.[31] In response to these efforts, small molecule probes inhibiting the activity of HDMs became an increasingly interesting area of study. Small molecule probes offer many distinct advantages for studying gene function over classical genetic approaches.[32,33] In addition to the relative ease of a chemical approach over a genetic one, chemical

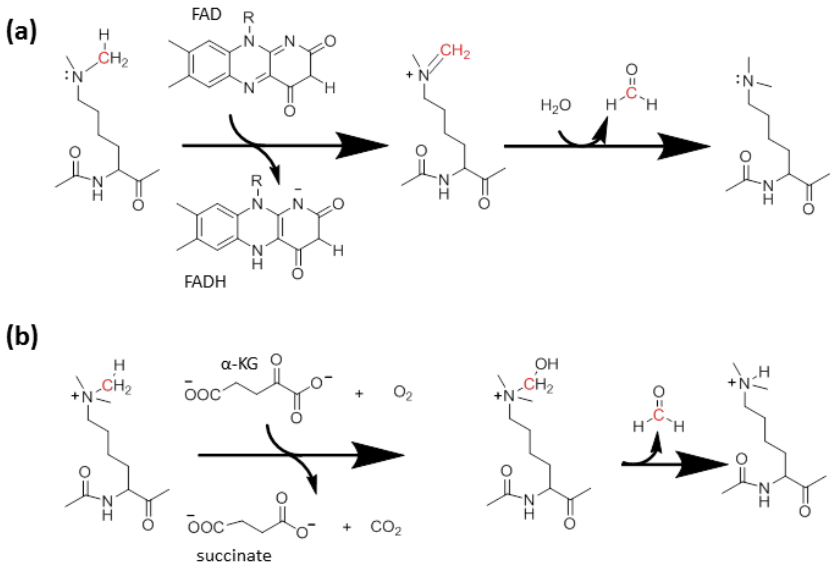

Figure 1.2: Mechanisms of histone lysine demethylation by FAD-dependent HDMs and JHDMs.

(a) The FAD-dependent mechanism of the amine oxidase proceeds via an imine intermediate formation, which is coupled to the reduction of FAD to FADH-. The imine carbon is then hydroxylated by addition of water, which subsequently decomposes to formaldehyde and the demethylated product. The formation of the imine intermediate makes demethylation of tri-methylated substrates by this mechanism impossible. (b) For demethylation of methylated lysines on histones by JHDMs, hydroxylation of the methyl group is coupled to decarboxylation of α-KG to succinate and proceeds via the action of the highly reactive Fe^{4+} in the active site. Since this mechanism involves direct hydroxylation of the methyl group, JHDMs are capable of demethylating mono, di, and tri-methyl lysine substrates.

probes may also be functionalized with linkers for target identification studies, offering a convenient forward chemical genetic approach, and may be further developed into therapeutics for targets with known disease involvement.[21,34]

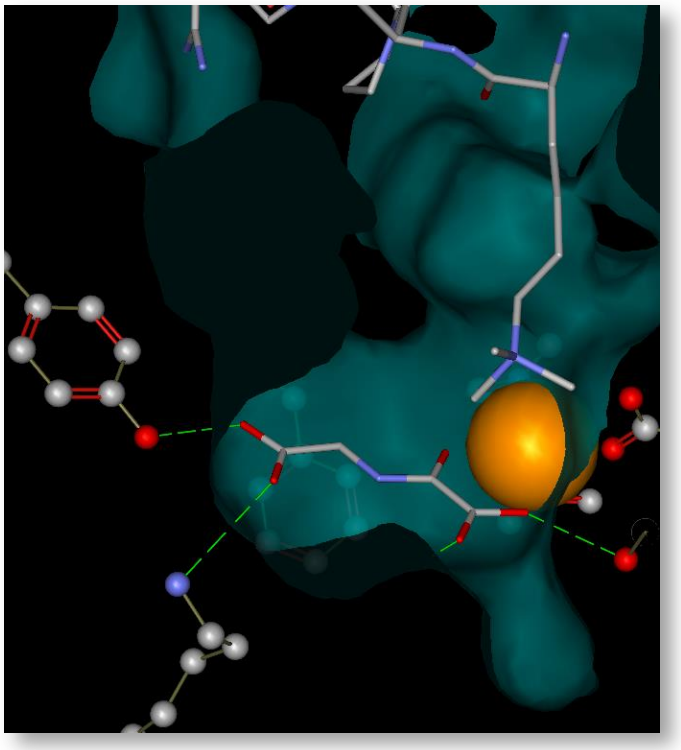

Figure 1.3: The orientation of the JHDM active site.

The metal ion (orange) is coordinated by two histidine and a glutamate within the JHDM active site (not shown). The α-KG co-factor (here represented by the inhibitor NOG) coordinates to the metal ion in the active site (red and grey stick structure below orange metal ion). The tri-methylated lysine substrate projects into the active site in proximity to the metal ion and the α-KG cofactor (blue and grey stick structure above orange metal ion).

Although a number of small-molecule inhibitors of HDMs have been created, none included elements capable of imparting specificity to the JHDMs. Most of these inhibitors were designed as either methyl-lysine mimics or α-ketoglutarate mimics. Although these are effective inhibitors in vitro due to high affinity binding with JHDMs, they have low specificity, reducing their utility as chemical probes for studies of the cellular functions of JHDMs.[35,36] This insight contributed to the process of designing, synthesizing, and validating methylstat as a cell active and selective inhibitor of JHDMs (Figure 1.4).[37] As opposed to previous inhibitors mimicking one of the two JHDM substrates (methyl-lysine and α-KG), methylstat was designed as a bivalent inhibitor. In the case of methylstat, a methyl-lysine mimic was designed based on a well-known HDAc inhibitor and covalently bound to an α-KG mimic with a four-carbon linker separating the two molecules.[38] The 4 carbon linker provides a similar distance and

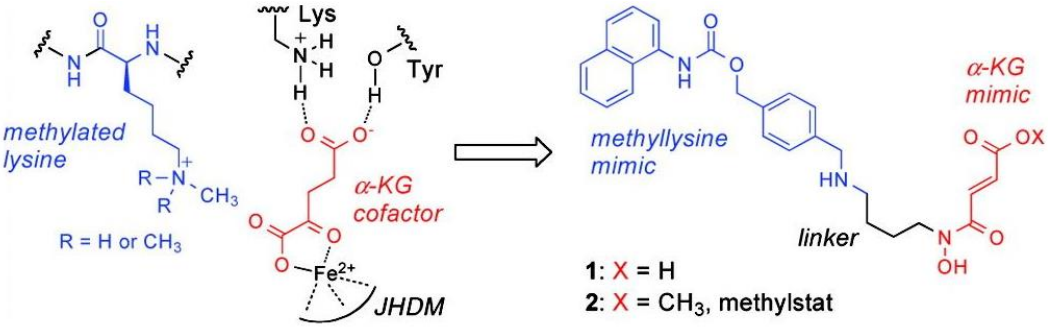

Figure 1.4: Design of Methylstat, a small-molecule probe selective for JHDMs.

The structure of methylstat was designed as a bivalent inhibitor by covalently linking a methyllysine mimic (blue) to an α-KG mimic (red) with a 4 carbon linker (black) in an orientation like that of the native substrates in the active site. The active form of methylstat (1) is generated by cleaving the ester from the α-KG mimic, whereas the prodrug form (2) is capable of crossing the cell membrane.

geometry to the observed native substrate and co-factor situated in the JHDM active site. The methyl-lysine mimic was designed to impart specificity, distinguishing JHDMs from other Fe^{2+} and α-KG dioxygenases, while the α-KG mimic inhibits Fe^{2+} activation and catalysis, yet stabilizes binding.[27]Biochemical evaluation of the acid form of methylstat showed that it inhibits multiple JHDMs including JMJD2A, JMJD2C (which demethylate H3K9me3 and H3K36me3), JMJD2E (which acts solely on H3K9me3), JMJD3 (an H3K27me3 demethylase), and PHF8 (an H3K9me2 demethlase). Methylstat inhibited each of these enzymes with IC_{50} values in the low micro molar range. Supporting specificity for JHDMs, methylstat did not show activity against the FAD-dependent HDM family (LSD1) or class I or II HDAcs.

Cellular evaluation of methylstat was carried out by assessing its ability to penetrate cells and inhibit a variety of JHDMs therein. Although the acid form of methylstat had proved effective in biochemical evaluations, this form was too polar to penetrate the cell. A methyl-ester pro-drug was thus designed to improve the cellular uptake. Once the methyl-ester is taken up by cells, it is cleaved to its active form by non-specific esterases. The methylstat pro-drug was evaluated for its ability to inhibit growth of the KYSE-150 cell line, an esophageal carcinoma cell line that has become dependent on JMJD2C for proliferation .[39,40] Methylstat effectively inhibited growth of the cell line, suggesting that methylstat inhibits JMJD2C in cells (Figure 1.5a). This was confirmed by expressing GFP-tagged JMJD2C in HeLa cells and performing a quantitative immunostain for its substrate (H3K9me3). Cells expressing the GFP-JMJD2C showed decreased methylation of the H3K9me3.[37] Addition of methylstat reversed this effect, exhibiting an increase in H3K9me3 methylation. This observation

confirmed that methylstat inhibited JMJD2C in cells (Figure 1.5b). Also, methylstat showed the ability to inhibit a variety of cellular demethylases, some of which are known JHDMs, and others that are yet to be a known demethylase (data not shown). This not only confirms the cellular activity of methylstat as a pan-JHDM inhibitor, it also reveals that a number of JHDMs that exist in cells have not yet been linked to their substrates. Taken together, these data prove that methylstat is a selective, bivalent, pan-JHDM inhibitor capable of inhibiting JHDMs in cells.

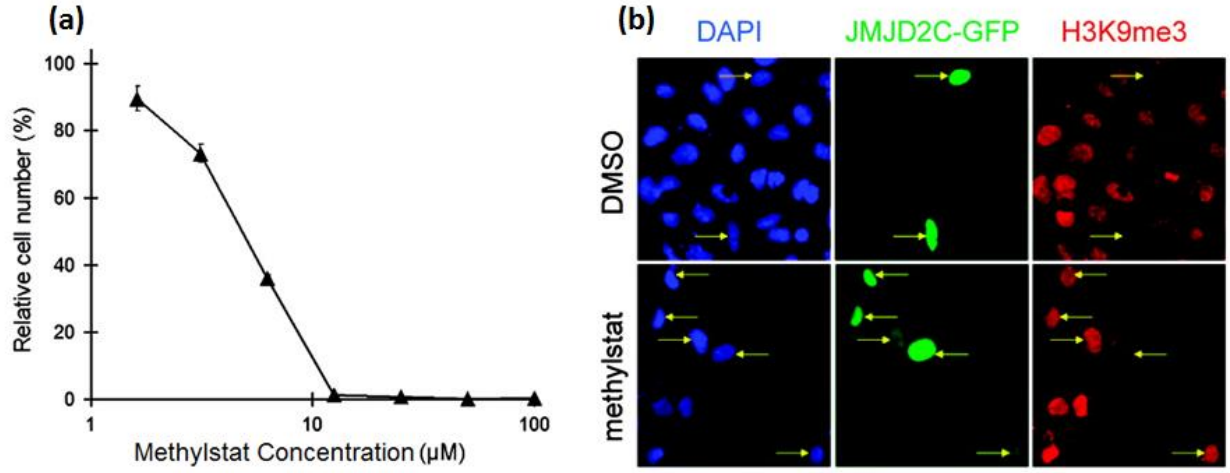

Figure 1.5: Methylstat inhibits the oncogenic JHDM, JMJD2C.

(a) Growth inhibition of KYSE150 cells in the presence of methylstat. KYSE150 cells depend on the activity of JMJD2C for survival. Cell viability was normalized to cells grown in the absence of methylstat (DMSO). (b) HeLa cells expressing GFP-labeled JMJD2C and immunostain for H3K9me3. DNA is stained with DAPI, GFP-JMJD2c is green and H3K9me3 is labeled with AlexaFluor 594. Treatment with methylstat causes hypermethylation of the H3K9me3 mark compared to DMSO control. This figure was adapted from Luo et al. (2011).[37]

1.2 Methylstat is a useful cellular tool for investigating phenotypic processes involving JHDMs.

1.2.1 Methylstat inhibits myogenesis via inactivation of the JHDM, UTX.

In order to prove that methylstat is a cellular probe that may be used for phenotypic investigations, we assayed its effects on myotube-differentiation of C2C12 mouse myocites. A necessary role of a JHDM, UTX, was established for myogenesis previously.[41] UTX was shown to demethylate the repressive H3K27me3 mark at muscle-specific genes including *myog* and *ckm,* thereby allowing expression of Myogenin and Creatine kinase, respectively, and differentiation to myotubes from C2C12 myocites. ShRNA knockdown of UTX blocked expression of muscle specific genes and inhibited formation of myosin heavy chain (MHC)-positive myotubes entirely.

We sought to recapitulate the effects of shRNA knock down of UTX using methylstat in order to inhibit the enzyme. We found that as little as 2 μM methylstat was sufficient to block myotube formation, and phenocopy the effects of UTX knockdown (Figure 1.6). Cells treated with methylstat over the course of their normal differentiation period showed a reduction in MHC-positive myotubes at 1 μM and no myotube formation at 2 μM or higher. The reduction of *myog* and *ckm* expression was also confirmed by reverse transcription PCR (RT-PCR). Although the 2 μM methylstat treatment was sufficient to produce an altered phenotype, global hypermethylation of the H3K27me3 mark was not obvious until higher concentrations (4 μM) were used.

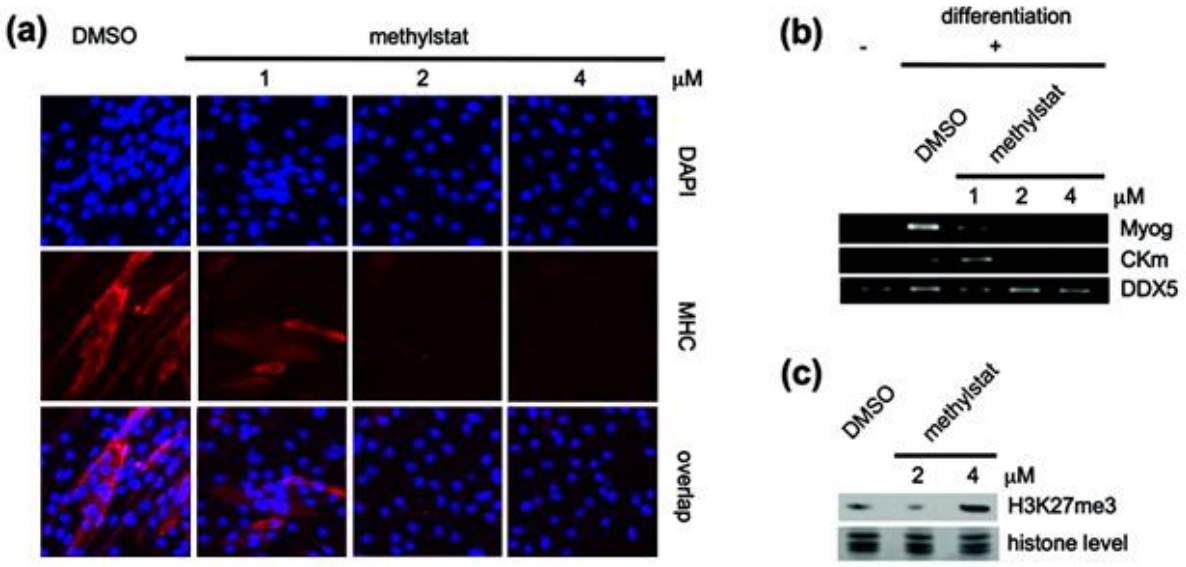

Figure 1.6: Methylstat prevents myogenesis through inhibition of the H3K27me3-demethylase UTX.

(a) Methylstat prevented C2C12 myotube formation in a concentration-dependent manner. Assayed by immunostaining myotube specific myosin heavy chain (MHC, red). Cell nuclei are stained with DAPI (blue). (b) Methylstat inhibits the expression of UTX-targeted genes, Myog and Ckm, during myogenesis. Assayed by RT-PCR. The housekeeper gene DDX5 is shown as a control. (c) Western blot showing that methylstat induces hypermethylation of H3K27me3 in C2C12 cells.

1.2.2 Methylstat causes G1 cell cycle arrest in acute myeloid leukemia cell lines presumably by blocking the activity of JHDM1B.

The cancer phenotype is characterized by uncontrolled cell proliferation. Recently, the cancer stem cell hypothesis has shed some light on the role of self-renewal machinery in carcinogenesis.[42–44] Specifically, it has been shown that epigenetic machinery, known to play roles in embryonic stem cell (ESc) self-renewal, can play a notable role in cancer cell transformation.[43] This led to the discovery of epigenetic mechanisms that play a role in the leukemic transformation of acute myeloid leukemia (AML).[42,45] Notably, these investigations revealed the role of a JHDM, JHDM1B, in silencing the tumor suppressor $p15^{Ink4b}$, thereby promoting cellular proliferation. Interestingly, shRNA knockdown of JHDM1B in AML cell lines restored expression and activity of $p15^{Ink4b}$ causing G1 cell cycle arrest in JHDM1B knockdown cells, and reducing AML cell line proliferation.

We followed up on this investigation by assessing the ability of methylstat to recapitulate the effects of JHDM1B knock down. First, the effect of methylstat on the G1/S phase transition was assessed. The AML cell line, U937, was selected for this investigation.[45] Cells were treated with DMSO, or 1 or 2 μM methylstat. Cells were treated for 24 hours, and cell cycle analysis was performed by staining the total DNA with propidium iodide (PI), and DNA content was measured by flow cytometry. The effect of methylstat on cell viability was assayed by incubating U937 cells with various concentrations of methylstat for a 48-hour period and then calculating cell viability using the CellTiterGlo assay from promega. The data was normalized to the untreated control

and used to calculate the GI_{50}, the concentration at which 50% of cell growth is inhibited.

We found treatment with 2 μM methylstat was sufficient to cause a significant increase in the percentage of G1 phase cells as compared to the DMSO control, consistently with the demonstrated effect of shRNA JHDM1B knock down (Figure 1.7). Furthermore, we found that low concentrations of methylstat are sufficient to disrupt cell proliferation in the AML cell line, U937 (GI_{50} = 0.8 μM). Although G1 cell cycle arrest was not apparent at the lower concentration tested (1 μM), this concentration was sufficient to inhibit cell proliferation significantly. Follow up experiments will include assessing the effect of methylstat on $p15^{Ink4b}$ expression by RT-PCR, and by Western blotting. We are intrigued by this data since it establishes that JHDMs may represent an attractive drug target for cancer therapeutics, and also that an analog of methylstat with increased JHDM isoform specificity could be a potential lead compound for such therapeutics.[21]

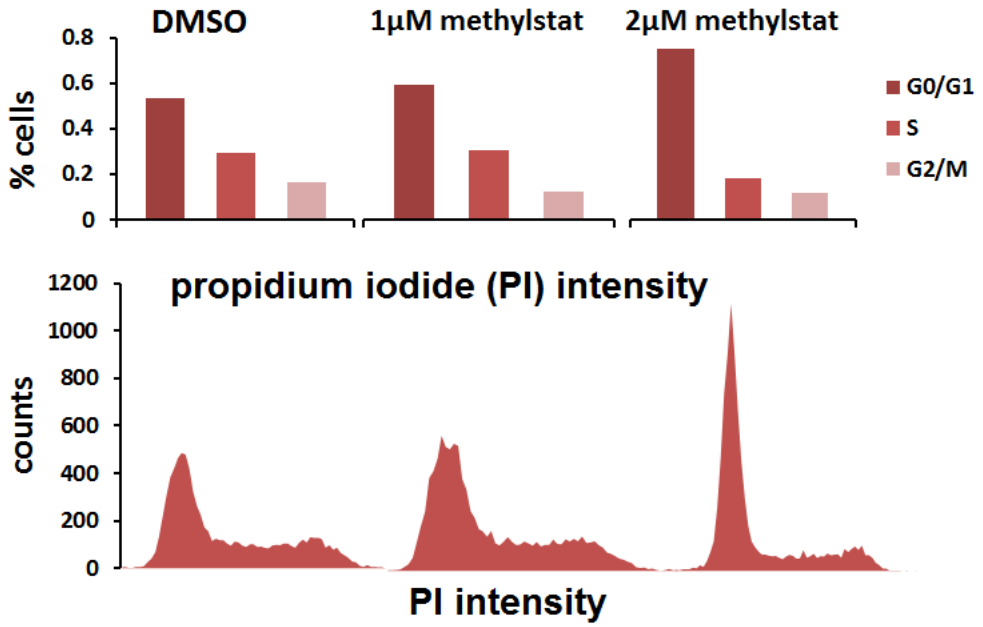

Figure 1.7: Methylstat causes G1 cell cycle arrest in U937 cells overexpressing JHDM1B.

Total cellular DNA was stained with propidium iodide (PI) and fluorescence activated cell scanning (FACS) was performed. The fraction of cells in the G1, S and G2/M phases of the cell cycle were determined (left upper panels); and the representative cell cycle analysis (FACS) data for each treatment are shown (left bottom panels). This data illustrates that a low dose of methylstat is sufficient to cause significant G1 cell-cycle arrest in U937 acute myeloid leukemia cells.

1.2.3 Cell-based screening of methylstat analogs: the search for a substrate class specific probe.[b]

An exciting opportunity exists for developing class-specific JHDM probes. Although methylstat is an excellent probe for identifying the global cellular activity of JHDMs over all, a probe with class or isoform specificity could be used to investigate specific cellular processes or could prove to be a useful lead compound for drug discovery. We began our efforts to identify class-specific probes by creating a library of methylstat analogs. The analogs were constructed by modifying each portion of the methylstat molecule. Two versions of the analog library were synthesized, one in which the α-KG mimic included an ester modification, and one in which the α-KG mimic terminates in the carboxylic acid. This was to allow whole-cell screening of the library, as well as *in vitro* validation of compounds causing hypermethylation of select histone marks. The library was screened in a whole-cell immunostaining assay using the esophageal carcinoma cell line KYSE-150, chosen due to the cell line's over expression of JMJD2C.[39] The assay was carried out by treating attached KYSE-150 cells in optical 96-well plates with 10 μM concentrations of each compound. Cells were then incubated for 48 hours and subject to immunostaining of various histone marks to assess hypermethylation. Four screens were carried out using antibiodies specific for H3K9me3, H3K27me3, H3K4me3, and H3K36me2 methyl marks, respectively. Wells in which significant hypermethylation of a histone mark was observed (relative to the DMSO control) were considered 'hits'.

[b] Methylstat analogs were synthesized by Dr. Wenqing Xu

Although some compounds produced a notable change in methylation levels of the histone marks selected, there was not a definitive way to compare the screening results in order to determine the specificity of various inhibitors. Furthermore, it is difficult to compare the levels of histone methylation observed just using an antibody as a reporter when four different antibodies were required.

We realized at this point that whole cell screening would not be sufficient to identify potent and selective JHDM isoform inhibitors, and determined that a more quantitative assay would be necessary. We thus set out to design and implement a quantitative JHDM binding assay that could be used to screen for isoform-specific JHDM active-site binders.

1.3 Quantitative analysis of histone demethylase probes using fluorescence polarization[c]

1.3.1 The need for a quantitative JHDM active site binding assay.

Historically, the major roadblock for discovery of class-specific JHDM inhibitors has been the lack of a uniform biochemical assay with which binding affinities of putative inhibitors can be quantified. Most established JHDM biochemical assays are enzyme inhibition assays.[36,46] Because of the self-destructive nature of JHDMs under biochemical reaction conditions, these assays typically require optimization for different JHDM isoforms.[47] In addition, they do not allow for accurate measurement of the dissociation constants of the JHDM probes. Thus, the IC_{50} values derived from these assays cannot be compared directly.

[c] Synthesis of methylstat^{fluor} was carried out by Dr. Wenqing Xu. Biochemical evaluation and assay development and optimization were carried out by Jessica Podoll and Dr. Xuan Dong, jointly.

In order to address this issue and facilitate discovery of novel and specific JHDM probes, a fluorescent analog of methylstat (methylstat^{fluor}) was designed and synthesized. Methylstat^{fluor} is comprised of the α-KG mimicking group of methylstat and its linker region conjugated to a fluorescein via a thiourea linkage to the secondary amine of the methylstat side chain (Figure 1.8). Methylstat^{fluor} showed similar fluorescent properties to fluorescein making its detection widely applicable to standard plate readers.

Once synthesized, methylstat^{fluor} was subsequently used to develop a fluorescence polarization (FP)-based binding assay.[48] This assay has allowed quantification of the binding affinities of multiple JHDM active site binders, has allowed binding affinities of native JHDM substrates to be quantified, and has enabled validation of the inhibitory mechanism of methylstat. Furthermore, this assay has been

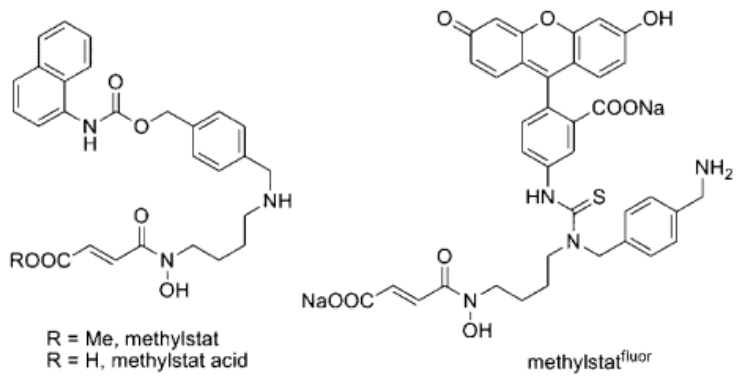

Figure 1.8: Structures of methylstat, methylstat acid, and methylstat^{fluor}.
Methylstat^{fluor} was constructed by attaching fluorescein isothiocyanate (FITC) to a free amine of methylstat.

miniaturized and adapted for high-throughput screening of JHDM active-site binders.

1.3.2 Evaluation of methylstat^{fluor} binding to three different classes of JHDMs.

Three JHDMs (JHDM1A, JMJD2A, and JMJD3) from three different classes were selected to assess the binding of methylstat^{fluor}. These three JHDMs were selected to represent a broad range of substrate specificity. JHDM1A, the first jmjC domain-containing protein to be identified as an HDM, is an H3K36me2 demethylase. JMJD2A selectively demethylates H3K9me2/3 and H3K36me2/3. Finally, JMJD3 is a H3K27me2/3 demethylase.[18,28,49] All three JHDMs were evaluated in a saturation binding experiment with methylstat^{fluor} by adapting a previously reported protocol.[50] FP signals were recorded using the Envision Multilabel plate reader (Perkin-Elmer), and expressed as the change in millipolarization ΔmP, where ΔmP is the mP of the JHDM/methylstat^{fluor} mixture after subtracting the mP of methylstat^{fluor} alone in assay buffer.

To determine the dissociation constants (K_d) of methylstat^{fluor} and the JHDMs, JHDM concentrations were plotted against ΔmP and the data were fitted in KaleidaGraph (v4.1.1, Synergy Software) using equation 1:

$$\Delta mP = \frac{P_{\min} - P_{max} \times \left(\frac{x}{K_d}\right)^n}{1+\left(\frac{x}{K_d}\right)^n} \quad (Eq.1)$$

Where, P_{max} and P_{min} are the maximum and minimum observed ΔmP values, respectively, x is the JHDM concentration, and n is the Hill coefficient of the binding

curve. Preliminary tests indicated that methylstat^{fluor} bound JHDM1A with the highest affinity among these three JHDMs; therefore, JHDM1A was used for assay optimization (Figure 1.9).

1.3.3 Optimization of the divalent metal cation for JHDM binding assays.

The initial assay buffer composition was adapted from previous reports on JHDM enzyme activity assays. These generally contain an Fe^{2+} salt and a reducing agent, sodium ascorbate, as Fe^{2+}, but not Fe^{3+}, is a cofactor for JHDM catalysis.[19,37] Our initial results showed that, although methylstat^{fluor} binds to JHDM1A with much higher affinity (K_d: 8.6 ± 1.1 nM) compared with JMJD2A and JMJD3, for which saturated binding was not obtained, the P_{max} was relatively low (<50 mP, Figure 1.10). In the absence of any additional metal ions, the P_{max} increased significantly (ca. 120 mP); however, the K_d of

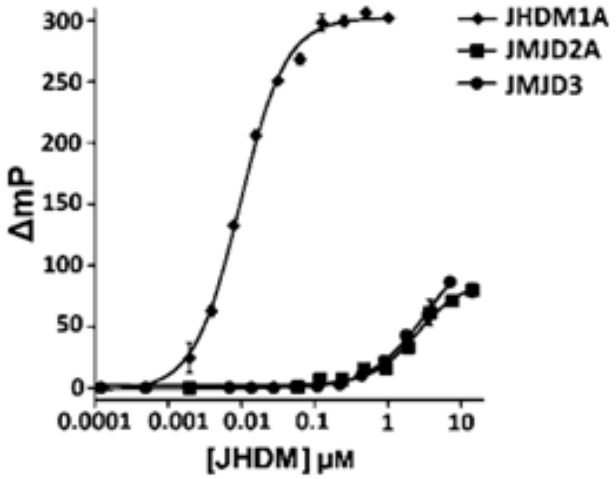

Figure 1.9: Binding of methylstatfluor to JHDM1A, JMJD2A, and JMJD3.
Only the binding of JHDM1A and methylstat^{fluor} reaches saturation at the highest concentrations tested.

JHDM1A for methylstat^{fluor} also increased significantly (19 ± 1.4 nM). Taken together, these results suggested the loss of the Fe^{2+} during protein purification and protein degradation in the presence of Fe^{2+}, a common problem for all Fe^{2+}- and α-KG-dependent hydroxylases.[36] To minimize the effects of Fe^{2+} oxidation, the binding assay was evaluated in the presence of Fe^{2+} under anaerobic conditions; the results were similar to those observed under ambient conditions in the presence of ascorbate. Because JHDM substrate binding necessitates the addition of a divalent metal cation, we next examined the binding in the presence of Ni^{2+} or Co^{2+}. Ni^{2+} and Co^{2+} were chosen because they exhibit increased stability under ambient conditions as compared to Fe^{2+}. Ni^{2+} and Co^{2+} have been shown to interact with native substrates as well as inhibitors in the JHDM active site in crystallographic studies; furthermore, these transition metals are capable of inhibiting enzyme activation without altering substrate or cofactor binding in the JHDM active site.[28,29,51–54] Replacement of Fe^{2+} with Ni^{2+} or Co^{2+} in the assay buffer afforded highly stable binding between methylstat^{fluor} and JHDM1A, with a much larger dynamic range (ca. 300 mP). The K_d of JHDM1A for methylstat^{fluor} calculated in the presence of Ni^{2+} (9.3 ± 0.5 nM) is more similar to that of the native condition than the K_d calculated in the presence of Co^{2+} (22 ± 1.4 nM). Hence, we chose to further optimize the FP assay in the presence of Ni^{2+}.

1.3.4 Stability of JHDM binding to methylstat^{fluor}.

We found the binding of JHDM1A and methylstat^{fluor} reached equilibrium after 4 h of incubation at room temperature, and the signals are stable over at least 24 h (Figure 1.11). The stabilizing effect of the Ni^{2+} buffer on JHDM1A was also observed by SDS-PAGE analysis (Figure 1.12). JHDM1A in assay buffer containing Fe^{2+} or no additional

metal showed significant decomposition after as little as 2 h, whereas JHDM1A in buffer containing Ni^{2+} showed no observable decomposition over the course of 24 h. In addition to the divalent metal ion, we have also optimized the buffer and fluorophore concentration. TRIS buffer provided more consistent results than other buffers such as MOPS and HEPES; a stable and reliable FP signal was achieved using 1 nM methylstat^{fluor}.

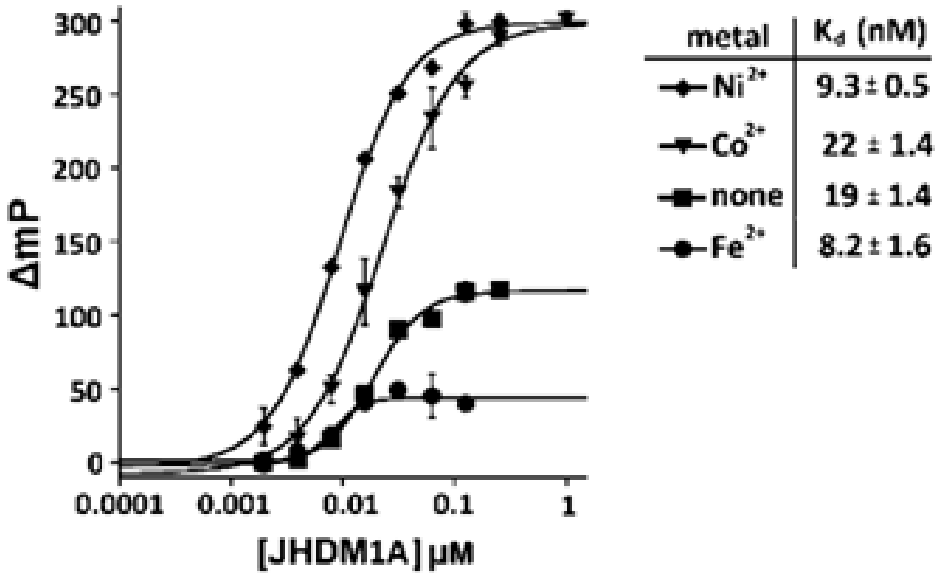

Figure 1.10: Metal ion optimization for FP binding.

Binding of methylstat^{fluor} to JHDM1A was measured with the addition of Fe^{2+}, no additional metal, or Ni^{2+} in assay buffer. Optimal binding between JHDM1A and methylstatf^{luor} was achieved by addition of Ni^{2+} to the assay buffer.

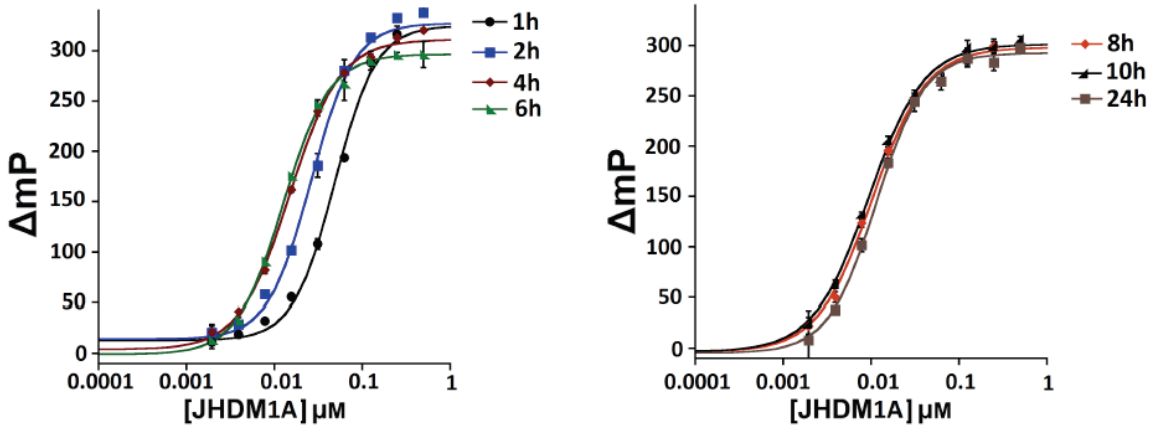

Figure 1.11: Binding of methylstatfluor to JHDM1A in the presence of Ni^{2+} is highly stable over time.

FP signals were measured at various time points over 24 hours. Once binding reached equilibrium (approximately 4 hours), signals stayed stable over the course of at least 20 hours.

1.3.5 JHDM FP-competition assays allow quantification of native substrate and inhibitor binding to the JHDM active site.

Since a protein-tracer pair with high binding affinity is required for appropriate resolution of non-fluorescent inhibitors in an FP competition assay, further development of the FP competition assay was performed using only JHDM1A.[55] Next, the ability of methylstat^{fluor} to serve as a tracer for FP competitive binding experiments was assessed and the appropriate concentration of JHDM1A for FP competition assays optimized. Typically, a protein concentration at which 50 to 80% of the fluorescent tracer is initially bound is used for FP competition assays but must be optimized to achieve a desirable dynamic range.[50,55–57] The competition assay was validated and optimized using pyridine 2,4-dicarboxylic acid (PDCA), a well-known α-KG mimic, as the competitive ligand.[58] The competition assay set up was similar to that of the binding assay except

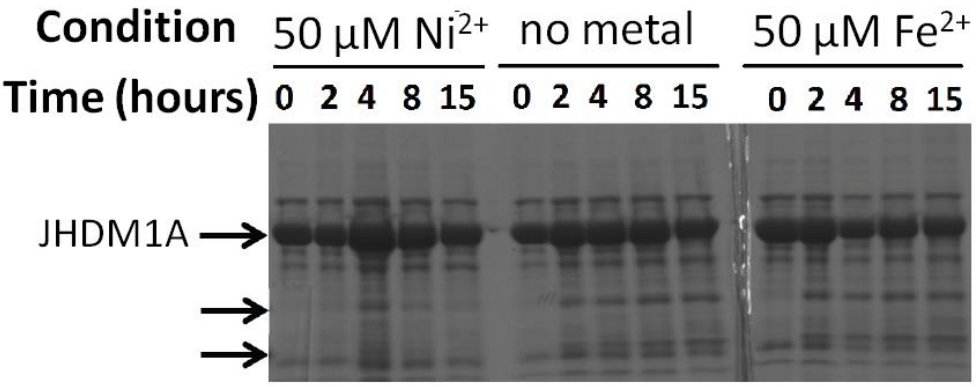

Figure 1.12: Addition of Ni^{2+} ion but not Fe^{2+} stabilizes JHDM1A.

JHDM1A was incubated in assay buffer in the presence or absence of metal ion (Ni^{2+} or Fe^{2+}) at room temperature over the indicated time. Samples were subjected to SDS-PAGE analysis followed by Coomassie staining. The bottom two arrows indicate the decomposed JHDM1A.

that a constant concentration of protein was used in each condition and the non-fluorescent inhibitor was titrated into the system (5 nM−2 mM). DMSO (1 μL, 1%) was added to each assay well as a vehicle for the inhibitor. Of the three JHDM1A concentrations tested, 60 nM JHDM1A afforded a large dynamic range appropriate for competition assays (Figure 1.13); therefore, 60 nM JHDM1A was selected as the protein concentration for the following FP competition studies. A series of JHDM probes was evaluated in the optimized FP competition assay. Probes evaluated in the assay included methylstat acid, the JHDM cofactor, α-KG, *N*-oxalylglycine (NOG, an α-KG mimic), and the substrate of JHDM1A, an H3K36me2 peptide (Figure 1.14). The results showed that all of the above molecules can displace methylstat^{fluor} from JHDM1A. Additionally, the IC_{50} values stabilized after approximately 4 h and remained stable for up to 24 h. These results not only suggest that methylstat^{fluor} binds both the substrate and α-KG cofactor-binding sites of JHDM1A but also confirms that methylstat acid is a competitive JHDM inhibitor. This competition assay also afforded the half inhibitory concentrations (IC_{50}) of these JHDM-binding molecules. The IC_{50} values were then used to calculate their dissociation constants (Ki) with JHDM1A using equation 2 and the online Ki calculator: [57]

$$K_i = \frac{[I]_{50}}{\frac{[L]_{50}}{K_d} + \frac{[P]_0}{K_d} + 1} \quad (Eq.2)$$

where, $[I]_{50}$ and $[L]_{50}$ are free inhibitor concentration and free ligand concentration at 50% inhibition, $[P]_0$ is free protein concentration at 0% inhibition, and K_d is the dissociation constant between protein JHDM1A and methylstat^{fluor}.

The ability to quantify binding of competitive inhibitors in the JHDM active site is an unprecedented development. Only the binding affinities of some JHDMs for histone peptides have been quantified by surface plasmon resonance. However, the binding affinity of α-KG for various JHDMs has never been reported.[36,51] Competitive binding assays designed for screening inhibitors have shown relative binding affinities, but report IC_{50} values of competitive inhibitors as opposed to K_i values. Although IC_{50} values are useful for assessing the relative effectiveness of inhibitors for a single enzyme, they are not directly comparable between enzymes or between different

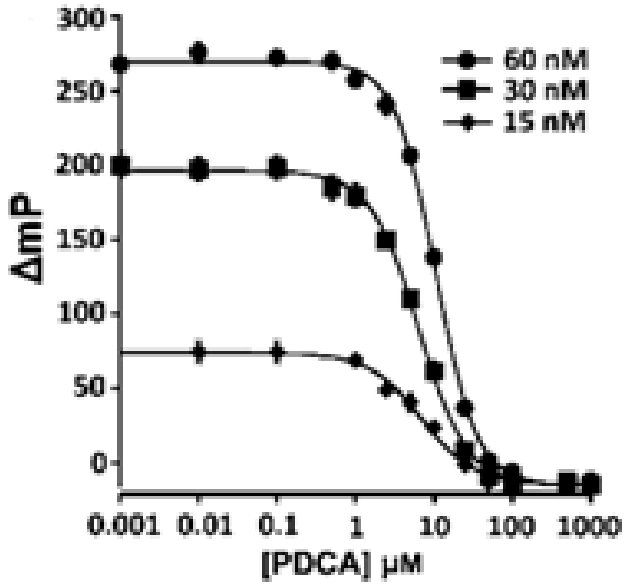

Figure 1.13: FP competition assay optimization.

15, 30, and 60 nM of JHDM1A were tested in the FP competition assay with PDCA.

assays and always depend on the individual assay conditions.[59] Further expansion of our FP binding assay to other JHDM isoforms may be extremely useful for assessing the specificities as well as the inhibitory mechanism of various JHDM probes.

1.3.6 The FP-competition assay was miniaturized and optimized for high-throughput screening.

The FP competition assay was further miniaturized to the 384-well plate format. The total volume for each assay was reduced to 20 µL, while the concentrations of JHDM1A (60 nM), methylstat^{fluor} (1 nM), and DMSO (1%) remained the same. For high-throughput screening purposes, we also evaluated the influence of detergent, Tween 20, on our FP assay. We found that addition of 0.1% Tween 20 to the assay buffer completely abolishes the binding, and 0.001% of Tween 20 is well tolerated. To

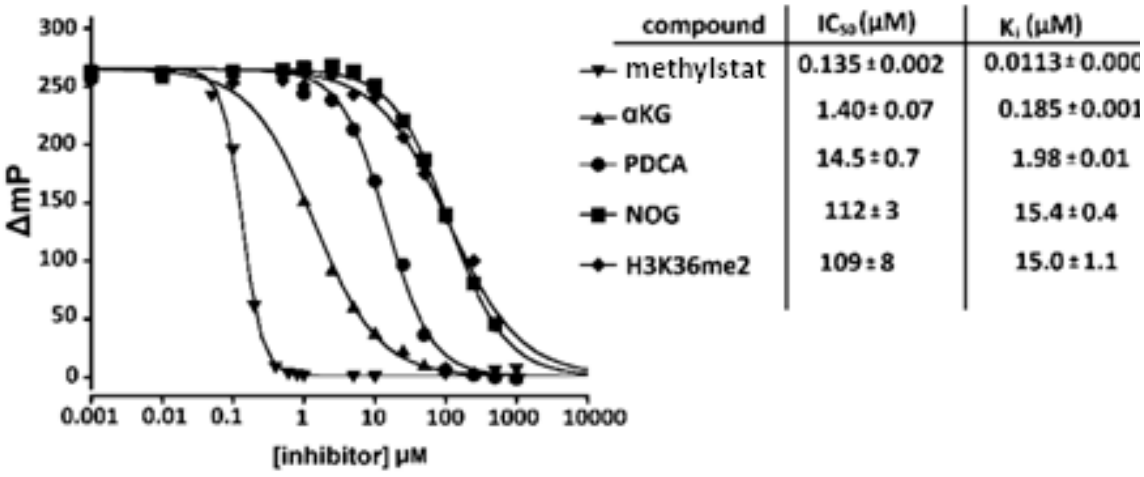

Figure 1.14: FP competition assay for known inhibitors and native substrates.

The FP competition assay was used to determine IC_{50} and K_i values for known JHDM probes.

calculate the Z′ factor, the statistical effect size of an HTS assay, we used methylstat (100 μM in DMSO) and DMSO only as positive and negative controls, respectively. Although the dynamic range of this assay decreased slightly (Figure 1.15), a high Z' factor value (0.78) was calculated,[60] which further demonstrates the robustness of this assay and its suitability for high-throughput screening.

1.4 Conclusions and future directions

The field of epigenetics is ever-growing and changing. As the epigenetic landscape has taken shape and the histone code revealed itself, there has been an established and growing need for tools with which to study the processes involved in epigenetic regulation of gene expression. Although it has been well established for

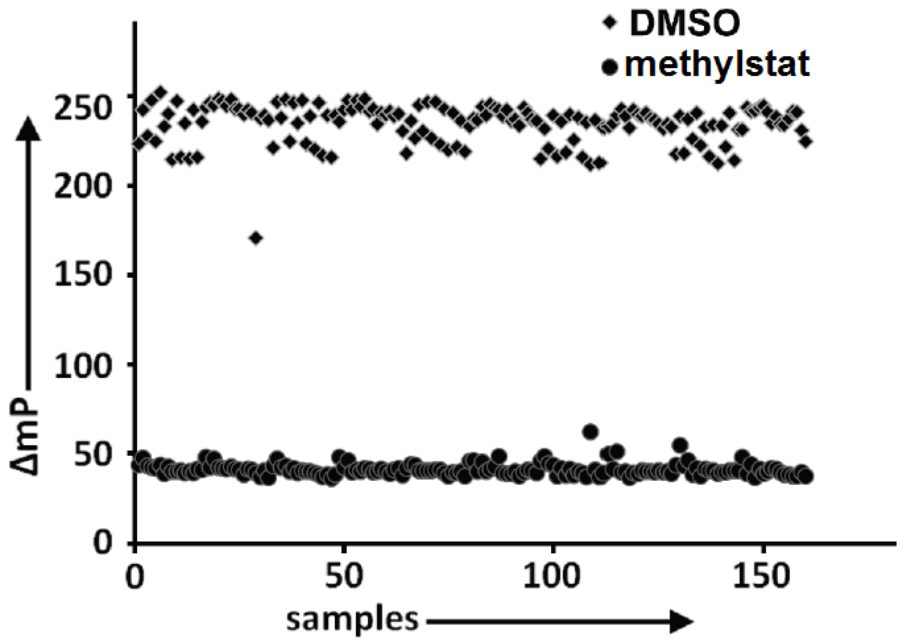

Figure 1.15: Z' determination to assess our FP competition assay as a HTS technique.

Methylstat^{fluor} can be used for high-throughput screening of JHDM inhibitors. DMSO and methylstat were used to represent 0% and 100% inhibition, respectively.

decades that that the histone code is written and erased enzymatically, it was only within the last decade that the dynamic nature of histone methylation, particularly the phenomenon of demethylation, discovered. Although two distinct mechanisms of histone methylation have been discovered, involving hydroxylation coupled to either an FAD or an α-KG cofactor, many of these enzymes targeting specific sites that are known to be dynamically regulated remain elusive. Furthermore, although demethylation activity has been hypothesized in the cascade of events underlying many processes of development and disease, many cases still exist in which the enzyme responsible has not yet been identified. In addition, the dysregulation of HDMs and JHDMs in multiple disease states has been identified, but there are no approved treatments targeting these enzymes as of yet.[21] The development of JHDM inhibitors, and isoform/substrate-specific JHDM inhibitors will fill many of the gaps in epigenetic research at both the basic science level, as well as the clinical level. The Wang lab developed methylstat in 2011; already, this cell active JHDM probe has been used to investigate the role of JHDMs in disease processes including angiogenesis.[61] However, the major limitation of methylstat is that it is a pan-JHDM probe, that is, it does not distinguish among various JHDM isoforms with differing substrate specificity. Potentially, a library of probes with specific and established targets within the JHDMs could serve to validate specific hypotheses without genetic intervention, and could potentially translate to use in the clinic. The Wang lab has thus sought to bring this aspiration to light by developing a highly quantitative binding assay that can be used to calculate the binding affinities of ligands to the JHDM active site. In doing so, we were able to calculate the binding affinities of known JHDM inhibitors as well as native

substrates including the α-KG cofactor, a feat which has never before been accomplished.

The Wang lab has further expanded the field of JHDM probe discovery by establishing an HTS technique based on the FP-competition assay. This screening technique was highly repeatable and robust. Although the work described here only produced a set of FP assays suitable for JHDM1A, other members of the Wang lab have been working to develop FP tracers for a variety of JHDMs. A tracer for JMJD2A has already been developed and used in a high-throughput screen. Already, the FP-HTS assay has been used to identify novel scaffolds capable of binding the active site of JHDM1a. Several of these have already been validated as cell-active JHDM inhibitors. Additionally, FP-binding and competition assays have been developed for the ten-eleven translocation (TET) proteins, which are 5-methylcytosine hydroxylases. Going forward, the Wang lab intends to continue to discover and validate substrate-class-specific JHDM probes and other techniques with which to study these essential epigenetic regulators.

1.5 Materials and methods

1.5.1 Cell culture

The human esophageal squamous cell carcinoma cell line, KYSE-150, was obtained from the German Collection of Microorganisms and Cell Cultures, Braunschweig, Germany. KYSE-150 cells were maintained in 49% RPMI 1640, 49% Ham's F12 supplemented 2% fetal calf serum (FCS), 1% penicillin/streptomycin, 5%CO2.^{3}> U937 cells were maintained in RPMI-1640 supplemented with 10% FCS, 1%

penicillin/streptomycin, 5% CO2 at 37 °C. All other cells were acquired from the American Type Culture Collection (ATCC) and were maintained at 37 °C in Dulbecco's modified Eagle's medium (DMEM) supplemented with 10% fetal calf serum (FCS), 1% penicillin/streptomycin, 5% CO2.The differentiation of C2C12 was induced by incubating cells in DMEM with 2% horse serum for approximately 6 days. Media and compounds for this experiment were refreshed every other day. The compounds were added as previously described.[37] 0.1% DMSO was added as the control. Western blotting was performed following standard protocols.

1.5.2 Immunostaining

Cells were seeded in in 96-well optical bottom plates at a density of 5000-10000. Cells were allowed to attach for 24 hours before treatment with compound. For whole cell screens, cells were treated for 48 hours before media was removed and the cells washed in D-PBS. Cells were fixed for 20 minutes in 4% para-formaldehyde in D-PBS. Cells were washed three times (10 minutes per wash) in cold D-PBS. Cells were permeabilized and blocked simultaneously in 0.5% Triton-X-100 1% BSA for 30 minutes. Next, cells were incubated with the appropriate primary antibody diluted 1:1000 in D-PBS overnight. The next day, cells were washed three timed in D-PBS and incubated with fluorescent antibodies as appropriate (either Alexafluor 488 goat anti-mouse, or Alexafluor 694 goat anti-rabbit from Invitrogen). Cells were washed three times in D-PBS, their nuclei stained with Hoechst 3342 and read using the Cellomics array-scan HCS plate reader. Mean average fluorescence intensity for each well was calculated relative to the cell count of that well and used as a measure of hypermethylation.

1.5.3 FACS cell cycle analysis.

U937 cells were grown in suspension under standard conditions or in the presence of methylstat. Cell density was determined by hemocytometer assisted counting. Cells were harvested by centrifuging for 2 minutes at 1000 rpm. Cells were fixed in ice cold 70% ethanol by adding the solution drop-wise to the cell pellet and vortexing. Cells were incubated for 30 minutes at 4°C. Cells were washed in D-PBS. 200 µl of a 50 µg/ml stock was added to the cell pellet to stain DNA. Total DNA content was obtained and analyzed using a Becton Dickenson FACScan flow cytometer and the FACScan software.

1.5.4 Purification of JHDMs.

Recombinant JHDM1A (1−517) and JMJD3 (1018−1590) were expressed as 6XHis fusion proteins using the pNIC28 and the pNH-TrxT expression vectors, respectively. The coding regions were verified by sequencing and the plasmids were transfected into BL21 Escherichia coli. Following expression, JHDM1A was purified using Ni SepharoseTM 6 Fast Flow beads (GE) by gravity chromatography according to the manufacturer's instructions. JMJD3 was purified using cobalt (high density) agarose beads (Gold Biotechnology) according to the manufacturer's protocol. JMJD2A was expressed and purified as described previously.[37] The purified proteins were exchanged into assay buffer, flash frozen in liquid nitrogen, and stored at −80 °C.

1.5.5 FP-binding assay conditions.

FP binding experiments were performed in black, low-binding, half area 96-well plates (Corning 3993). Then 80 µL of JHDM1A (2.44 nM to 2.50 µM in 2-fold dilution) in

assay buffer (50 μM $NiCl_2$, 25 mM TRIS, 100 mM NaCl, pH 7.5) were added to experimental wells. After 10 min, 20 μL of methylstat^{fluor} (5 nM in assay buffer) was then added to each well. Wells containing protein only were subtracted from assay wells as background. Plates were incubated at room temperature and read five times at each time point (1, 2, 4, 6, 8, 10, and 24 h), and the average values at each time point were used for the calculation of the polarization values. Binding curves were fit using KaleidaGraph (v4.1.1, Synergy Software).

1.5.6 FP competition assay.

Known JHDM active site binders (methylstat, α-KG, PDCA, NOG, or peptide H3K36me2) were tested for their ability to compete the binding of methylstatf^{luor} to JHDM1A. Then 2-fold serial dilutions of compounds were prepared as 100x solutions in DMSO. Then 80 μL of JHDM1A (75 nM in assay buffer) were added to each well, to which 1 μL of the above compound solutions were added. The mixtures were incubated at room temperature for 30 min prior to addition of 20 μL of methylstatf^{luor} (5 nM in assay buffer). Controls containing 3 and JHDM1A or JHDM1A and the competing compound were included for background subtraction. Each experiment was performed in duplicate. The assay plates were incubated at room temperature for 4 h before signals were recorded by the Envision Multilabel plate reader. The calculated data was fitted using KaleidaGraph (v4.1.1, Synergy Software).

1.5.7 Z' factor determination.

The FP competition assay was miniaturized to 20 μL in the 384well plate format. 15 μL of JHDM1A (80 nM in assay buffer: 50 μM $NiCl_2$, 100 mM NaCl, 0.001% Tween

20, 25 mM TRIS, pH 7.5) were added to each experimental well of a black 384well plate (Corning: 3677) using MicroFlo dispenser (Biotek). 200 nL of DMSO or 2 (10 mM in DMSO) was transferred to each experimental well using a CyBi-Well 96-channel simultaneous pipettor (Cybio). The assay plate was incubated at room temperature with rocking for 30 minutes prior to the addition of 5 µL of 3 (4 nM in assay buffer) to each well using MicroFlo dispenser. The signals were recorded after incubation for 4 hours at room temperature, and a *Z*'-factor of 0.78 was calculated based on the following equation:

$$Z' = 1 - \frac{3 \times (\sigma_{max} + \sigma_{min})}{\mu_{max} - \mu_{min}}$$

σ_{max} and σ_{min} are the standard deviations of the maximum and minimum observed signals, respectively, and μ_{max} and μ_{min} are means of the maximum and minimum observed signal, respectively.[60]

1.6 References

1. Biel, M., Wascholowski, V. & Giannis, A. Epigenetics--an epicenter of gene regulation: histones and histone-modifying enzymes. *Angew. Chem. Int. Ed. Engl.* **44,** 3186–216 (2005).

2. Felsenfeld, G. & Groudine, M. Controlling the double helix. *Nature* **421,** 448–53 (2003).

3. Kouzarides, T. Chromatin modifications and their function. *Cell* **128,** 693–705 (2007).

4. Goldberg, A. D., Allis, C. D. & Bernstein, E. Epigenetics: a landscape takes shape. *Cell* **128,** 635–8 (2007).

5. Strahl, B. D. & Allis, C. D. The language of covalent histone modifications. *Nature* **403,** 41–5 (2000).

6. Upadhyay, A. K. & Cheng, X. in *Epigenetics Dis.* (Gasser, S. M. & Li, E.) **3,** 107–124 (Springer Basel, 2011).

7. Khalil, A. M. & Rinn, J. L. RNA-protein interactions in human health and disease. *Semin. Cell Dev. Biol.* **22,** 359–365 (2011).

8. Shi, J. *et al.* The Polycomb complex PRC2 supports aberrant self-renewal in a mouse model of MLL-AF9;NrasG12D acute myeloid leukemia. *Oncogene* **32,** 930–938 (2012).

9. Qiu, J. *et al.* The X-linked mental retardation gene PHF8 is a histone demethylase involved in neuronal differentiation. *Cell Res.* **20,** 908–18 (2010).

10. Bernstein, B. E., Meissner, A. & Lander, E. S. The mammalian epigenome. *Cell* **128,** 669–81 (2007).

11. Fischle, W., Wang, Y. & Allis, C. D. Histone and chromatin cross-talk. *Curr. Opin. Cell Biol.* **15,** 172–183 (2003).

12. Shilatifard, A. Chromatin modifications by methylation and ubiquitination: implications in the regulation of gene expression. *Annu. Rev. Biochem.* **75,** 243–269 (2006).

13. Suganuma, T. & Workman, J. L. Crosstalk among Histone Modifications. *Cell* **135,** 604–607 (2008).

14. Lee, J. S., Smith, E. & Shilatifard, A. The Language of Histone Crosstalk. *Cell* **142,** 682–685 (2010).

15. Klose, R. J. & Zhang, Y. Regulation of histone methylation by demethylimination and demethylation. *Nat. Rev. Mol. Cell Biol.* **8,** 307–18 (2007).

16. Allis, C. D., Bowen, J. K., Abraham, G. N., Glover, C. V & Gorovsky, M. a. Proteolytic processing of histone H3 in chromatin: a physiologically regulated event in Tetrahymena micronuclei. *Cell* **20,** 55–64 (1980).

17. Shi, Y. *et al.* Histone demethylation mediated by the nuclear amine oxidase homolog LSD1. *Cell* **119,** 941–53 (2004).

18. Tsukada, Y. *et al.* Histone demethylation by a family of JmjC domain-containing proteins. *Nature* **439,** 811–6 (2006).

19. Shi, Y. & Whetstine, J. R. Dynamic regulation of histone lysine methylation by demethylases. *Mol. Cell* **25,** 1–14 (2007).

20. Anand, R. & Marmorstein, R. Structure and mechanism of lysine-specific demethylase enzymes. *J. Biol. Chem.* **282,** 35425–9 (2007).

21. Højfeldt, J. W., Agger, K. & Helin, K. Histone lysine demethylases as targets for anticancer therapy. *Nat. Rev. Drug Discov.* **12,** 917–30 (2013).

22. Kawazu, M. *et al.* Histone demethylase JMJD2B functions as a co-factor of estrogen receptor in breast cancer proliferation and mammary gland development. *PLoS One* **6,** e17830 (2011).

23. Xiang, Y. *et al.* JARID1B is a histone H3 lysine 4 demethylase up-regulated in prostate cancer. *Proc. Natl. Acad. Sci. U. S. A.* **104,** 19226–31 (2007).

24. Duncan, E. M. & Allis, C. D. *Epigenetics and Disease*. *Epigenetics Dis.* 69–90 (Springer Basel, 2011). doi:10.1007/978-3-7643-8989-5

25. Chen, Z. *et al.* Structural insights into histone demethylation by JMJD2 family members. *Cell* **125,** 691–702 (2006).

26. Ozer, A. & Bruick, R. K. Non-heme dioxygenases: cellular sensors and regulators jelly rolled into one? *Nat. Chem. Biol.* **3,** 144–53 (2007).

27. Hausinger, R. P. *FeII/alpha-ketoglutarate-dependent hydroxylases and related enzymes. Crit. Rev. Biochem. Mol. Biol.* **39,** 21–68 (2004).

28. Couture, J., Collazo, E., Ortiz-Tello, P. A., Brunzelle, J. S. & Trievel, R. C. Specificity and mechanism of JMJD2A, a trimethyllysine-specific histone demethylase. *Nat. Struct. Mol. Biol.* **14,** 689–95 (2007).

29. Ng, S. S. *et al.* Crystal structures of histone demethylase JMJD2A reveal basis for substrate specificity. *Nature* **448,** 87–91 (2007).

30. Mosammaparast, N. & Shi, Y. Reversal of histone methylation: biochemical and molecular mechanisms of histone demethylases. *Annu. Rev. Biochem.* **79,** 155–79 (2010).

31. Cloos, P. a C., Christensen, J., Agger, K. & Helin, K. Erasing the methyl mark: histone demethylases at the center of cellular differentiation and disease. *Genes Dev.* **22,** 1115–40 (2008).

32. Spring, D. R. Chemical genetics to chemical genomics: small molecules offer big insights. *Chem. Soc. Rev.* **34,** 472 (2005).

33. Stockwell, B. R. Chemical genetics: ligand-based discovery of gene function. *Nat. Rev. Genet.* **1,** 116–125 (2000).

34. Sumranjit, J. & Chung, S. J. Recent advances in target characterization and identification by photoaffinity probes. *Molecules* **18,** 10425–51 (2013).

35. Cole, P. a. Chemical probes for histone-modifying enzymes. *Nat. Chem. Biol.* **4,** 590–7 (2008).

36. Rose, N. R., McDonough, M. A., King, O. N. F., Kawamura, A. & Schofield, C. J. Inhibition of 2-oxoglutarate dependent oxygenases. *Chem. Soc. Rev.* **40,** 4364–97 (2011).

37. Luo, X. *et al.* A selective inhibitor and probe of the cellular functions of Jumonji C domain-containing histone demethylases. *J. Am. Chem. Soc.* **133,** 9451–9456 (2011).

38. Simonini, M. V *et al.* The benzamide MS-275 is a potent, long-lasting brain region-selective inhibitor of histone deacetylases. *Proc. Natl. Acad. Sci. U. S. A.* **103,** 1587–92 (2006).

39. Cloos, P. a C. *et al.* The putative oncogene GASC1 demethylates tri- and dimethylated lysine 9 on histone H3. *Nature* **442,** 307–11 (2006).

40. Ishimura, A. *et al.* Jmjd2c histone demethylase enhances the expression of Mdm2 oncogene. *Biochem. Biophys. Res. Commun.* **389,** 366–71 (2009).

41. Seenundun, S. *et al.* UTX mediates demethylation of H3K27me3 at muscle-specific genes during myogenesis. *EMBO J.* **29,** 1401–11 (2010).

42. He, J., Nguyen, A. T. & Zhang, Y. KDM2b/JHDM1b, an H3K36me2-specific demethylase, is required for initiation and maintenance of acute myeloid leukemia. *Blood* **117,** 3869–80 (2011).

43. Vincent, A. & Van Seuningen, I. On the epigenetic origin of cancer stem cells. *Biochim. Biophys. Acta* **1826,** 83–8 (2012).

44. Shackleton, M., Quintana, E., Fearon, E. R. & Morrison, S. J. Heterogeneity in cancer: cancer stem cells versus clonal evolution. *Cell* **138,** 822–9 (2009).

45. Nakamura, S. *et al.* JmjC-domain containing histone demethylase 1B-mediated p15(Ink4b) suppression promotes the proliferation of leukemic progenitor cells through modulation of cell cycle progression in acute myeloid leukemia. *Mol. Carcinog.* 1–13 (2011). doi:10.1002/mc.20878

46. Krishnan, S., Collazo, E., Ortiz-Tello, P. a & Trievel, R. C. Purification and assay protocols for obtaining highly active Jumonji C demethylases. *Anal. Biochem.* **420,** 48–53 (2011).

47. Mantri, M., Zhang, Z., McDonough, M. a & Schofield, C. J. Autocatalysed oxidative modifications to 2-oxoglutarate dependent oxygenases. *FEBS J.* **279,** 1563–75 (2012).

48. Xu, W. *et al.* Quantitative analysis of histone demethylase probes using fluorescence polarization. *J. Med. Chem.* **56,** 5198–5202 (2013).

49. De Santa, F. *et al.* The histone H3 lysine-27 demethylase Jmjd3 links inflammation to inhibition of polycomb-mediated gene silencing. *Cell* **130,** 1083–94 (2007).

50. Rossi, A. M. & Taylor, C. W. Analysis of protein-ligand interactions by fluorescence polarization. *Nat. Protoc.* **6,** 365–87 (2011).

51. Horton, J. R. *et al.* Enzymatic and structural insights for substrate specificity of a family of jumonji histone lysine demethylases. *Nat. Struct. Mol. Biol.* **17,** 38–43 (2010).

52. Sekirnik, R., Rose, N. R., Mecinović, J. & Schofield, C. J. 2-Oxoglutarate oxygenases are inhibited by a range of transition metals. *Metallomics* **2,** 397–9 (2010).

53. Chang, Y. *et al.* Structural basis for G9a-like protein lysine methyltransferase inhibition by BIX-01294. *Nat. Struct. Mol. Biol.* **16,** 312–7 (2009).

54. Sengoku, T. & Yokoyama, S. Structural basis for histone H3 Lys 27 demethylation by UTX / KDM6A. 2266–2277 (2011). doi:10.1101/gad.172296.111.heterochromatin

55. Huang, X. Fluorescence polarization competition assay: the range of resolvable inhibitor potency is limited by the affinity of the fluorescent ligand. *J. Biomol. Screen.* **8,** 34–8 (2003).

56. Nikolovska-Coleska, Z. *et al.* Development and optimization of a binding assay for the XIAP BIR3 domain using fluorescence polarization. *Anal. Biochem.* **332,** 261–73 (2004).

57. Fang, X. & Wang, R. The Ki Calculator For Fluorescence-Based Competitive Binding Assays. (2004). at <sw16.im.med.umich.edu/software/calc_ki>

58. Cole, P. a. Chemical probes for histone-modifying enzymes. *Nat. Chem. Biol.* **4,** 590–7 (2008).

59. Krohn, K. A. & Link, J. M. Interpreting enzyme and receptor kinetics: keeping it simple, but not too simple. *Nucl. Med. Biol.* **30,** 819–826 (2003).

60. Zhang, J.-H. A Simple Statistical Parameter for Use in Evaluation and Validation of High Throughput Screening Assays. *J. Biomol. Screen.* **4,** 67–73 (1999).

61. Cho, Y. *et al.* A histone demethylase inhibitor, methylstat, inhibits angiogenesis in vitro and in vivo. *RSC Adv.* **4,** 38230 (2014).

Chapter 2 : Development and initial screening efforts of a natural-product-like library of indole alkaloids

2.1 Introduction

2.1.1 Bioactive plant natural products and indole alkaloids

Plant secondary metabolites represent a highly diverse wealth of chemical structures. Although these were formerly thought to be waste products of higher metabolism, they are now recognized as bioactive compounds that take part in plant defense systems as well as communication and sensory activities.[1] The plant alkaloids represent a highly bioactive array of plant secondary metabolites which have been used throughout history in herbal medicine.[2,3] One chemical moiety represented in an array of plant alkaloids is the indole, and alkaloids that contain this moiety are known as the indole alkaloids. Indole alkaloids are relatively common in modern medicine and have been used to treat cancers (vinblastine) and hypertension (reserpine and ajmaline).[4] The indole moiety is also common in psychoactive compounds such as serotonin and its analogs, and indole amine hallucinogens including psilocybin, and LSD (Figure 2.1).[5]

2.1.2 Natural products are not well suited for technology driven drug discovery.

Although medicinal plants and natural products have historically been the mainstay of drug discovery, when high-throughput technologies came into the limelight, natural-product-based drug discovery largely fell by the wayside. This is largely because plant secondary metabolites are not user-friendly from a screening perspective.[6]

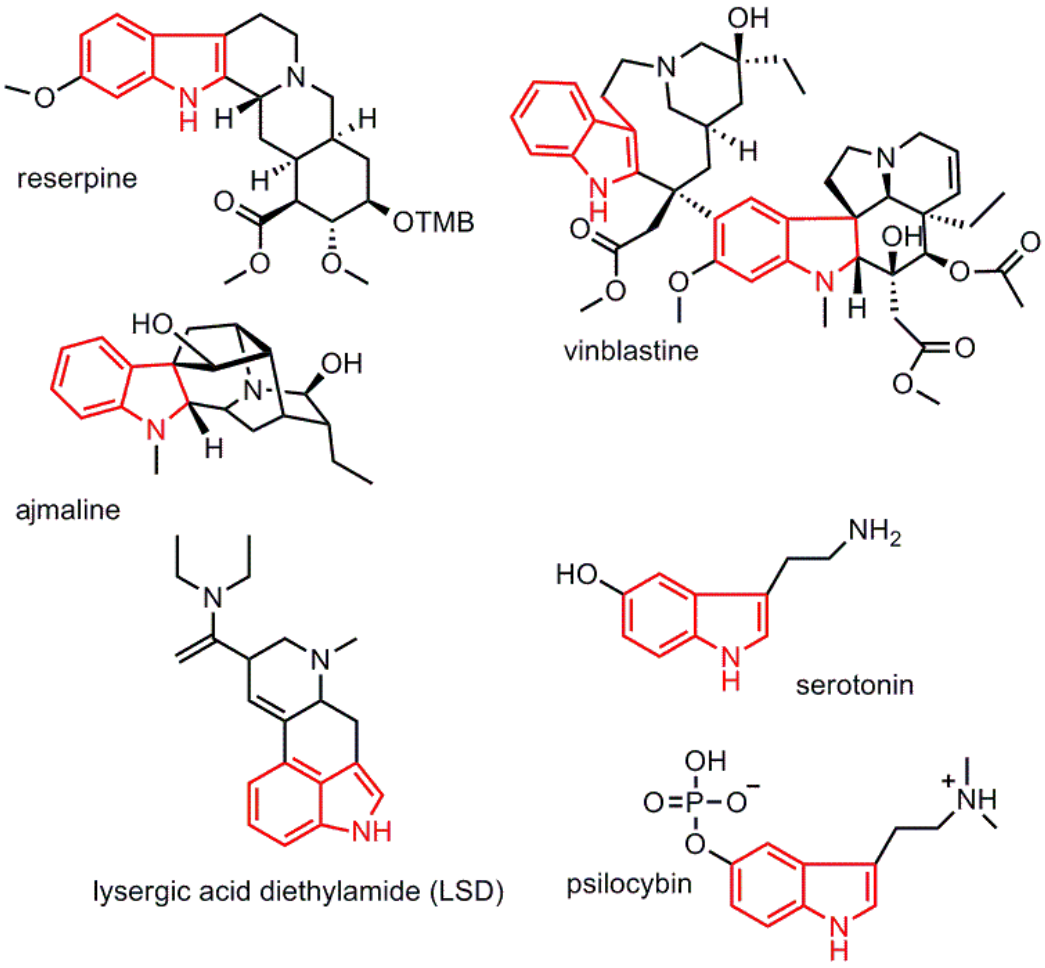

Figure 2.1: The indole moiety is present in molecules with diverse bioactivities.

The indole moiety (red) is present in an array of bioactive compounds, examples of which are illustrated here. These include, but are not limited to, antihypertensives (reserpine and ajmaline), chemotherapeutics (vinblastine), and a variety of psychoactive compounds including serotonin, psilocybin and lysergic acid diethylamide (LSD, which is semi-synthetic).

Firstly, isolation of active components from natural materials remains a challenge. This is because plant secondary metabolites represent such a small fraction of the overall mass of their plant of origin. To complicate matters further, the secondary metabolites are present as a complex mixture, making separation of a single active component difficult, to say the least.[7] Although synthetic efforts toward total synthesis of bioactive alkaloids exist, there has not been a systematic approach identified that could potentially afford a screening library of natural products with relative ease.[8,9] These issues have directed drug discovery away from natural products in favor of large, synthetic screening libraries.[10,11]

2.1.3 High-throughput screening of large, synthetic libraries has had limited success for challenging targets and identifying antibiotics.

Large libraries for high-throughput screening (HTS) are designed to be 'drug-like' based on existing pharmaceuticals and a set of chemical properties known as 'Lipinski's rule of five'.[12] Although such compound libraries are expansive, and known to produce leads for targets considered 'druggable' in the human genome, they are unsuitable as drug candidates for more challenging targets (such as protein-protein interactions) and have not had any success as antimicrobials.[13,14] A notable example of the shortcomings of synthetic-compound library HTS was observed in the late 1990s during a screening effort carried out by GlaxoSmithKline (GSK). This process involved screening up to 500,000 compounds in over 70 different biochemical screens in an effort to identify novel antibiotics.[14] These screens yielded just five possible lead compounds, none of which was suitable for clinical use. With numerous technologies designed to identify target proteins, and efficient synthesis strategies, natural products

or derivatives of natural products still represent a far larger portion of known pharmaceuticals than compounds identified from randomly synthesized libraries.[15]

The root of this issue comes down to chemical diversity. While drug-like libraries are easily synthesized and follow a set of rules that should contribute to their success as pharmaceuticals, their chemical diversity is minimal. Chemical space has been estimated to comprise up to 10^{200} compounds; the largest of screening campaigns will include 10^6 structures.[16] Even if each structure were entirely unique chemically, this would still represent only a tiny fraction of the possible chemical diversity. It has thus been estimated that only 10% of the proteins encoded in the human genome are druggable by what are considered 'drug-like' molecules. Furthermore, the vast majority of known antibiotics show chemical properties that diverge from typical drug-like molecules.[14,17] Based on these observations, it is clear that an alternate approach to compound library design is necessary to identify drug candidates for novel targets and antibiotics, specifically.

2.2 Development of a natural-product-like library to bridge the gap between natural product and HTS drug discovery.[d]

The Wang lab sought to address the gap in screening library quality by developing a bio-inspired natural-product-like library of indole alkaloids. Although the library is purely synthetic in origin, it occupies a chemical space more similar to that of natural product drugs while maintaining a modular and systematic synthetic route. Furthermore, because of the relative ease of synthesis, analogs of hit compounds are

[d] Synthesis of the indole alkaloid pilot library was carried out by Dr. Yongxiang Liu

easily attainable, creating a situation in which functional probes and analogs of hits are readily available for studies involving immobilizing the compound, fluorescence labeling, or structure-activity relationship (SAR) investigations.

Synthesis of the library was broken into three components: assembly of building blocks (to form a functionalized indole), cyclization of the functionalized indoles to fused or spiro-tetracyclic indolines, and various modifications of indoline skeletons. These

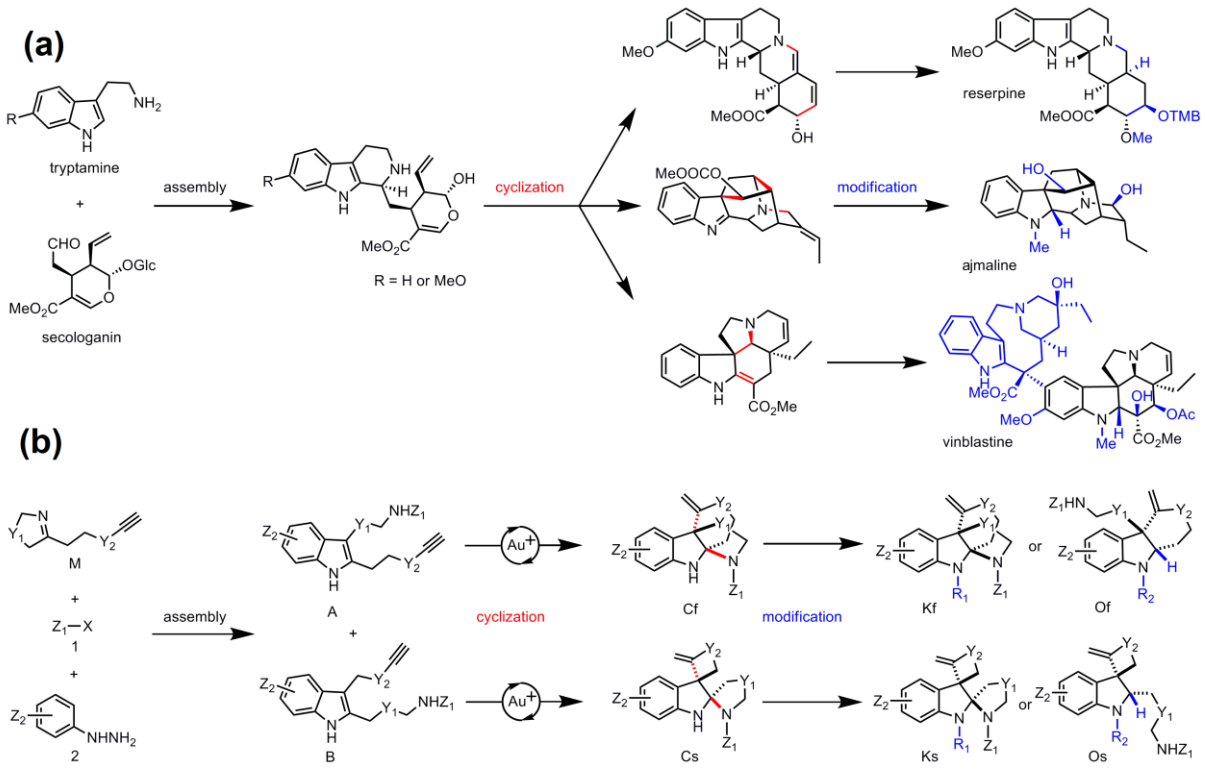

Figure 2.2: Synthetic strategy for polycyclic indole alkaloids in nature, and for the Wang lab's synthetic indole alkaloid library.

(a) Biosynthesis proceeds via assembly of building blocks including tryptamine is the indole source. Later steps which include cyclization and functionalization are accomplished enzymatically. (b) For the Wang lab's synthetic library, assembly of the indole is accomplished by Fischer indole synthesis followed by gold-catalyzed cyclization and finally modification of the cyclized products.

three steps were designed to mimic the complex enzymatic pathways that afford these structures in nature (Figure 2.2). Assembly of the building blocks, accomplished in nature via synthesis of the indole-containing precursor, tryptamine, is performed in the Wang group via Fischer indole synthesis in a one-pot, three-component reaction, generating a series of indoles with sufficient side chain diversity that allows cyclizations to multiple unique skeletons in later steps (Figure 2.2).[18–20] These are cyclized using gold catalysis, which results in fused or spiro-tetracyclic indoline formation from the indoles.[21] The final step is ring-opening, and reduction or alkylation of indoline skeletons. When indole alkaloids are synthesized in their natural environment, there is no purification of the 'final' structure from the intermediates and byproducts of synthesis.[22] The result is a complex mixture of secondary metabolites in which an intermediate of another bioactive compound is also bioactive. Likewise, the indole alkaloid library created in the Wang lab includes all intermediates of each matured indoline compound as a screening compound. Although the library is still expanding, the pilot library used in initial screening efforts totaled 120 indolines containing 26 distinct skeletons (Figure 2.3).

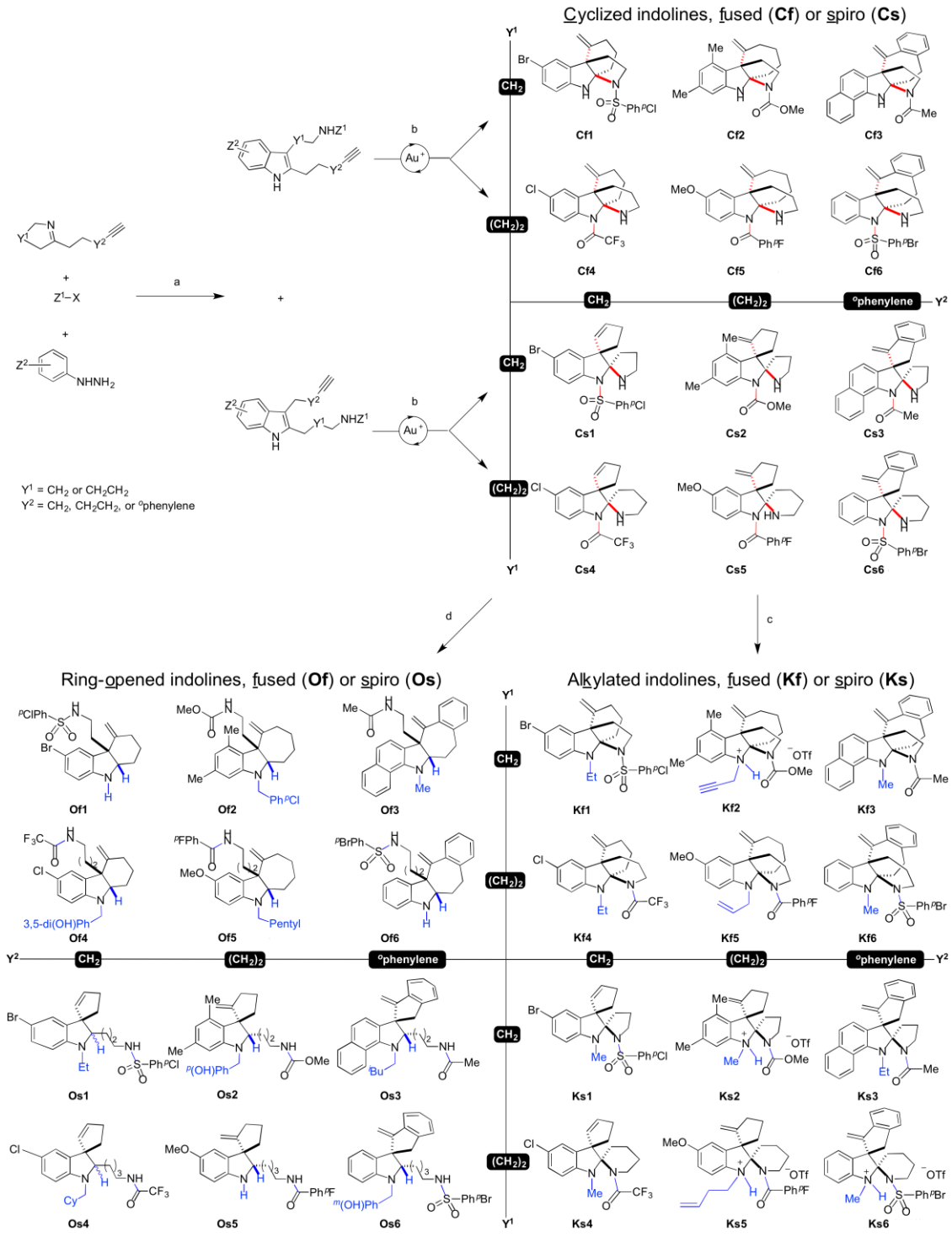

Figure 2.3: Skeletal diversity of the indole alkaloid library.

2.3 Initial screening efforts.

Based on the vast array of bioactivities represented by natural indole alkaloids, we sought to screen the synthetic indole alkaloid library in an array of bioassays. The goal of this investigation was to assess the breadth of bioactivities possessed by the synthetic indole library and how closely the diversity of bioactivities mimics those of natural indole alkaloids. We first chose to screen our library for its ability to inhibit cancer cell and bacterial growth based on the use of indole alkaloids such as the vinca indoles (such as vinblastine, vindoline and vincristine) in cancer therapy as well as the antibacterial activity of indole alkaloids isolated from natural product extracts.[23]

Notable hits resulting from these screening efforts were investigated further. The initial investigations are discussed here and some are ongoing. The goal of these initial screens was to get an idea of the potential impact of this library and its potential bioactivities.

Figure 2.4: Initial screening heat map.

The 120-compound pilot library was screened for their ability to inhibit growth of two cancer cell lines (MCF-7 and HCT116), Gram-positive bacteria (*Staphylococcus aureus,* ATCC 25923), and Gram-negative bacteria (*Escherichia coli*, ATCC 25922). Growth in the presence of compound was normalized to the growth in the presence of vehicle only (DMSO). The red brightness indicates the extent to which growth was inhibited by a compound. Black indicates no inhibition at all and very bright red indicates nearly complete inhibition of growth.

2.3.1 Cancer cell line screening.

The pilot library was first screened for growth inhibition of a colorectal carcinoma cell line (HCT116) and a breast adenocarcinoma cell line (MCF7). Compounds were screened at a concentration of 20 µM over a period of 48 hours. Cell growth was normalized to a DMSO control and the known microtubule polymerization inhibitor, vinblastine, was added as a positive control. Cell viability was assessed using the CellTiter-Glo^{TM} cell viability kit from Promega, which measures ATP as a proxy of active cell metabolism to distinguish living from dead cells. Our initial screen using the pilot

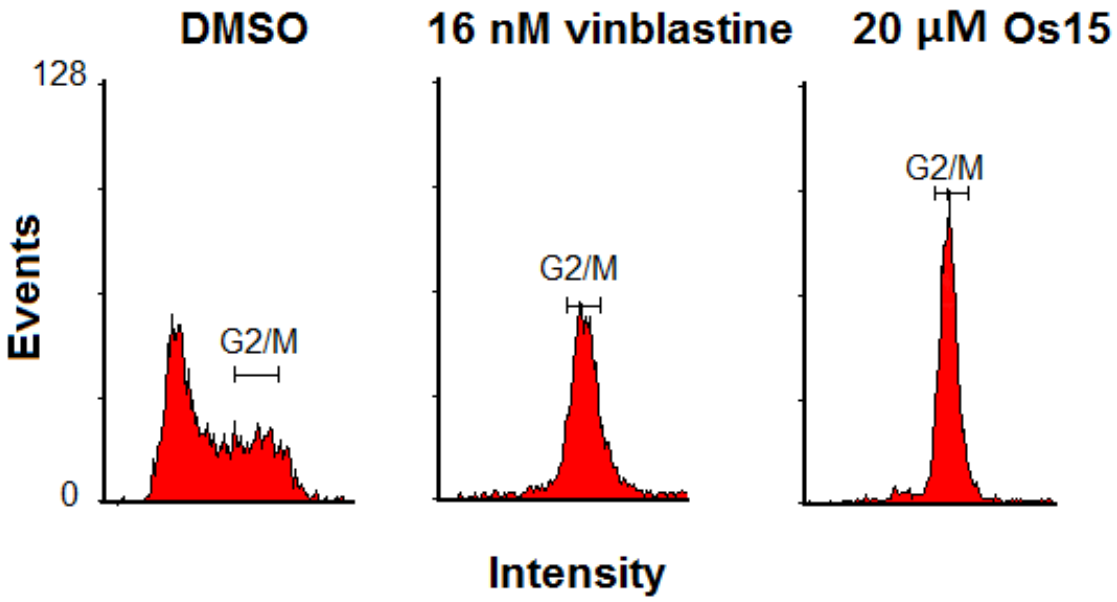

Figure 2.5: Treatment of HCT116 cells with Os15 results in G2/M cell cycle arrest.

Cells were treated with vehicle (DMSO), vinblastine (16 nM), or Os15 (20 µM). Treatment concentrations of vinblastine and Os15 were the concentrations at which 100% growth inhibition was observed. Os15 caused G2/M cell cycle arrest as compared to the untreated control and treatment with vinblastine.

library of 120 compounds identified a number of compounds that inhibited more than 80% of cell growth for both cancer cell lines tested. Some of these specifically inhibited growth of HCT116 cells (Figure 2.4). Several of the most potent growth inhibitors were further profiled for their effect on the cell cycle.

2.3.2 One alkaloid identified from screening causes G2/M phase arrest.

Several indole alkaloids that showed significant growth inhibition of both HCT116 cells and MCF7 cells were examined for their effects on the cell cycle using fluorescence-activated cell sorting (FACS). Cells were passaged into 6-well plates and allowed to attach overnight. Attached cells were then treated with the concentration of indole alkaloid at which no observable growth was seen (the GI_{90}). Cells were incubated with compound for 24 hours followed by DNA staining with propidium iodide (PI) and FACS cell cycle analysis. Vinblastine was included as a positive control. Intriguingly, cells treated with compound Os15 showed a cellular DNA content profile indicating that the compound causes G2/M phase cell cycle arrest similarly to vinblastine (Figure 2.5).[24] These results indicate that the activity of Os15 causes G2/M phase arrest in rapidly dividing cells. This type of growth inhibition is very useful in the treatment of many cancers and is the mechanism of action of the vinca alkaloids (including vinblastine and vincristine) as well as Taxol.[24,25] Future follow-up on these results could include analysis of the effect of compound Os15 on tubulin polymerization and somatic cell toxicity tests.

2.3.3 Bacterial growth inhibition screen.

In order to assess the range of activity of our library against bacterial growth and proliferation, an initial viability screen was performed. We selected a representative Gram-positive species (*S. aureus*) and a Gram-negative species (*E. coli*) for our initial screen to assess general growth inhibition by Gram class. The strains *Staphylococcus aureus* ATCC 25923 and *Escherichia coli* ATCC 25922 were selected since they are commonly used antibiotic susceptibility reference strains.[26] The effect of alkaloids on cell viability was assessed by diluting an overnight bacterial culture 200,000-fold into plates containing a screening concentration of each alkaloid (20 µM). Viability was assessed after 5 hours of growth using the BacTiter-Glo™ Microbial Cell Viability Assay according to the manufacturer's instructions (www.promega.com).

2.3.4 One indoline identified from the bacterial growth inhibition screen proved interesting as an antibiotic lead compound.[e]

Although there were not many compounds with desirable growth inhibitory effects against our Gram-negative model (*E.* coli ATCC 25922), we were encouraged by two compounds that showed reasonable antibacterial activity against our Gram-positive model, *S. aureus* 25923. The compound showing the greatest and most specific growth inhibition of *S. aureus* in the initial screen and little inhibitory activity against mammalian cells, known as Of4 (Figure 2.6), was further evaluated for its minimum inhibitory concentrations (MICs) against MSSA 25923 and MRSA BAA-44.[27,28] The MIC value for both MSSA and MRSA was 32 µg/ml. Notably, the MRSA strain, BAA-44, is a multi-drug resistant strain and is resistant to a wide variety of antibiotics. The observation that the

[e] Synthesis and SAR investigations of Of4 were carried out by Patrick Barbour.

MIC of Of4 in both MSSA 25923 (a strain with no notable resistance phenotypes) and MRSA BAA-44 indicates that it exerts its antimicrobial effect via a mechanism that is distinct from any of the antibiotics to which BAA-44 harbors resistance.

An initial structure-activity relationship (SAR) study of Of4 was undertaken by synthesizing a number of analogs in which the halogen on the aromatic indoline ring, the modification on the indoline nitrogen, as well as the side chain were modified. Through this SAR strategy, a more active analog of Of4 was identified, known as **4k** (Figure 2.6). **4k** differs from Of4 by replacement of tri-fluoro acetic acid (TFA) on the sidechain with benzyloxycarbonyl, and a reduction of the sidechain length by one carbon. This analog afforded an 8-fold increase in antibiotic activity against MSSA. The MIC of **4k** was also determined for three other MRSA strains with unique resistance profiles. The MIC in each of these strains was consistent at 4 µg/ml. These results indicate that Of4 and **4k** are exerting their antibiotic effects via a general mechanism that is present in a variety of *S. aureus* stains. Further profiling of **4k** against other bacterial species will indicate whether it acts via a mechanism that is conserved amongst all or most bacteria. Furthermore, profiling of **4k** against members of the antibiotic resistant ESKAPE (*Enterococci, Staphylococcus, Klebsiella, Acinetobacter, Pseudomonas, and Escherichia*) pathogens will be very informative as to whether or not Of4/**4k** exert their effects via an entirely unique mechanism.

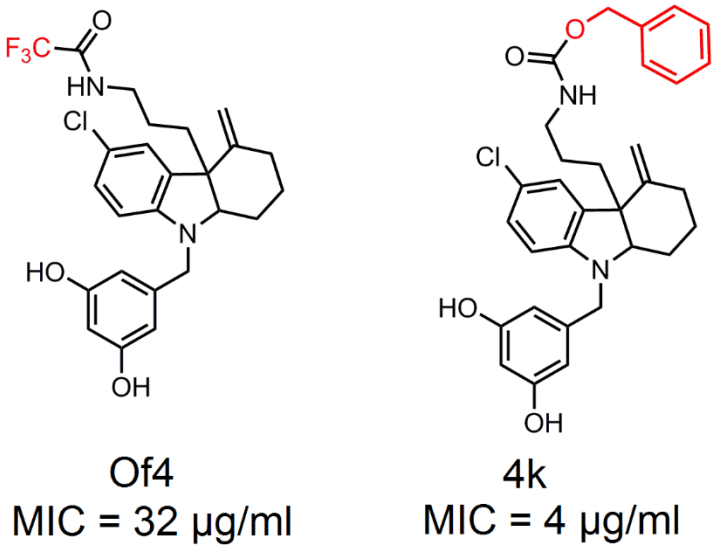

Figure 2.6: Structures of Of4 and 4k.

Of4 was identified by growth inhibition screening of the indole alkaloid library against *S. aureus* (ATCC25923). The MIC of Of4 in MSSA and a multidrug-resistant MRSA strain (ATCC BAA-44) is 32 µg/ml. The slight modification of Of4 to 4k (replacement of TFA with a benzyloxycarbonyl group) affords an 8-fold improvement in the MIC against both strains (4 µg/ml).

2.4 Summary of results and conclusion.

Initial screens involving the natural-product-like library of indole alkaloids have revealed that the library is highly bioactive and that the 26 unique skeletons as well as side chain and ring-opening, reduction or alkylation modifications provide sufficient diversity to afford a wide range of biological activities. As illustrated by the heat map of our initial biological screening results, there are a number of compounds that have cell-line or species specificity. Already, this investigation has afforded at least one compound capable of causing G2/M-phase cell cycle arrest, a well-known mechanism of currently used cancer therapeutics. Further insight into this compound's mechanism of action could potentially reveal its utility as an alternative cancer therapeutic or back

up for vinca alkaloid-resistant cancers. Os15 could also give insight into a novel mechanism by which to achieve G2/M-phase arrest in rapidly dividing cells. Furthermore, these initial screening efforts have already afforded a potentially novel antibiotic that is capable of exerting its effects in both multi-drug resistant MRSA as well as MSSA. SAR investigations of this compound afforded an analog with 8-fold improved antibacterial activity in multiple strains of MRSA with different antibiotic resistance profiles. Going forward, we will continue to screen our natural-product-like library of indoline compounds in a variety of cell-based and biochemical screens. In addition, further expansion of the library using similar synthetic strategies will result in a highly diverse, and efficiently synthesized library of compounds that is well suited for biological screening efforts.

2.6 Materials and methods

2.6.1 Mammalian cell culture

All cells were acquired from the American Type Culture Collection (ATCC) and were maintained at 37 °C in Dulbecco's modified Eagle's medium (DMEM) supplemented with 10% fetal calf serum (FCS), 1% penicillin/streptomycin, and maintained at 37°C and 5% CO_2.

2.6.2 Cell viability screens

White, flat-bottom, 384-well plates (Corning 3570) were used for all screens. For mammalian cell screening, cells were prepared from a preparative cell culture by trypsin separation of cells from the flask followed by concentration by centrifugation and cell

count determination (using a hemocytometer). Cells were plated into the 384-well plates at a density of 5000 cells per well in Dulbecco's modified Eagle's medium (DMEM) supplemented with 10% fetal calf serum (FCS), 1% penicillin/streptomycin. Cells were allowed to attach overnight. Compounds were added to the plates using the CyBio pintool from a 4 mM 96-well source plate to a final concentration of 20 µM. Cells were incubated for 48 hours and viability assessed using the CellTiter-Glo™ Mammalian Cell Viability Assay (Promega).

For bacterial growth inhibition screens, plates were prepared by the addition of 35 µl of MHB using a BioTek MicroFlo select reagent dispenser. Compounds, from a 4 mM 96-well source plate, were then pinned into each well of the 384-well plate using the CiBy pin-tool from CyBio. Next, an overnight culture of MSSA ATCC 25923 was diluted 25,000-fold and 5 µl of this dilution was added to each well of the 384-well plate. The final concentration of alkaloids used in the screen was 20 µM, and the final dilution of bacteria inoculated was 1:100,000. Compounds were screened in quadruplicate. Plates were incubated at 37°C with shaking for 5 hours and the BacTiter-Glo™ Microbial Cell Viability Assay was performed according to the manufacturer's instructions.

2.6.3 GI_{50} and GI_{90} determination.

Cell viability assays were carried out using CellTiter-Glo luminescent cell viability assay kit (Promega). Cells were seeded (20,000 cells/well) on white, cell-culture treated 96-well plates (Corning: 3917) with Dulbecco's modified Eagle's medium (DMEM) supplemented with 10% fetal calf serum (FCS), 1% penicillin/streptomycin. The final volume of media in each well was 100 µL. Cells were incubated at 37 °C in 5% CO_2/95% air for 16 hours. The medium was removed from each well and replaced with

99 µL of warmed fresh medium. To each well 1 µL of compound in DMSO was added to achieve final concentrations of 0.5-32 µg/mL. Each dose was performed in triplicate. After incubation at 37 °C for another 24 hours, the plates were equilibrated to room temperature for 30 minutes. Next, 100 µL of CellTiter-Glo reagent (Promega) was added to each well and mixed for 2 minutes on an orbital shaker. The plate was incubated at room temperature for another 10 minutes to stabilize the luminescence signal. The luminescence of each sample was recorded in an Envision Multilabel Plate Reader (Perkin Elmer), and normalized to positive and negative controls (ellipticine and DMSO, respectively). The data were fit using KaleidaGraph software and the GI_{50} and GI_{90} values were determined as the concentrations at which 50 and 90% of growth was inhibited.

2.6.4 Propidium iodide staining and FACS cell cycle analysis.

HCT116 cells were grown under standard conditions and supplemented with vehicle (1% DMSO), vinblastine (16 nM) or compound Os15 (20 µM) for 24 hours. Cell density was determined by hemocytometer-assisted counting. Cells were harvested by centrifuging for 2 minutes at 1000 rpm. Cells were fixed in ice-cold 70% ethanol by adding the solution drop-wise to the cell pellet and vortexing. Cells were then incubated for 30 minutes at 4°C. Cells were washed in PBS and 200 µl of a 50 µg/ml propidium iodide stock was added to the cell pellet to stain DNA. Total DNA content was obtained and analyzed using a Becton Dickenson FACScan flow cytometer and the FACScan software.

2.6.5 Broth microdilution minimum inhibitory concentration (MIC) testing.

Alkaloids were prepared in 96-well microplates (USA Scientific CytoOne 96-well TC plate, cat: CC7682-7596) at twice the intended final concentration and two-fold serial dilutions were performed down the columns of the plate to afford a suitable concentration range. The inoculum was prepared by diluting a bacterial day culture (OD_{600} 0.150-0.4) to OD_{600} 0.002. This dilution was further diluted two-fold when added to 96 well microplates for a final inoculum concentration of OD_{600} 0.001. All plates were incubated at 37°C with shaking for overnight (18 hours) and results were interpreted. The MIC was defined as the lowest concentration at which no observable growth was present.

2.7 References

1. Verpoorte, R. Exploration of nature's chemodiversity: the role of secondary metabolites as leads in drug development. *Drug Discov. Today* **3,** 232–238 (1998).

2. Peng, W. *et al.* Areca catechu L. (Arecaceae): A review of its traditional uses, botany, phytochemistry, pharmacology and toxicology. *J. Ethnopharmacol.* (2015). doi:10.1016/j.jep.2015.02.010

3. Yvette Fofie, N., Sanogo, R., Coulibaly, K. & Kone Bamba, D. Minerals salt composition and secondary metabolites of Euphorbia hirta Linn., an antihyperglycemic plant. *Pharmacognosy Res.* **7,** 7 (2015).

4. Ban, Y., Murakami, Y., Iwasawa, Y., Tsuchiya, M. & Takano, N. Indole alkaloids in medicine. *Med. Res. Rev.* **8,** 231–308

5. Halberstadt, A. L. & Geyer, M. A. Multiple receptors contribute to the behavioral effects of indoleamine hallucinogens. *Neuropharmacology* **61,** 364–381 (2011).

6. Dias, D. a., Urban, S. & Roessner, U. A Historical Overview of Natural Products in Drug Discovery. *Metabolites* **2,** 303–336 (2012).

7. Littleton, J., Rogers, T. & Falcone, D. Novel approaches to plant drug discovery based on high throughput pharmacological screening and genetic manipulation. *Life Sci.* **78,** 467–75 (2005).

8. Meseguer, B., Alonso-Díaz, D., Griebenow, N., Herget, T. & Waldmann, H. Natural Product Synthesis on Polymeric Supports-Synthesis and Biological Evaluation of an Indolactam Library. *Angew. Chem. Int. Ed. Engl.* **38,** 2902–2906 (1999).

9. Lo, M. M. C., Neumann, C. S., Nagayama, S., Perlstein, E. O. & Schreiber, S. L. A library of spirooxindoles based on a stereoselective three-component coupling reaction. *J. Am. Chem. Soc.* **126,** 16077–16086 (2004).

10. Nielsen, T. E. & Schreiber, S. L. Towards the optimal screening collection: A synthesis strategy. *Angew. Chemie - Int. Ed.* **47,** 48–56 (2008).

11. Rodriguez, R. in *Mod. Tools Synth. Complex Bioact. Mol.* 513–518 (2012). doi:10.1002/9781118342886.ch15

12. Lipinski, C. A., Lombardo, F., Dominy, B. W. & Feeney, P. J. Experimental and computational approaches to estimate solubility and permeability in drug discovery and development settings. **46,** 3–26 (2001).

13. Overington, J. P., Al-Lazikani, B. & Hopkins, A. L. How many drug targets are there? *Nat. Rev. Drug Discov.* **5,** 993–996 (2006).

14. Payne, D. J., Gwynn, M. N., Holmes, D. J. & Pompliano, D. L. Drugs for bad bugs: confronting the challenges of antibacterial discovery. *Nat. Rev. Drug Discov.* **6,** 29–40 (2007).

15. Leeds, J. A., Schmitt, E. K. & Krastel, P. Recent developments in antibacterial drug discovery: microbe-derived natural products--from collection to the clinic. *Expert Opin. Investig. Drugs* **15,** 211–226 (2006).

16. Dobson, C. M. Chemical space and biology. *Nature* **432,** 824–828 (2004).

17. O'Shea, R. & Moser, H. E. Physicochemical properties of antibacterial compounds: Implications for drug discovery. *J. Med. Chem.* **51,** 2871–2878 (2008).

18. Austin, M. B., O'Maille, P. E. & Noel, J. P. Evolving biosynthetic tangos negotiate mechanistic landscapes. *Nat. Chem. Biol.* **4,** 217–222 (2008).

19. DeLuca, V. *et al.* Biosynthesis of Indole Alkaloids: Developmental Regulation of the Biosynthetic Pathway from Tabersonine to Vindoline in Catharanthus roseus. *J. Plant Physiol.* **125,** 147–156 (1986).

20. Yeo, S. J., Liu, Y. & Wang, X. A one-pot three-component reaction for the preparation of highly functionalized tryptamines. *Tetrahedron* **68,** 813–818 (2012).

21. Liu, Y., Xu, W. & Wang, X. Gold(I)-catalyzed tandem cyclization approach to tetracyclic indolines. *Org. Lett.* **12,** 1448–51 (2010).

22. Kutchan, T. Alkaloid Biosynthesis -- The Basis for Metabolic Engineering of Medicinal Plants. *Plant Cell* **7,** 1059–1070 (1995).

23. Tanaka, J. C. A., da Silva, C. C., de Oliveira, A. J. B., Nakamura, C. V. & Dias Filho, B. P. Antibacterial activity of indole alkaloids from Aspidosperma ramiflorum. *Brazilian J. Med. Biol. Res.* **39,** 387–391 (2006).

24. Jordan, M. A., Thrower, D. & Wilson, L. Mechanism of Inhibition of Cell Proliferation by Vinca Alkaloids. *Cancer Res.* **51,** 2212–2222 (1991).

25. Horwitz, S. B. *et al.* Taxol: mechanisms of action and resistance. *Ann. N. Y. Acad. Sci.* **466,** 733–744 (1986).

26. CLSI. *Performance Standards for Antimicrobial Susceptibility Testing ; Seventeenth Informational Supplement*. **27,** (2007).

27. CLSI. *Methods for Dilution Antimicrobial Susceptibility Tests for Bacteria That Grow Aerobically ; Approved Standard — Eighth Edition*. **29,** (2009).

28. Michael Barbour, P., Podoll, J. D., Marholz, L. J. & Wang, X. Discovery and initial structure–activity relationships of N-benzyl tricyclic indolines as antibacterials for methicillin-resistant Staphylococcus aureus. *Bioorg. Med. Chem. Lett.* **24,** 5602–5605 (2014).

Chapter 3 : Discovery and profiling of resistance-modifying agents (RMAs) identified from the indole alkaloid screening library

3.1 Introduction

3.1.1 Antibiotic discovery: a historical perspective

The vast majority of antibiotic classes were discovered during the “golden era” of antibiotic discovery spanning the 1940s through the 1960s.[1,2] Although one of the foremost antibiotics, penicillin, was discovered serendipitously, there are notable examples of highly systematic screening approaches that were introduced to further antibiotic discovery. These were developed by Paul Ehrlich and Selman Waksman and adopted widely in the pharmaceutical industry to unearth the vast majority of antibiotics

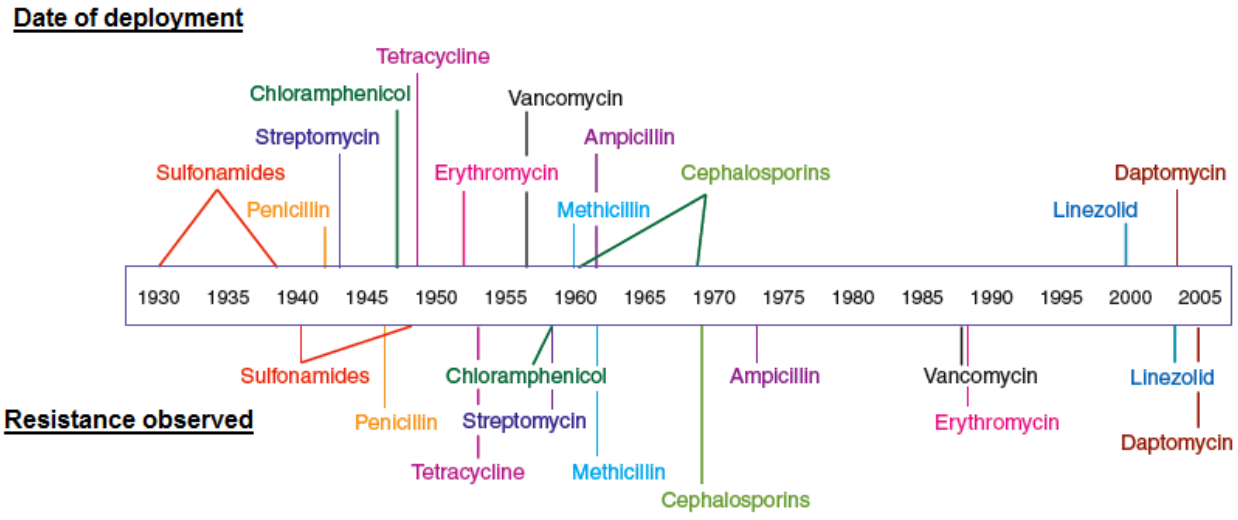

Figure 3.1: Timeline of antibiotic deployment and observed resistance.

The approximate date of deployment is on the top of the timeline, and the date of observed resistance on the bottom. Clearly, antibiotic resistance has been observed for all antibiotics in use. In addition, our ability to develop novel antibiotics has slowed. Adapted from Clatworthy et al.(2007).[5]

known today.[3,4] The “Waksman platform” involved taking advantage of natural biological warfare: Streptomyces isolated from soil samples were screened for their antimicrobial activity by assessing zones of inhibition on agar plates. The active compounds were then identified and isolated. The isolated, purified active components are used clinically today as antibiotics.

After twenty years of success, however, the Waksman platform stopped producing novel hits, forcing the pharmaceutical industry to begin investigating new approaches including HTS of compounds against whole cells, as well as genetically identified essential proteins.[4] Despite these efforts, only two novel antibiotic classes have seen clinical use, oxazolidinones and lipopeptides (Figure 3.1).[5] Paradoxically, the increase in screening and assay technology has not been accompanied by an increase in antibiotic discovery.[6,7] Although this is concerning from a general drug-discovery perspective, the issue requires immediate attention due to the rapid development of antibiotic resistance among pathogenic microorganisms.

3.1.2 Antibiotic resistance: an ongoing worldwide health concern

Antibiotics generally function by targeting essential cellular processes, and either induce cell death (bactericidal), or arrest growth (bacteriostatic). The major processes targeted by antibiotics include DNA replication, transcription of DNA to RNA, translation of RNA to protein, cell wall synthesis, or other metabolic processes (Figure 3.2a). Antibiotic resistance is largely driven by targeting these essential processes, which supplies the selective pressure necessary for antibiotic resistance development either through gene mutation or via acquisition of extracellular DNA expressing resistance determinants (Figure 3.2b).[8]

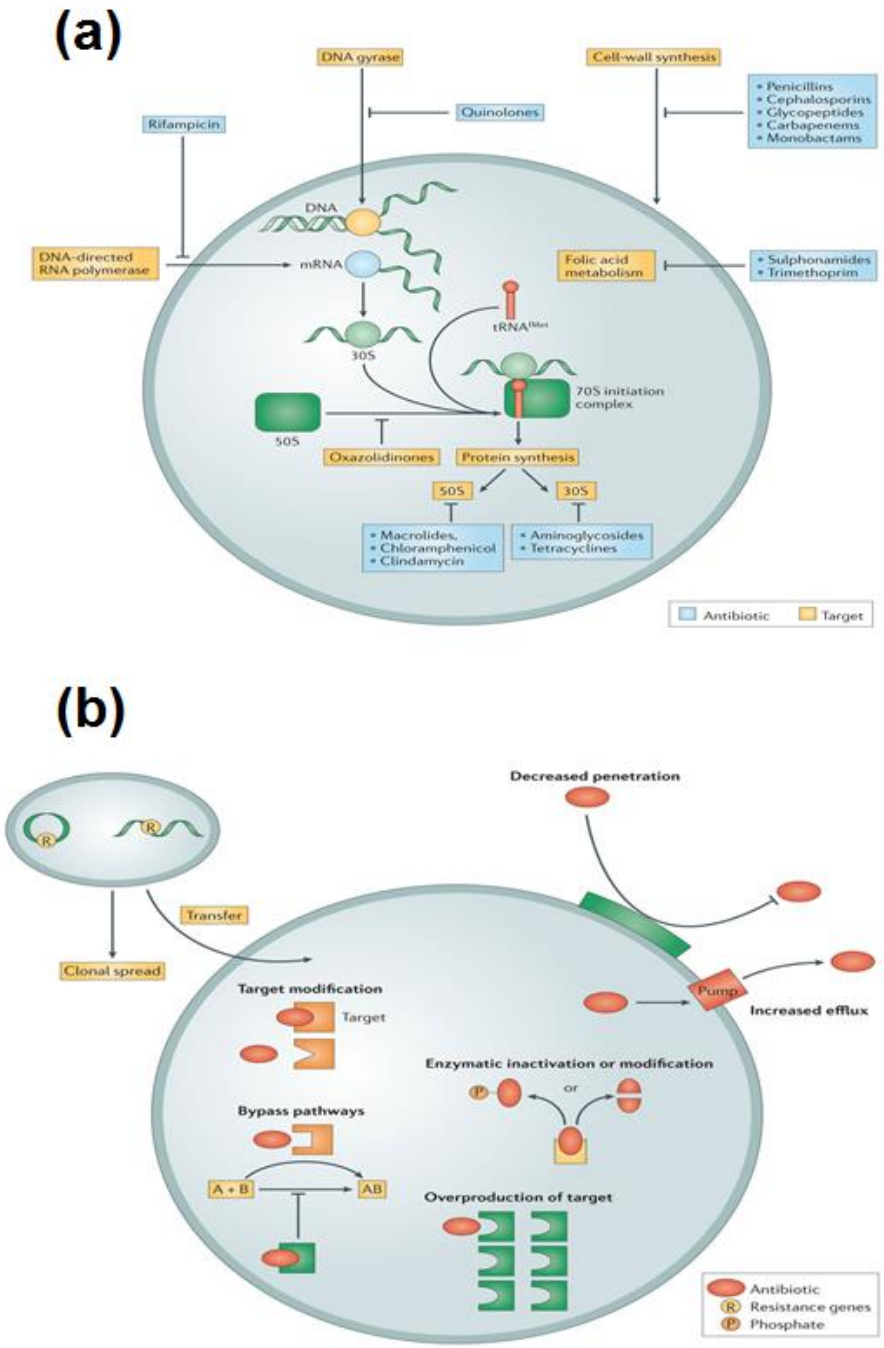

Figure 3.2: Common antibiotic targets and mechanisms of resistance.

(a) Although there are over 200 known essential bacterial genes, the vast majority of successful antibiotics only target a few essential pathways. (b) The rise of antibiotic resistance driven by a few general mechanisms, some of which require acquisition of resistance genes from external sources. The mechanisms of resistance include modification of the antibiotic target or complete bypass of the pathway targeted by the antibiotic, enzymatic inactivation of the antibiotic, efflux of the antibiotic, or modification of the cell to exclude entry of the antibiotic. This figure was adapted from Lewis (2013).[2]

Antibiotic resistance is an urgent world health concern that is aggravated by a lack of novel antibiotic discovery.[7] Although development of antibiotic analogs had previously kept resistant pathogens at bay, the rapid onset of antibiotic resistance has now created a situation where there are not enough analogs in the antibiotic pipeline to combat imminent resistance emergence.[6] Methicillin-resistant *Staphylococcus aureus* (MRSA) is particularly concerning in this regard. Prior to the introduction of penicillin in the 1940s, the mortality of patients who developed invasive *Staphylococcus* infections was nearly 80%, but this statistic was drastically reduced by the introduction of penicillin in the clinic.[9] In just a few years, however, resistance to penicillin mediated by β-lactamase emerged, which led to the introduction of β-lactam antibiotics such as methicillin, which are resistant to degradation by β-lactamase. It was not long, however, before *Staphylococcus aureus* developed methicillin resistance in the form of an alternative penicillin binding protein (PBP), PBP2a, which binds poorly to β-lactams and can therefore catalyze peptidoglycan crosslinking in their presence.[10] In addition to methicillin resistance, a number of MRSA strains have developed resistant phenotypes against multiple drugs used in the clinic, thus limiting treatment options for bacterial infections and threatening the onset of a post-antibiotic era.[11] Of the estimated 2,000,000 illnesses and 23,000 deaths in 2013 that are directly associated with antibiotic resistant bacteria in the United States, MRSA was directly responsible for 80,000 illnesses and 11,000 deaths.[12] Although vancomycin as well as some antibiotic analogs are still effective for the treatment of MRSA, strains that are resistant to these last-line-of-defense treatments have already become a problem.[13]

Along with novel cures to many formerly fatal diseases, the antibiotic era also allowed for the overuse and misuse of antibiotics in agriculture as well as clinical settings, according to the CDC.[12] Compounding the issue further, in conjunction with the emergence of an array of antibiotics, pathogenic microorganisms began responding to the added selective pressure by evolving or acquiring modes of resistance. Although in many instances, modification or functionalization of antibiotic cores afforded antibiotic analogs capable of circumventing the resistance mechanisms, microbes continue to acquire and evolve mechanisms that are rendering them resistant to more and more antibiotics in clinical use.

3.1.3 Resistance-modifying agents offer an alternative approach to conventional antibiotics.

Resistance-modifying agents (RMAs) offer a promising solution to the global antibiotic resistance crisis.[14] These target non-essential resistance-conferring genes and gene products to restore antibiotic sensitivity. A notable advantage of RMAs is that they are capable of extending the usable lifespan of known antibiotics that have already been optimized for large-scale production and that have well-studied toxicity profiles. For example, clavulanic acid is a serine β-lactamase inhibitor that is commonly used in combination with amoxicillin under the brand name Augmentin, among others, to treat infections resulting from β-lactamase-producing bacteria.[15] Clavulanic acid deactivates β-lactamase by irreversibly acylating the catalytic serine residue in the active site of the β-lactamase enzyme that would otherwise function to breakdown the β-lactam antibiotic. Although the clavulanic acid/β-lactam combination is effective for serine β-lactamases, it is ineffective against metallo-β-lactamases and does nothing to combat β-

lactam resistance mediated by the alternative penicillin-binding-protein, PBP2a, encoded in MRSA.[16] Although efforts have been underway to discover more novel RMAs, thus far, only those that are β-lactamase inhibitors have been successfully brought to market. β-lactam antibiotics are one of the most widely used antibiotics and have inspired numerous research efforts to overcome bacterial resistance. In addition to β-lactamase inhibitors, other classes of compounds have been reported to potentiate the activity of β-lactam antibiotics, such as compounds interfering bacterial cell wall synthesis and compounds affecting resistance-sensing pathways.[17–20]

Given the need for novel approaches to antibiotic discovery, we undertook an effort to seek out compounds with the capacity to potentiate a variety of antibiotics. RMA screens for three antibiotics (methicillin, tetracycline, and vancomycin) were carried out using our indole alkaloid library. As the library expands, we intend to expand this screening to include more antibiotic classes and a variety of microbial species.

3.2 RMA screening efforts.

Screening for RMAs was performed using a modified broth microdilution assay, and our previously synthesized library of natural-product-like indole alkaloids.[21,22] First, minimum inhibitory concentrations were established for each antibiotic in a resistant species. Most commonly, the multi-drug resistant MRSA strain ATCC BAA-44 was used, as it possesses resistance to a variety of commonly used antibiotic classes. Vancomycin RMA screens were carried out using a vancomycin-resistant *S. aureus* strain (VRSA) NR-46421 (a.k.a., VRS11a, BEI Resources).

3.2.1 Screening for compounds capable of modulating methicillin, tetracycline, and vancomycin resistance in *S. aureus*.

The indole alkaloid library was screened for the ability to potentiate the activity of methicillin and tetracycline in MRSA ATCC BAA-44, and vancomycin in vancomycin-resistant *S. aureus* (VRSA) NR-46421 (a.k.a., VRS11a, BEI Resources), since BAA-44 does not possess the vancomycin resistance phenotype. First, the minimum inhibitory concentration (MIC) of each antibiotic in the corresponding *S. aureus* strain was assessed and determined to be 128 µg/mL (methicillin, BAA-44), 64 µg/mL (tetracycline, BAA-44), and 512 µg/mL (vancomycin, NR 46421). This was determined using the standard Clinical Laboratory Standards Institute (CLSI) broth microdilution method.[36] For each screen, Mueller Hinton Broth (MHB) was supplemented with methicillin at ¼ of its MIC value (i.e., 32 µg/mL), or vancomycin or tetracycline at 1/8 of its MIC value (i.e. 64 and 16 µg/mL, respectively). To each well, 20 µM of each individual indoline alkaloid was added and the plates were incubated at 37 ^{o}C for 18 hours.

Nine indoline alkaloids were identified that reduced the MIC of methicillin in BAA-44 to 32 µg/mL or lower, representing an 8% hit rate for this screen. Furthermore, one compound was identified that was capable of reducing the MIC of tetracycline in BAA-44 and two compounds were identified that were capable of potentiating vancomycin in VRSA (NR-46421). One compound (Kf18) was a hit compound in the methicillin screen as well as the vancomycin screen. Further evaluation of Kf18 showed that it had no antiproliferative effect on its own (MIC > 128 µg/mL). Furthermore, in addition to its potentiating effect in MRSA and VRSA, Kf18 also potentiates vancomycin in vancomycin-resistant *E. faecium* (VRE) HM-968 (a.k.a., ERV102, BEI Resources). VRE

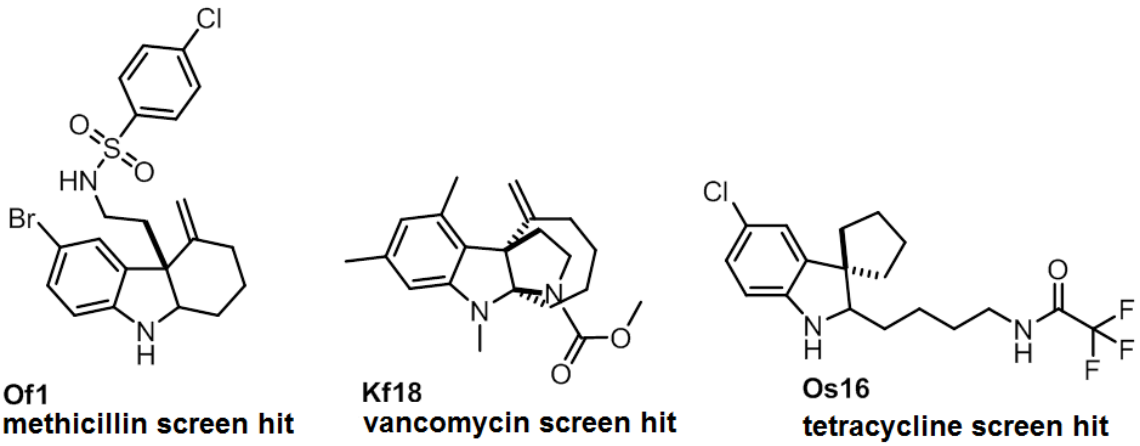

Figure 3.3: Hit compounds from RMA screening efforts.

Of1 was identified from a screen for compounds capable of potentiating methicillin in MRSA ATCC BAA-44 and Os16 was identified from a screen for compounds capable of potentiating tetracycline in the same strain. Kf18 was identified from an initial screen for compounds capable of potentiating vancomycin in a VRSA strain (NR-46421), and a counter-screen in VRE (HM-968).

HM-968 is highly resistant to vancomycin, with an MIC of 512 µg/mL, and it is known to express the *vanA* gene, the most prevalent determinant that allows the bacteria to construct alternative cell wall lacking the D-Ala-D-Ala moiety targeted by vancomycin.[23] The most potent lead resulting from each screen is illustrated in figure 3.3.

Although the remainder of this report deals solely with evaluation of hits generated from the methicillin RMA screen, follow up on the scope of activity of Kf18 as well as SAR are ongoing in the Wang lab.

3.3 Evaluation of hits generated from the β-lactam RMA screen

3.3.1 Identification of the most potent lead compound.

We further evaluated the ability of these nine compounds to potentiate methicillin by assessing the MIC of methicillin in MRSA using the standard microdilution method in medium supplemented with 20 µM of each alkaloid. Of1 (Figure 3.3) was found to be the most active compound, capable of reducing the MIC of methicillin from 128 to 8 µg/mL. Hence, Of1 re-sensitizes this multi-drug resistant MRSA strain to methicillin, since *S. aureus* with an MIC ≤8 µg/mL is defined as methicillin-sensitive.

3.4 Characterization of Of1 as a β-lactam selective RMA and toxicity evaluation.

3.4.1 Evaluation of the RMA scope of Of1.f

We evaluated the ability of OF11 to potentiate other antibiotics in MRSA by determining their MIC values in the presence and absence of 20 μM Of1. In addition to methicillin, we tested other β-lactam antibiotics, such as oxacillin (i.e., the replacement of methicillin, a narrow spectrum antibiotic), amoxicillin/clavulanic acid (amox/clav, an extended spectrum antibiotic), cephalexin and cefazolin (first-generation cephalosporins), and meropenem and imipenem (carbapenems). Antibiotics from other structural classes tested include streptomycin (aminoglycoside), rifampicin (ansamycin), tetracycline (tetracycline), ciprofloxacin (quinolone), erythromycin and azithromycin (macrolides), clindamycin (lincosamide), vancomycin (glycopeptide), and linezolid (oxazolidinone).

The results showed that Of1 potentiates all β-lactam antibiotics with variable fold of potentiation (Table 3.1). Although this MRSA strain is not resistant to carbapenems such as imipenem and meropenem, Of1 still showed 8- and 16-fold potentiation of these, respectively. In addition, Of1 showed weak potentiation of rifampicin (2-fold), but did not potentiate any other classes of antibiotics, such as ciprofloxacin, tetracycline, vancomycin and linezolid. It should be noted that MRSA ATCC BAA-44 is highly resistant to azithromycin, erythromycin, streptomycin, and clindamycin; 20 μM of Of1 was unable to lower their MICs to 256 μg/mL, the highest concentration tested.

[f] The investigation of the scope of Of1 was carried out with assistance from Shane Walls

Table 3.1: Of1 selectively potentiates β-lactam antibiotics in multi-drug resistant MRSA.

Compound	MIC (μg/mL)	MIC (+Of1)[a] (μg/mL)	fold opotentiation	sensitive range[b] (μg/mL)
Of1	>128	-	-	-
methicillin	128	8	16	≤8
oxacillin	64	0.5	128	≤2
amox/clav	32/16	4/2	8	≤4/2
meropenem	4	0.25	16	≤4
imipenem	8	1	8	≤4
cephalexin	256	16	16	≤8
cefazolin	128	4	32	≤8
rifampicin	2	1	2	≤1
tetracycline	64	64	1	≤4
ciprofloxacin	8	8	1	≤1
azithromycin	>256	>256	-	≤2
erythromycin	>256	>256	-	≤0.5
clindamycin	>256	>256	-	≤0.5
streptomycin	>256	>256	-	-
vancomycin	1	1	1	≤2
linezolid	2	2	1	≤4

[a]MIC value in the presence of 20 μM Of1; [b]values obtained from Clinical Laboratory Standards Institute (CLSI) Performance Standards for Antimicrobial Testing; 17th informational supplement.

Furthermore, we evaluated Of1's potentiation effect for β-lactam antibiotics in a methicillin-sensitive *S. aureus* (MSSA) strain (ATCC: 25923). Surprisingly, we found Of1 does not potentiate any β-lactams tested, such as methicillin, amox/clav, and cefazolin (Table 3.2). In addition the ability of Of1 to potentiate β-lactams in a resistant *Enterococcus faecium* strain (HM-968, BEI resources) was tested. We found that Of1 did indeed potentiate amoxicillin at least 4-fold.

3.4.2 Evaluation of the anti-proliferative activity of Of1 in MRSA and MSSA.

To evaluate the anti-proliferative activity of Of1 alone, we performed the standard microdilution assay for Of1 using both MRSA (ATCC: BAA-44) and MSSA (ATCC: 25923) strains. The MICs of Of1 against both strains were found to be higher than 128 μg/mL, the highest concentration tested. Considering the effective concentration (20 μM or approximately 10 μg/mL) required to re-sensitize MRSA to methicillin, this result suggests that Of1 has a synergistic effect with methicillin, but does not itself target any essential genes or gene products.

Table 3.2: MIC values of Of1 or β-lactam antibiotics in the presence or absence of Of1 in MSSA ATCC 25923.

β-lactams	MIC (μg/ml)	MIC + 20 μM Of1 (μg/ml)
Of1	>128	-
methicillin	4	4
oxacillin	0.5	0.5
amox/clav	0.125/ 0.0625	0.125/ 0.0625
cephalexin	4	4
cefazolin	0.5	0.5

3.4.3 Determination of Of1's minimum re-sensitizing concentrations (MRCs) for MRSA.

Next we determined Of1's MRC for MRSA with three common β-lactam antibiotics: oxacillin, amox/clavulanic acid and cefazolin. A modified broth microdilution assay was used. This involves incubating MRSA with Of1 in 2-fold series dilution in the presence of each individual antibiotic at its highest sensitive concentration (i.e., 2, 4/2, and 8 μg/mL, respectively) as determined by the clinical and laboratory standards institute (CLSI).[22] As shown in table 3.3, Of1 re-sensitizes BAA-44 to all three antibiotics, and the MRC of Of1 is dependent on the antibiotic used. We have also determined the MRC values for another three MRSA strains. Strain 33592 (ATCC) behaves similarly to BAA-44, and the MRC for all three antibiotics are 4 μg/mL. BAA-1683 is not resistant to cefazolin, but is resistant to both oxacillin and amox/clav. The MRC for oxacillin is found to be >32 μg/mL (the highest concentration tested), and the

Table 3.3: Of1's minimum re-sensitizing concentrations (MRCs) for MRSA strains.[a]

β-Lactams	BAA-44	33592	700789	BAA-1683
oxacillin	2	4	>32	>32
amox/clav	4	4	4	4
cefazolin	4	4	-[b]	-[b]

[a]All MIC values are in μg/mL; all MRSA strain names are ATCC numbers; [b]this strain is not resistant to the antibiotic indicated.

MRC for amox/clav is 4 µg/mL, similar to the other two strains. Strain 700789 (ATCC) is particularly interesting, because it is known to possess intermediate resistance to vancomycin, and is therefore a vancomycin-intermediate-resistant *S. aureus* (VISA). Our results showed that Of1 is able to re-sensitize this VISA strain to amox/clav at 4 µg/mL.

3.4.4 Mammalian cytotoxicity of Of1.[g]

To evaluate the cytotoxicity of Of1 in mammalian cells, we treated human liver hepatocellular carcinoma HepG2 cells with Of1 at various concentrations for 24 hours. The remaining viable cells were determined using the CellTiter-Glo™ mammalian viability assay (Promega). Of1 showed weak inhibition (ca. 10%) of the growth of

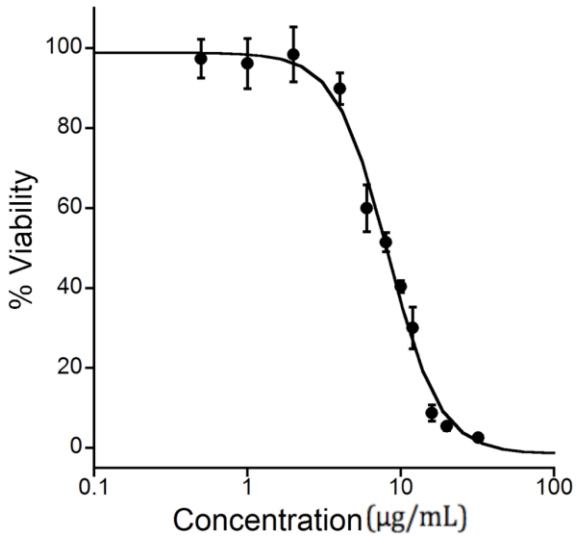

Figure 3.4: Growth inhibition of HepG2 cells by Of1.

Of1 showed weak growth inhibition at its minimum re-sensitizing concentration for MRSA.

[g] Toxicity of Of1 in mammalian cells was evaluated by Dr. Wei Wang

HepG2 cells at 4 μg/mL, its MRCs for all MRSA strains to amox/clav or cefazolin. The half growth inhibitory concentration (GI_{50}) of Of1 in HepG2 cells is determined as 8.2 μg/mL by fitting the data using KaleidaGraph (v4.1.1, Synergy Software, Figure 3.4).

3.5 Structure-activity relationship studies of Of1.[h]

3.5.1 Rationale for the structure-activity-relationship (SAR) study of Of1.

Intrigued by the unique activity of Of1, we sought to conduct a structure-activity relationship (SAR) study in order to identify regions of the Of1 structure that may be modified to improve its activity and toxicity profile. Of1 has been identified as an RMA for β-lactam antibiotics in MRSA. However, it did show some toxicity against mammalian cells. Furthermore, although our initial evaluations of Of1 have clearly demonstrated its activity, these did not indicate which regions of the molecule are necessary to maintain its activity in cells. The knowledge gleaned from an SAR study would reveal regions of Of1 that are functionally significant and would furthermore reveal regions that may be modified to afford functional probes such as a fluorescent analog for localization investigations as well as a biotin-conjugated probe that could potentially be immobilized and used in pull-down experiments.

3.5.2 Functional assays to assess the activities and cytotoxicity of Of1 analogs.[i]

In order to conduct an SAR investigation of Of1, several series of Of1 analogs were synthesized. These were then evaluated for their ability to re-sensitize MRSA to a collection of β-lactam antibiotics including amoxicillin in combination with clavulanic acid

[h] Analogs of Of1 were synthesized by Dr. Le Chang
[i] Cytotoxicity evaluation was carried out by Dr. Wei Wang

(a.k.a., Augmentin, one of the top three most prescribed antibiotics), cefazolin (a first-generation cephalosporin), and meropenem (an ultra-broad-spectrum carbapenem). Amoxicillin/clavulanic acid and cefazolin re-sensitizing experiments were performed using MRSA ATCC BAA-44 in which the MICs of these two antibiotics were found to be 32/16 µg/mL and 128 µg/mL, respectively. Experiments using meropenem were performed using MRSA ATCC 33592, since this strain has demonstrated greater level of resistance to meropenem, with an MIC of 16 µg/mL. To assess activity of each analog as RMA, a modified broth microdilution assay was employed as described previously.[21] Briefly, this involves incubating MRSA with Of1 or each of its analogs in 2-fold serial dilution in the presence of each individual antibiotic at its Clinical Laboratory Standards Institutes (CLSI)-defined sensitive concentrations. For amoxicillin/clavulanic acid, the sensitive concentration is 4/2 µg/mL (8-fold potentiation), for cefazolin 8 µg/mL (16-fold potentiation) and for meropenem, 4 µg/mL (4-fold potentiation).[24] Following overnight incubation, plates were examined for bacterial growth, or lack thereof. Of1 analogs were tested at concentrations ranging from 0.50-32 µg/mL. The minimum re-sensitizing concentration (MRC) was defined as the concentration of Of1 analog at which no overnight growth was observed in the presence of a sensitive concentration of antibiotic. Compounds that displayed similar or improved RMA activity relative to Of1 were further tested for their toxicity against the growth of human cervical adenocarcinoma HeLa cells by incubating a range of concentrations of each compound with cells for 24 hours and assessing viability at each concentration using the CellTiter-Glo^{TM} mammalian viability assay (Promega). The half growth inhibitory concentration (GI_{50}) of each analog was determined by fitting the data using KaleidaGraph (v4.1.1, Synergy Software).

3.5.3 Of1 modification scheme.[j]

Our initial SAR investigation of Of1 was carried out by modification of the indoline and sulfonamide nitrogens, addition and/or substitution of groups around the aromatic indoline ring, and modifications of the Of1 side chain.[25] MRC data for each analog are shown in tables 3.4-3.6, which are organized by the location on the molecule at which the modification was made.

3.5.4 Notable patterns in the activity of the first series of Of1 analogs.

We first assessed the MRC activity of analogs that contained modifications to the indole nitrogen, the sulfonamide nitrogen, or both. We found that modification at either or both sites abolished RMA activity altogether and thus concluded that these nitrogens must remain un-modified (Table 3.4).

Analogs involving modifications on the aromatic indoline ring were tested next (Table 3.5). In order to test the necessity of the bromine (R_2) at the 5-position of the indoline, analogs were synthesized in which the bromine was replaced with various functional groups (**6b, 6c** and **6e**). In case each case, RMA activity was abolished or greatly diminished. Moving the bromine to other positions on the indoline (e.g., **6i**, **6h**, and **6g**) also significantly reduced RMA activity. We thus concluded that the presence of a halogen at the R_2 position is necessary for RMA activity.

[j] Synthesis of Of1 analogs was performed by Dr. Le Chang

We further evaluated the effect of switching the halogen at the R_2 position. We found that RMA activity is optimal with bromine at R_2. However, replacing the R_2 bromine with chlorine (**6a**) significantly reduced mammalian toxicity (Table 3.5). Several analogs in which an additional halogen was added at the 7-position of indoline were synthesized. We found that when the R_2 halogen is chlorine, fluorine at R_4 significantly reduces RMA activity (**6j**); however, when both R_2 and R_4 are chlorine (**6k**), the RMA activity remains similar to that of Of1. Maintaining bromine at the R_2 position and adding fluorine at R_4 (**6l**), however, yields slightly improved RMA activity and reduced mammalian toxicity with respect to Of1.

Table 3.4: MRC values for indoline and sulfonamide nitrogen modifications.

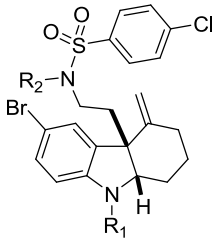

1a-f

Compound	R_1	R_2	amox/clav[a, b]	cefazolin[a, b]	meropenem[a ,c]
1a	Me	-	>32	>32	>32
1b	SO_2Ph^pCl	-	>32	>32	>32
1c	$COPh^pCl$	-	>32	>32	>32
1d	-	Me	>32	>32	>32
1e	-	SO_2Ph^pCl	>32	>32	>32
1f	-	$COPh^pCl$	>32	>32	>32

[a]: All MRC values are in μg/mL; [b]: MRSA ATCC BAA-44; [c]: MRSA ATCC 33592.

Table 3.5: MRC and GI_{50} values for the substitutions of indoline aromatic ring.

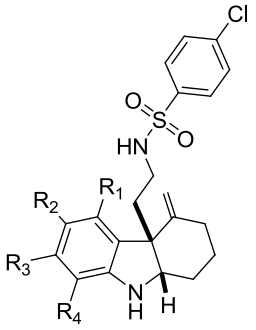

6a-l

Compound	R_1	R_2	R_3	R_4	amox/clav[a b]	cefazolin[a b]	meropenem[a c]	GI_{50}[d]
Of1	H	Br	H	H	4	4	4	17.1
6a	H	Cl	H	H	8	4	8	35
6b	H	Me	H	H	16	16	32	-
6c	H	MeO	H	H	>32	>32	>32	-
6d	H	F	H	H	16	16	16	-
6e	H	H	H	H	16	16	16	-
6f	H	H	phenylene		>32	>32	>32	-
6g	H	H	H	Br	>32	32	8	-
6h	H	H	Br	H	16	16	16	-
6i	Br	H	H	H	32	16	16	-
6j	H	Cl	H	F	16	16	32	-
6k	H	Cl	H	Cl	4	4	4	13.6
6l	H	Br	H	F	2	4	4	18.1

[a]: MRC values are in µg/mL; [b]: MRSA ATCC BAA-44; [c]: MRSA ATCC 33592; [d]: HeLa cells, GI_{50} values are in µg/mL.

Based on this series of modifications on the aromatic indoline ring, we concluded that in order to maintain RMA activity, the identity of the R_2 position must be a halogen (bromine or chorine) and that the R_2 position may be functionalized with a second halogen to improve or maintain activity.

Next, SAR investigations of the Of1 side chain were performed. For this portion of our SAR investigation, we maintained the bromine group at the 5-position of the indoline moiety. We included several analogs in this portion of our study with fluorine at the 7-position of indoline, since **6l** showed similar activity but lower mammalian cytotoxicity with respect to Of1 (Table 3.6). We first discovered that removing the side chain (R_2) entirely resulted in severely reduced activity in the presence or absence of the R_1 fluorine (**11a, 11b**). Likewise, replacing the sulfonamide with an amide (e.g., **12a**, **12b**, and **12c**) resulted in abolished RMA activity. We discovered the necessity of the phenyl ring by replacing it with a pyridine ring (**12m**) which resulted in a loss of RMA activity. Next the side chain phenyl ring was modified. When the chlorine at the *para* position relative to the sulfonamide was removed from Of1, the RMA activity is reduced at least two fold (**12d**). We thus attempted to modify the phenyl ring on the side chain with a series of functional groups. For these experiments, we synthesized analogs in which the chlorine was maintained and an additional chlorine was added to the meta or ortho position, respectively (**12i**, **12j**). These di-substituted products did not result in improved RMA activity; however, in the presence of the fluorine at the 7-position of indoline (R_1), reduced toxicity was observed for the di-substituted analogue **13f**.

Table 3.6: MRC and GI_{50} values for Of1 analogues with modifications on the side chain.

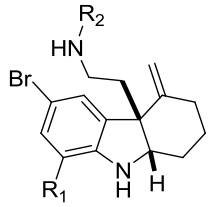

12a-n, 13a-m

Compound	R_1	R_2	amox/clav[a, b]	cefazolin[a, b]	meropenem[a ,c]	GI_{50}[d]
Of1	H	SO_2Ph^pCl	4	4	4	17.1
11a	H	H	32	32	32	-
11b	F	H	>32	32	16	16.2
12a	H	TFA	>32	>32	32	-
12b	H	COBu	>32	>32	32	-
12c	H	$COPh^pCl$	>32	>32	>32	-
12d	H	SO_2Ph	8	8	16	-
12e	H	SO_2Ph^pMe	>32	>32	>32	-
12f	H	SO_2Ph^pF	>32	>32	>32	-
12g	H	SO_2Ph^pBr	4	4	8	40
12h	H	SO_2Ph^pI	4	4	32	33
12i	H	$SO_2Ph^{3,4}Cl$	4	2	4	12.8
12j	H	$SO_2Ph^{2,4}Cl$	8	>32	4	-
12k	H	SO_2Ph^pCN	16	8	16	-
12l	H	SO_2Ph^pNHAc	>32	>32	32	-
12m	H	$SO_2{}^5Py$	32	32	32	-
12n	H	$SO_2Ph^pNO_2$	>32	>32	>32	-
12o	H	$SO_2Ph^pNH_2$	16	16	16	-
13a	F	SO_2Ph^pOMe	8	4	8	49
13b	F	SO_2Ph^pMe	4	4	4	22
13c	F	SO_2Ph^pF	4	4	4	18.3
6l	F	SO_2Ph^pCl	2	4	4	18.1
13d	F	SO_2Ph^pBr	1	1	1	22
13e	F	SO_2Ph^pI	4	2	4	19.6
13f	F	$SO_2Ph^{3,4}Cl$	4	4	4	31
13g	F	SO_2Ph^pNHAc	32	32	16	32
13h	F	SO_2Ph^pCN	8	4	4	17.0
13i	F	$SO_2Ph^pCF_3$	4	4	4	8.7

[a]: MRC values are in µg/mL; [b]: MRSA ATCC BAA-44; [c]: MRSA ATCC 33592; [d]: HeLa cells, GI_{50} values are in µg/mL.

The remainder of our modifications focused on the para position of the phenyl ring. Replacing the chlorine with a fluorine (i.e., **12f**) abolished RMA activity entirely; however, this same modification in combination with the R_1 as a fluorine (i.e., **13c**) resulted in similar RMA activity relative to Of1. A similar trend was also observed when the chlorine was replaced with an iodine in the absence (**12h**) or presence (**13e**) of the R_1 fluorine. Interestingly, when the chlorine is replaced with a methyl group (**12e**), RMA activity is lost; however, it is regained when fluorine is added at the R_1 position (**13b**), in addition, the mammalian toxicity of this analogue is reduced in this case. This trend was also observed when the chlorine was replaced with a cyanide (**12k, 13h**). Although substituting a methoxy group for the chlorine in the presence of the R_1 fluorine (**13a**) results in slightly reduced activity, the mammalian toxicity is significantly reduced.

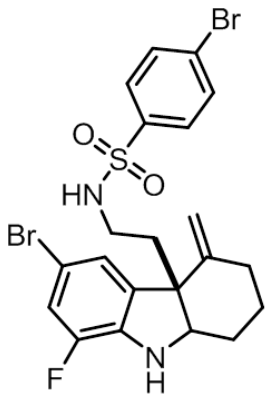

13d

Figure 3.5: Compound 13d.

This analog of Of1 shows reduced toxicity against mammalian cells relative to Of1 and increased potency as an RMA.

Likewise, replacing the chlorine with a bromine (**12g**) resulted in slightly reduced RMA activity, this analog demonstrated a significant decrease in mammalian toxicity (Table 3.6). Intriguingly, when we added the R_1 fluorine (**13d**) to this molecule, we observed a significant (at least four fold) increase in RMA activity as well as decreased toxicity relative to Of1 (Figure 3.5).

3.5.5 Synergistic activity and hemolytic activity of the more potent Of1 analog, 13d.[k]

In order to assess the synergy of **13d** in combination with β-lactam antibiotics, we first investigated the antibacterial activity of **13d** against both MRSA and methicillin-sensitive *S. aureus* (MSSA) strains. For this experiment, we employed a standard microdilution assay using MRSA ATCC BAA-44, MRSA ATCC 33592 and MSSA ATCC 25923. The assay was performed by following the procedure outlined by CLSI.[22] The minimum inhibitory concentrations (MICs) of **13d** against all strains was higher than 64 µg/mL, the highest concentration tested. Since **13d** exhibited no anti-proliferative effect on its own, we decided to confirm its synergistic activity with the three antibiotics tested in this report by performing the checkerboard (CB) test for synergy and calculating the fractional inhibitory concentration index (FICI) for each antibiotic tested in combination with **13d.** CB assays and FICIs were set up and calculated as described previously.[26] Briefly, **13d** was diluted across 96-well microplates in MHB (8-0.016 µg/mL)**,** and to each plate, either amoxicillin/clavulanic acid (128-1 µg/mL), cefazolin (128-1 µg/mL), or meropenem (16-0.125 µg/mL) was diluted down the plate. Thusly, each well of the 96-well plate contained a unique concentration combination of **13d** and antibiotic. FICI was

[k] Hemolytic activity assays were performed by Shane Walls

calculated by the following formula: FICI = FICA + FICB, where FICA is the MIC of drug A in combination with B divided by the MIC of drug A on its own, and FICB is the MIC of drug B in combination divided by the MIC of drug B on its own. A FICI that is less than 0.5 indicates a synergistic drug interaction, a FICI in a range of 0.5-1 denotes an additive drug interaction, and an FICI greater than 1 indicates an antagonistic interaction. The FICI of **13d** for amoxicillin/clavulanic acid, cefazolin, and meropenem were 0.0315, 0.0156, and 0.0315, respectively. This result confirms the synergistic action of **13d** in combination with all antibiotics tested in this study.

We further evaluated toxicity of **13d** by conducting a standard hemolytic assay as previously described.[27,28] This assay measures the amount of hemoglobin leakage in compound-treated human red blood cells (hRBCs) and is used to measure the amount of membrane damage induced by drug treatment. The hemolytic activity assay was conducted for multiple concentrations of **13d**. It caused less than 2% hemolysis of red blood cells at 64 μg/mL (64-fold above its MRC), the highest concentration tested. We thus concluded that compound **13d** shows an insignificant level of toxicity against hRBCs.

Collectively, these results indicate that **13d** is a more potent analog of Of1, with increased RMA activity, decreased toxicity, and potent synergy with multiple classes of β-lactam antibiotics. Furthermore, **13d** shows no antiproliferative effect against MRSA or MSSA on its own.

3.6 Conclusions and future directions.

Through specialized low-throughput screening of a tricyclic indoline library, we were able to identify a number of compounds with significant potentiating activity for methicillin in MRSA. Additional screening efforts have identified unique indolines from the same library with the ability to potentiate vancomycin in both MRSA and VRE, as well as others capable of potentiating tetracycline.

Follow-up on one of the methicillin potentiating compounds, Of1, revealed that it is a highly specific RMA for a wide variety of β-lactam antibiotics in multiple MRSA strains, with no growth-attenuating effect on its own and no super-sensitizing effect in non-resistant organisms. The highly tuned specificity of Of1 for β-lactam antibiotics in β-lactam-resistant bacteria largely rules out the general potentiation mechanisms, such as efflux pump inhibition and enhancement of membrane permeability.[32] Instead, Of1 may selectively a target a β-lactam-specific resistance mechanism, such as β-lactam-induced expression of *mecA* and/or *blaZ*, which encode PBP2a and β-lactamase, respectively.[33–37] Because Of1 can potentiate the combination of amoxicillin and β-lactamase inhibitor clavulanic acid, and Of1 does not have the reactive β-lactam functional group, it is highly likely that Of1 modifies the resistance of MRSA via an unknown mechanism. Although Of1 showed potentiating effects in both MRSA and VRE, we did not observe an effect in β-lactam resistant Gram-negative organisms including *Klebsiella pneumoniae, or Enterobacter fecalis*. We hypothesize that this may be due to the physiochemical properties of Of1 being unfavorable for penetration into the Gram-negative cell.[38,39] We are currently investigating approaches to make Of1 more favorable for uptake into both Gram-positive and Gram-negative cells. However,

investigation of the molecular target of Of1 will shed some light on whether or not a conserved target for the drug exists in Gram-negative bacteria.

Following the initial evaluation of Of1, we set out to identify elements of its structure that contribute to its RMA activity and potentially make a more potent analog with reduced toxicity in mammalian cells. A number of structural analogs were synthesized by Wang group chemists and were evaluated for their ability to potentiate three representative β-lactam antibiotics (amoxicillin/clavulanic acid, cefazolin, and meropenem) in MRSA. The toxicity of active analogs was evaluated in mammalian cells. We found that neither the aniline nor the sulfonamide nitrogen can tolerate further modification. While the sulfonamide group on the side chain is crucial for the RMA activity, modifications of both aromatic systems can further fine-tune the RMA activity and the mammalian toxicity. Notably, we discovered that adding fluorine to the 7-position of the indoline increases RMA activity of the compound in multiple instances, including those in which another modification has reduced or eliminated RMA activity. Furthermore, we discovered that a number of substitutions may be added to the phenyl ring on the side chain, which will allow the development of additional Of1 analogues for the discovery of its cellular target, a stepping stone to understanding the β-lactam resistome.[40] In addition, we have discovered a more potent analogue of Of1, compound **13d**, with reduced mammalian toxicity and low hemolytic activity. We were able to confirm the synergistic activity of **13d** by calculating its FICI and showed that it is highly synergistic in combination with all antibiotics tested.

3.7 Materials and methods

3.7.1 Bacterial strains and reagents.

Strains ATCC BAA-44 (MRSA) and ATCC 25923 (MSSA) were gifts from Daniel Feldheim and Charles McHenry's laboratories, respectively. VRE HM-968 and VRSA NR-46421 were obtained from BEI resources. Strain ATCC 33592 700789, BAA-1683, and HepG2 (ATCC HB-8065) cells were purchased from the ATCC**.** All antimicrobial compounds were purchased from Sigma-Aldrich. The growth media used for all MIC experiments was Mueller Hinton Broth (MHB) purchased from HIMEDIA through VWR (cat: 95039-356). Freshly drawn human blood for the hemolytic assay was gingerly harvested from Mr. Shane Walls, who literally put his blood, sweat and tears into this investigation.

3.7.2 Broth Microdilution antibiotic susceptibility tests.

The minimal inhibitory concentrations (MICs) of active **1** analogs were determined by the broth microdilution method detailed in the Clinical and Laboratory Standards Institute handbook.[22] The inoculum was prepared by diluting a bacterial day culture (OD_{600} 0.15□0.4) to OD_{600} 0.002. This dilution was further diluted two fold when added to 96 well microplates (USA Scientific CytoOne 96-well TC plate, cat: CC7682-7596) for a final inoculum concentration of OD_{600} 0.001. All plates were incubated at 37°C with shaking for 18 hours before results were interpreted.

3.7.3 Resistance-modifying agent (RMA) screens.

The RMA screens were conducted by first preparing 96-well plates containing 50 µl per well 64 µg/ml methicillin in Mueller Hinton Broth. Next, 500 nL of each indoline (4 mM in DMSO) was pinned to the assay plate using the CyBi-Well 96-channel simultaneous pipettor (Cybio). These plates were inoculated with 50 µL bacteria diluted to OD_{600} 0.002. The final concentration of methicillin for the screen was 32 µg/mL (¼ of the methicillin MIC), the final concentration of each alkaloid was 20 µM, and the final inoculum concentration was OD600 0.001. All plates were incubated at 37°C with shaking for 18 hours before results were interpreted.

3.7.4 Determination of MIC in the presence of Of1.

The MRSA strain ATCC BAA-44 and the methicillin-sensitive S. aureus (MSSA) strain ATCC 25923 were used to determine the MIC values of various antimicrobial compounds in the presence of 20 µM Of1. The experiment was conducted similarly to the CLSI MIC determination described previously; however, MHB was supplemented with 40 µM Of1 prior to set up and inoculation. The final concentration of Of1 after inoculation with BAA-44 was 20 µM.

3.7.5 MRC testing.

MRC screens were performed as described previously.[21] Briefly, antibiotic MIC values where *S. aureus* is considered susceptible were determined from the CLSI handbook supplement.[24] The RMA was diluted to 5 mg/mL in DMSO. Antibiotic was prepared at twice the intended final concentration in Mueller Hinton Broth (MHB). For amoxicillin/clavulanic acid, the initial concentration was 8/4 µg/mL, for meropenem 8

µg/mL and for cefazolin 16 µg/mL. 50 µL of the antibiotic containing media was added to each well of 96 well plates and 100 µL was added to the top row. 1.28 µL of 5 mg/mL alkaloid solution was added to the top row of each plate to afford a concentration of 64 µg/mL in the top row of each plate and two fold serial dilutions were performed down the columns. Once the plates were prepared, a day culture of MRSA was diluted to OD_{600} 0.002 and 50 µL were added to each well. The final concentration of MRSA added was OD_{600} 0.001, the final concentration of amoxicillin/clavulanic acid was 4/2 µg/mL, the final concentration of meropenem was 4 µg/mL the final concentration of cefazolin was 8 µg/mL, and the highest concentration of 1 analog tested was 32 µg/mL. Plates were incubated overnight at 37°C with shaking. The MRC value was determined as the concentration of **1** analog in the presence of antibiotic at which there was no observable overnight growth.

3.7.6 FICI checkerboard test

Checkerboard assays were performed as described previously.[26] Antibiotics were diluted down the columns of a 96-well microplate, while **13d** was diluted across the rows. Plates were prepared containing concentrations of antibiotics and **13d** two-fold higher than the intended final concentrations and were prepared in duplicate. All antimicrobial compounds were purchased from Sigma-Aldrich. The growth media was Mueller Hinton Broth (MHB) purchased from HIMEDIA through VWR (cat: 95039-356). The inoculum was prepared by diluting a bacterial day culture (OD_{600} 0.15-0.4) to OD_{600} 0.002. This dilution was further diluted two fold when added to 96 well microplates for a final inoculum concentration of OD_{600} 0.001. All plates were incubated at 37°C with shaking for 18 hours before results were interpreted.

3.8 References

1. Roemer, T. & Boone, C. Systems-level antimicrobial drug and drug synergy discovery. *Nat. Chem. Biol.* **9,** 222–31 (2013).

2. Lewis, K. Platforms for antibiotic discovery. *Nat. Rev. Drug Discov.* **12,** 371–87 (2013).

3. Fleming, A. On the antibacterial action of cultures of a penicillium, with special reference to their use in the isolation of B. influenzæ. *Br. J. Exp. Pathol.* **10,** 226–236 (1929).

4. Schatz, A., Bugle, E. & Waksman, S. A. Streptomycin, a Substance Exhibiting Antibiotic Activity Against Gram-Positive and Gram-Negative Bacteria.*. *Exp. Biol. Med.* **55,** 66–69 (1944).

5. Clatworthy, A. E., Pierson, E. & Hung, D. T. Targeting virulence: a new paradigm for antimicrobial therapy. *Nat. Chem. Biol.* **3,** 541–8 (2007).

6. Coates, A. R. M., Halls, G. & Hu, Y. Novel classes of antibiotics or more of the same? *Br. J. Pharmacol.* **163,** 184–94 (2011).

7. Payne, D. J. Microbiology. Desperately seeking new antibiotics. *Science* **321,** 1644–5 (2008).

8. Davies, J. & Davies, D. Origins and evolution of antibiotic resistance. *Microbiol. Mol. Biol. Rev.* **74,** 417–33 (2010).

9. Lowy, F. D. Antimicrobial resistance : the example of Staphylococcus aureus. **111,** 1265–1273 (2003).

10. Stryjewski, M. E. & Corey, G. R. Methicillin-Resistant Staphylococcus aureus: An Evolving Pathogen. *Clin. Infect. Dis.* **58 Suppl 1,** S10–9 (2014).

11. Cohen, M. L. Epidemiology of drug resistance: implications for a post-antimicrobial era. *Science* **257,** 1050–5 (1992).

12. Center for Disease Control and Prevention. *Antibiotic resistance threats*. (2013).

13. Bal, a. M. *et al.* Vancomycin in the treatment of meticillin-resistant Staphylococcus aureus (MRSA) infection: End of an era? *J. Glob. Antimicrob. Resist.* **1,** 23–30 (2013).

14. Abreu, A. C., McBain, A. J. & Simões, M. Plants as sources of new antimicrobials and resistance-modifying agents.Abreu, A. C., McBain, A. J., & Simões, M.

(2012). Plants as sources of new antimicrobials and resistance-modifying agents. Natural Product Reports, 29(9), 1007–21. doi:10.1039/c2np200. *Nat. Prod. Rep.* **29,** 1007–21 (2012).

15. Reading, C. & Cole, M. Clavulanic acid: a beta-lactamase-inhiting beta-lactam from Streptomyces clavuligerus. *Antimicrob. Agents Chemother.* **11,** 852–7 (1977).

16. Rossolini, G. M. Acquired metallo-beta-lactamases: an increasing clinical threat. *Clin. Infect. Dis.* **41,** 1557–8 (2005).

17. Worthington, R. J. & Melander, C. Overcoming resistance to β-lactam antibiotics. *J. Org. Chem.* **78,** 4207–13 (2013).

18. Worthington, R. J., Richards, J. J. & Melander, C. Small molecule control of bacterial biofilms. *Org. Biomol. Chem.* **10,** 7457–74 (2012).

19. Wang, H. *et al.* Discovery of wall teichoic acid inhibitors as potential anti-MRSA β-lactam combination agents. *Chem. Biol.* **20,** 272–84 (2013).

20. Pasquina, L. W., Santa Maria, J. P. & Walker, S. Teichoic acid biosynthesis as an antibiotic target. *Curr. Opin. Microbiol.* **16,** 531–7 (2013).

21. Podoll, J. D. *et al.* Bio-inspired synthesis yields a tricyclic indoline that selectively resensitizes methicillin-resistant Staphylococcus aureus (MRSA) to β-lactam antibiotics. *Proc. Natl. Acad. Sci. U. S. A.* **110,** 15573–15578 (2013).

22. CLSI. *Methods for Dilution Antimicrobial Susceptibility Tests for Bacteria That Grow Aerobically ; Approved Standard — Eighth Edition*. **29,** (2009).

23. Périchon, B. & Courvalin, P. VanA-type vancomycin-resistant Staphylococcus aureus. *Antimicrob. Agents Chemother.* **53,** 4580–4587 (2009).

24. CLSI. *Performance Standards for Antimicrobial Susceptibility Testing ; Seventeenth Informational Supplement*. **27,** (2007).

25. Chang, L. *et al.* Structure-activity relationship studies of the tricyclic indoline resistance-modifying agent. *J. Med. Chem.* **57,** 3803–17 (2014).

26. Sopirala, M. M. *et al.* Synergy testing by Etest, microdilution checkerboard, and time-kill methods for pan-drug-resistant Acinetobacter baumannii. *Antimicrob. Agents Chemother.* **54,** 4678–83 (2010).

27. Meng, H. & Kumar, K. Antimicrobial activity and protease stability of peptides containing fluorinated amino acids. *J. Am. Chem. Soc.* **129,** 15615–22 (2007).

28. Wang, F. *et al.* Solubilized gramicidin A as potential systemic antibiotics. *Chembiochem* **13,** 51–5 (2012).

29. Marholz, L. J., Chang, L., Old, W. M. & Wang, X. Development of substrate-selective probes for affinity pulldown of histone demethylases. *ACS Chem. Biol.* **10,** 129–37 (2015).

30. Giepmans, B. N. G., Adams, S. R., Ellisman, M. H. & Tsien, R. Y. The fluorescent toolbox for assessing protein location and function. *Science* **312,** 217–24 (2006).

31. Kocaoglu, O. *et al.* Selective penicillin-binding protein imaging probes reveal substructure in bacterial cell division. *ACS Chem. Biol.* **7,** 1746–53 (2012).

32. Blair, J. M. a., Webber, M. a., Baylay, A. J., Ogbolu, D. O. & Piddock, L. J. V. Molecular mechanisms of antibiotic resistance. *Nat. Rev. Microbiol.* **13,** 42–51 (2014).

33. Stapleton, P. D. & Taylor, P. W. Methicillin resistance in Staphylococcus aureus: mechanisms and modulation. *Sci. Prog.* **85,** 57–72 (2002).

34. Zhang, H. Z., Hackbarth, C. J., Chansky, K. M. & Chambers, H. F. A proteolytic transmembrane signaling pathway and resistance to beta-lactams in staphylococci. *Science* **291,** 1962–5 (2001).

35. Chambers, H. F. Methicillin resistance in staphylococci : molecular and biochemical basis and clinical Methicillin Resistance in Staphylococci : Molecular and Biochemical Basis and Clinical Implications. *Microbiology* **10,** (1997).

36. Arêde, P., Ministro, J. & Oliveira, D. C. Redefining the role of the β-lactamase locus in methicillin-resistant Staphylococcus aureus: β-lactamase regulators disrupt the MecI-mediated strong repression on mecA and optimize the phenotypic expression of resistance in strains with constitutive mecA . *Antimicrob. Agents Chemother.* **57,** 3037–45 (2013).

37. Llarrull, L. I., Toth, M., Champion, M. M. & Mobashery, S. Activation of BlaR1 protein of methicillin-resistant Staphylococcus aureus, its proteolytic processing, and recovery from induction of resistance. *J. Biol. Chem.* **286,** 38148–58 (2011).

38. O'Shea, R. & Moser, H. E. Physicochemical properties of antibacterial compounds: Implications for drug discovery. *J. Med. Chem.* **51,** 2871–2878 (2008).

39. Brown, D. G., May-dracka, T. L., Gagnon, M. M. & Tommasi, R. Trends and Exceptions of Physical Properties on Antibacterial Activity for Gram-Positive and Gram-Negative Pathogens. (2014).

40. Wright, G. D. The antibiotic resistome: the nexus of chemical and genetic diversity. *Nat. Rev. Microbiol.* **5,** 175–86 (2007).

Chapter 4 : Investigations of the molecular mechanism of synergy between Of1 and β-lactam antibiotics

4.1 Introduction

4.1.1 β-lactams: the first wonder drug.

Before the twentieth century, bacterial infections were handled very differently than they are today. Prior to the discovery of antibiotics, treatment for skin and wound infections included amputation or removal of the infected tissue, or maggot therapy to remove necrotic tissue.[1,2] In the early 1900s, however, Paul Ehrlich developed a profound hypothesis: that organic compounds could be used to cure a disease with no ill-effects to the host.[3] Ehrlich's 'magic bullet' hypothesis marked the beginning of the modern 'antibiotic era'.

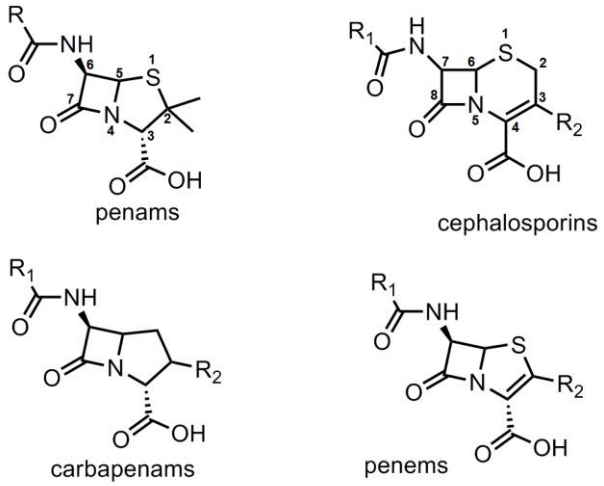

Figure 4.1: Representative classes of β-lactam antibiotics.

The class of β-lactam depends on the identity of the five or six membered ring fused to the four-membered lactam ring. Modification of the R-groups can confer favorable physiochemical properties as well as resistance to β-lactamases by steric interference.

Years after Ehrlich's initial contribution to the antibiotic field, Alexander Fleming made a serendipitous discovery. Fleming had been studying properties of staphylococci when fungal contamination on one of his plates resulted in death of the colonies in proximity to the mold on the plate.[4,5] Intrigued by the potential antibacterial activity of the mold, Fleming pursued purification and identification of the active component. In 1940, this goal was realized through the efforts of Howard Florey and Ernest Chain, who were able to purify the active component: penicillin.[6] Further testing of penicillin revealed that it is an effective antibiotic against both Gram-positive and Gram-negative bacteria, providing treatment for diseases such as scarlet fever, staphylococci infections and syphilis. Penicillin also had the added advantage that it caused no ill-effects to the host, a true 'magic bullet'. The class of antibiotics to which penicillin belongs, the β-lactams, has rightfully gained the reputation of being some of the safest and most effective antibiotics in history.[7]

4.1.2 Structure and function of β-lactams.

The β-lactam class of antibiotics is characterized by its four-membered β-lactam ring which, with the exception of monobactams, is fused to a five- or six-membered ring (Figure 4.1).[8] The β-lactams are categorized by their structural features as penams (such as penicillin, ampicillin and methicillin), cephalosporins (such as cefazolin and cefepime), penems (including faropenem) and carbapenams (exemplified by imipenem and meropenem). The defining characteristic of these subcategories is the character of the ring fused to the β-lactam ring (Figure 4.1). Although the structure of the β-lactam core contributes to its stability and therefore its reactivity and effectiveness as an antibiotic, another important feature of β-lactams is the character of sidechains

extending from the 6-amino group of penicillin (Figure 4.2).[9] These properties vary to some degree among naturally occurring β-lactams. However, the discovery of a means to create semi-synthetic β-lactams via 6-aminopenicillanic acid (6-APA) enabled manipulation of the drugs to allow more favorable physiochemical properties, bioavailability profiles, and a means to thwart some antibiotic resistance mechanisms.[10]

In bacteria, β-lactam antibiotics target the penicillin-binding-proteins (PBPs), which are key enzymes of cell wall synthesis.[11] The bacterial cell wall includes a rigid layer of peptidoglycan, a polymer of sugars and amino acids, which imparts rigidity and shape to the cell (Figure 4.3).[12] The peptidoglycan chain is composed of alternating units of the sugars *N*-acetylglucosamine (NAG) and *N*-acetylmuramic acid (NAM). Nam and NAG are linked together via a β-1,4 glycosidic bond. A short polypeptide branches from C-3 of NAM. The polypeptide chains protruding from NAM are cross-linked in a transpeptidation reaction catalyzed by PBPs that enables formation of the mesh-like peptidoglycan of the bacterial cell wall. The crosslinking step of peptidoglycan synthesis is crucial to maintain cell wall strength in bacteria. Without it, the cells would succumb to osmotic lysis from the pressure of its contents.[13] By inhibiting PBPs, β-lactam antibiotics cause bacterial cell death. One of the most important features of PBPs as an antibiotic target is that they are unique to bacteria, making β-lactam antibiotics one of the safest and most effective medicines known.

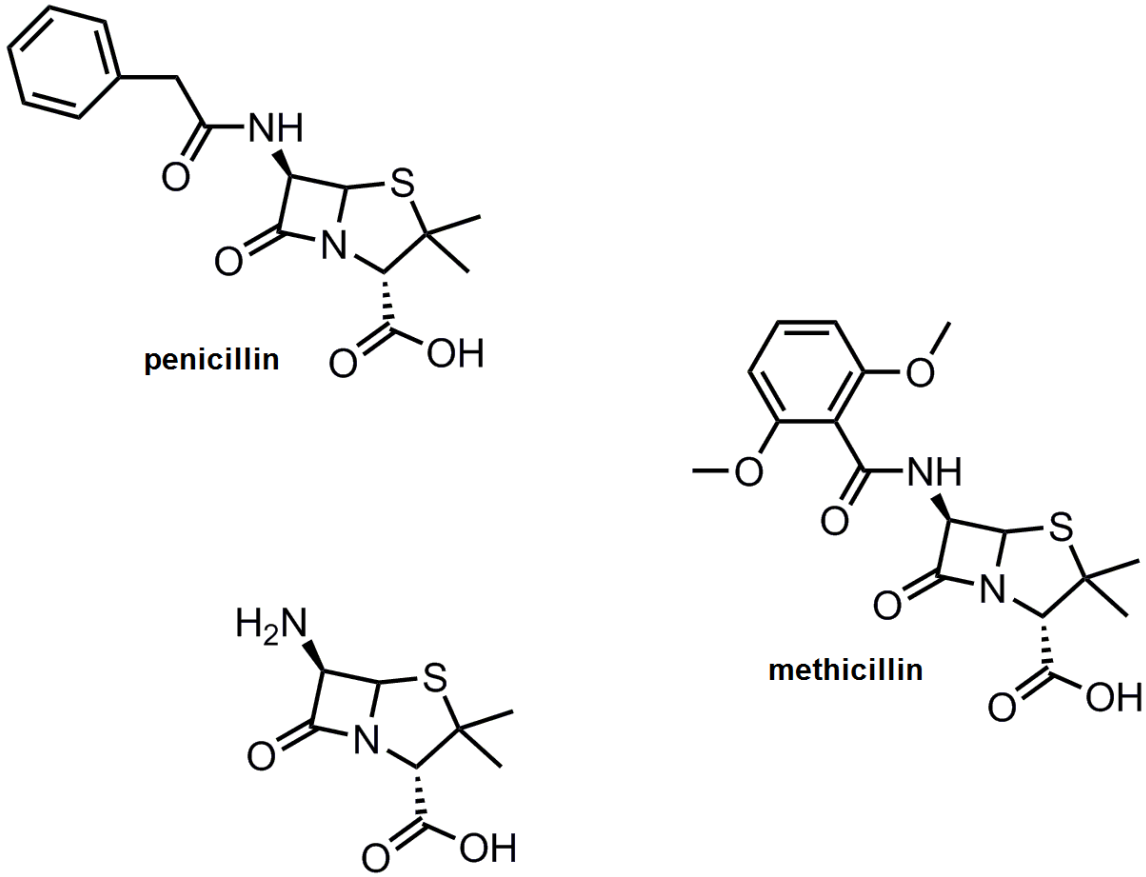

Figure 4.2: Structures of penicillin, 6-aminopenicillanic acid (6-APA) and methicillin.

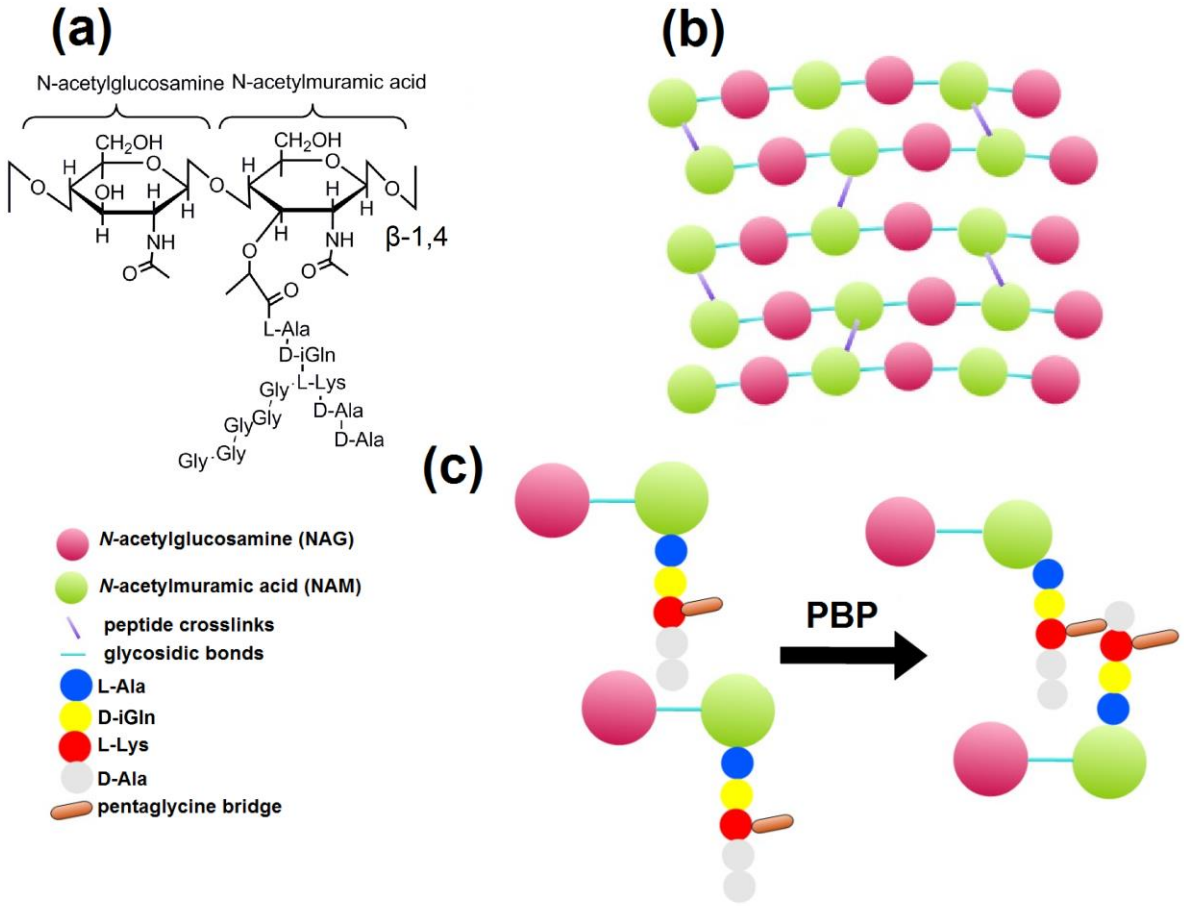

Figure 4.3: Structure of cell wall peptidoglycan.

The bacterial cell wall is largely composed of a mesh-like polymer known as peptidoglycan. (a) The backbone of peptidoglycan is made up of repeating units of a disaccharide composed of *N*-acetylglucosamine (NAG) and *N*-acetylmuramic acid which is functionalized with a short polypeptide. (b) The overall structure of peptidoglycan is realized through crosslinking the NAM peptides to form a sturdy mesh-like structure. (c) Penicillin binding proteins (PBPs) catalyze the crosslinking reaction of peptidoglycan synthesis. In Gram-positive bacteria, this is accomplished with the pentaglycine interbridge linking D-Ala to L-Lys.

4.1.3 β-lactam resistance is driven by β-lactamase and PBP2a.

The discovery and use of β-lactams in the clinic was closely followed by discovery of β-lactam resistance mechanisms in clinically significant pathogens.[14] This initial resistance phenotype came in the form of β-lactamase.[14–16] In most cases, β-lactamase is acquired and maintained on a resistance plasmid in *S. aureus* carrying this and other resistance genes.[17] β-Lactamase is expressed from a functioning unit of DNA known as the *bla* operon. In addition to β-lactamase, the *bla* operon includes two regulatory elements: a repressor (BlaI) and a sensor (BlaR1).[18] All three elements are expressed under the control of a single promoter (Figure 4.4). β-lactamase disables penicillin and other susceptible β-lactam antibiotics by enzymatically cleaving the β-lactam ring, the functional inhibitor (Figure 4.5). This action renders the antibiotic completely ineffective. In order to preserve β-lactam antibiotics, a semi-synthetic analog of penicillin, known as methicillin, was synthesized by the addition of di-methoxy benzoic acid and introduced in 1961 (Figure 4.2)**.**[9] The methicillin sidechain afforded

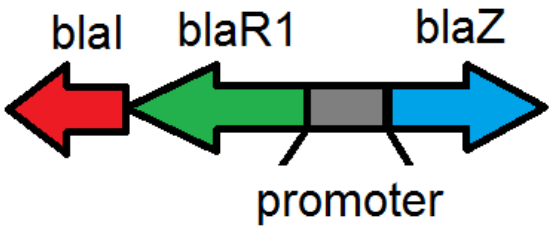

Figure 4.4: Organization of the bla operon.

The genes encoding β-lactamase (blaZ, blue) as well as its regulatory machinery, (blaR1 and blaI, green and red, respectively) are clustered together and expressed divergently from a single promoter.

effective resistance to β-lactamase due to the analog's poor affinity for the enzyme active site. Analogs of methicillin allowed further improvement of the drug, affording the similarly designed β-lactams oxacillin, cloxacillin and naficillin, which are more active *in vitro* than methicillin and have improved bioavailability profiles. Although these β-lactamase-resistant structural analogs seemed to provide a much-needed solution to β-lactam resistance in *S. aureus*, it was not long before methicillin-resistant *S. aureus* (MRSA) began to appear, first in the hospital setting. Currently, in addition to hospital-acquired MRSA isolates (HA-MRSA), community-acquired MRSA (CA-MRSA) is on the rise.[19] MRSA in all of its forms has become a world-wide health concern. In the United States alone, 80,000 cases of invasive MRSA infections were recorded in 2013, 11,000 of which resulted in death.[20]

The first instance of MRSA was reported in 1961, only two years after the introduction of methicillin in the clinic.[19] MRSA arises due to the chromosomal acquisition of a *Staphylococcal* cassette chromosome (SCC) containing the *mecA* gene (SCC*mec*), which expresses an alternative PBP, PBP2a. PBP2a binds poorly to β-lactam antibiotics. The antibiotics therefore have little effect on its activity.[21,22] Although transpeptidation of peptidoglycan by PBP2a is less efficient than when catalyzed by other PBPs, expression of PBP2a while under antibiotic pressure allows cells to catalyze the crosslinking in the presence of nearly all β-lactam antibiotics.[22]

Like the *bla* operon expressing β-lactamase and its regulatory elements, SCC*mec* contains the *mecA* gene (expressing PBP2a), as well as genes expressing a repressor (MecI) and a sensor (MecR1), and two recombinases that allow insertion of SCC*mec* into the chromosome.[23]

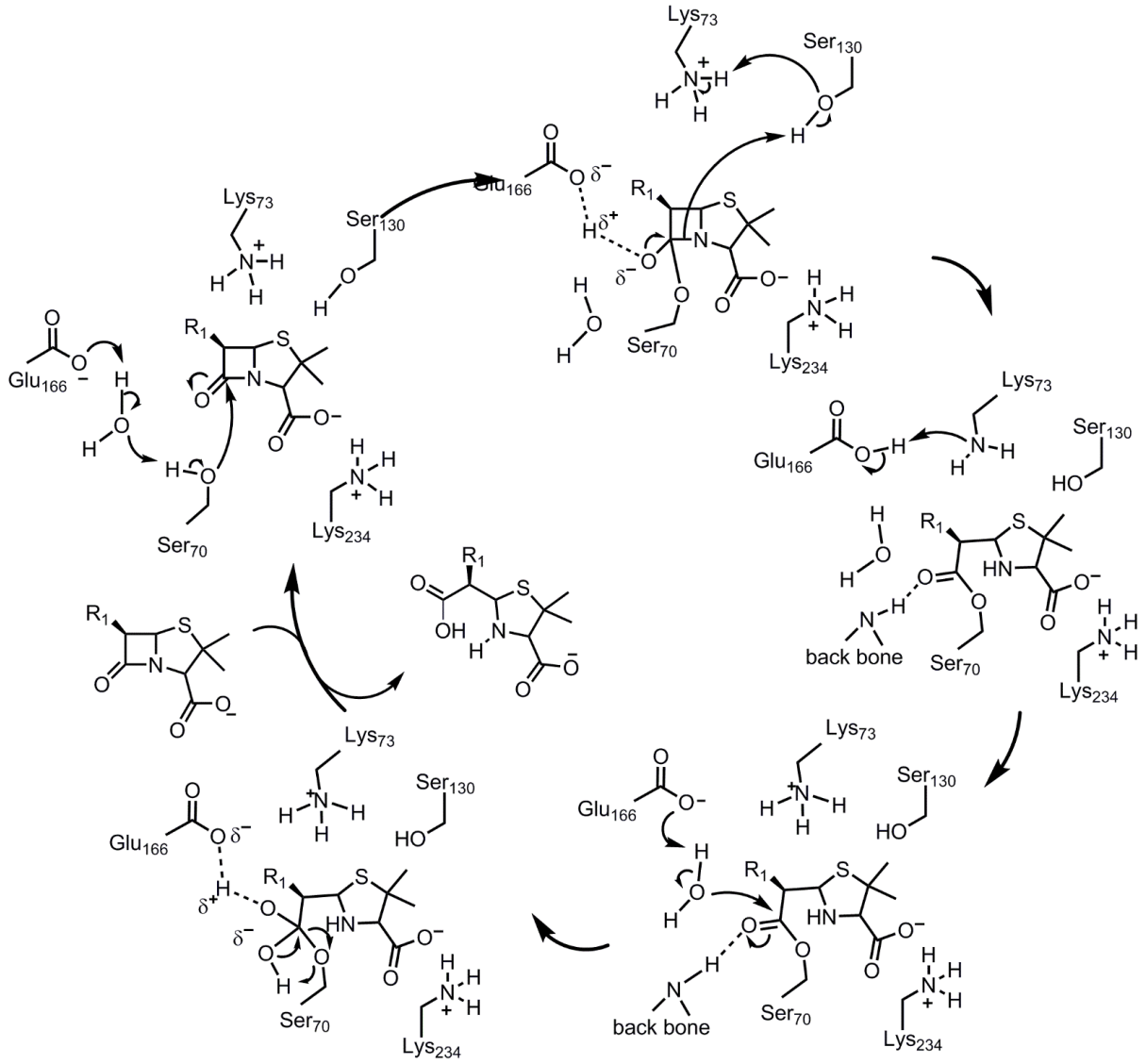

Figure 4.5: Enzymatic mechanism of serine β-lactamase.

A water molecule in the active site is activated by Glu_{166}. This, in turn, activates the hydroxyl group of Ser_{70} which performs nucleophilic attack on the carbonyl of the β-lactam ring, and forms a covalent enzyme-substrate intermediate. Re-formation of the carbonyl is accompanied by protonation of the β-lactam nitrogen and cleavage of the C-N bond. The covalent intermediate is broken-down via a second water activation event by $Glu_{166,}$ and subsequent nucleophilic attack on the carbonyl by the resulting hydroxide ion. This final step regenerates the enzyme for continued hydrolysis of β-lactam antibiotic molecules. Drawn based on Drawz and Bonomo (2010).[16]

There are eight known variants of SCC*mec*.[17,24] These are based on differences in the *mec* operon and the presence of other resistance determinants within the cassette (Figure 4.6). Although all variants encode the resistance determinant, PBP2a, some are missing or have insertions in the *mecR1* and *mecI* genes rendering them nonoperational. In these cases, expression of PBP2a is under control of the regulatory machinery contained in the *bla* operon.[25,26]

4.1.4 Expression of β-lactam resistance determinants is inducible in the presence of antibiotics through the activity of a two-component regulatory system.

Induction of *Staphylococcus aureus* β-lactam resistance machinery proceeds via a two-component signal transduction pathway in the presence of β-lactam antibiotics.[27–29] The pathways responsible for induction of β-lactamase and PBP2a are remarkably similar and the induction and resistance machinery are located on genetic elements known as the *bla operon* and the *mec* operon region of SCC*mec*, illustrated in figures 4.4 and 4.6, respectively.[25,30,31] Induction of gene expression from the *bla* operator proceeds under the control of the BlaR1 (the sensor) and the BlaI (gene repressor) proteins via a three-step, two-component process (Figure 4.7). First, the presence of β-lactam in the growth milieu is detected by the BlaR1 sensor domain located on the extracellular portion of the plasma membrane. Next, acylation of the sensor domain by the β-lactam results in an auto-proteolytic event between amino acids R293 and R294 of BlaR1, which allows the protease domain to act on BlaI. Finally, cleavage of BlaI between Asn101 and Phe102, and thus its removal from the DNA, promotes expression of β-lactamase (from the *blaZ* gene) as well as increased expression of the regulatory machinery. [28,32–35]

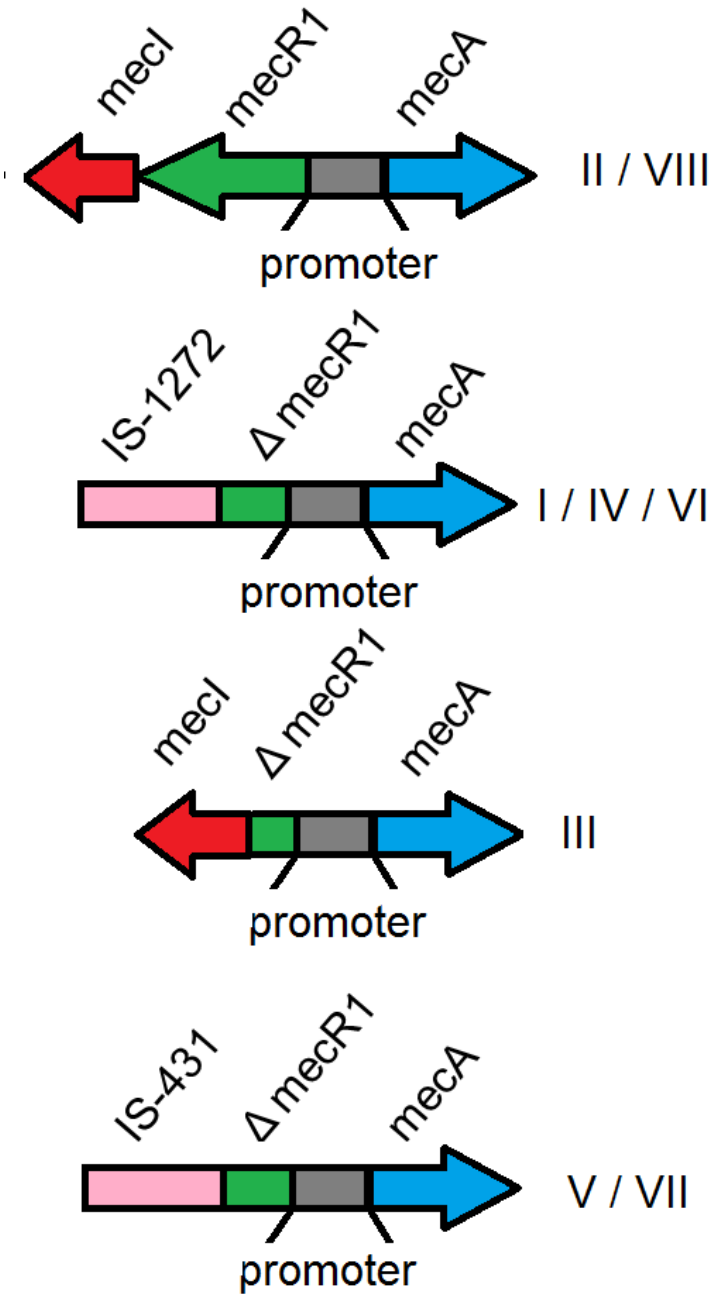

Figure 4.6: Comparison of SCCMec types in MRSA.

SCCMec subtypes are classified based on their size and whether or not their regulatory genes are intact. There are eight (I-VIII) SCCMec subtypes. Genes encoding mecA (blue), mecI (red) and mecR1 (green) are shown along with disrupting insertional sequences (IS, pink). All contain the full mecA gene which expresses PBP2a, but only types II and VIII have the fully functional regulatory machinery. In some cases, the mecR1 gene (green) which encodes the sensor is truncated with no other insertions (SCCMecIII). More commonly, the genes encoding mecR1 and mecI are disrupted by IS-1272 or IS-431.[17,24]

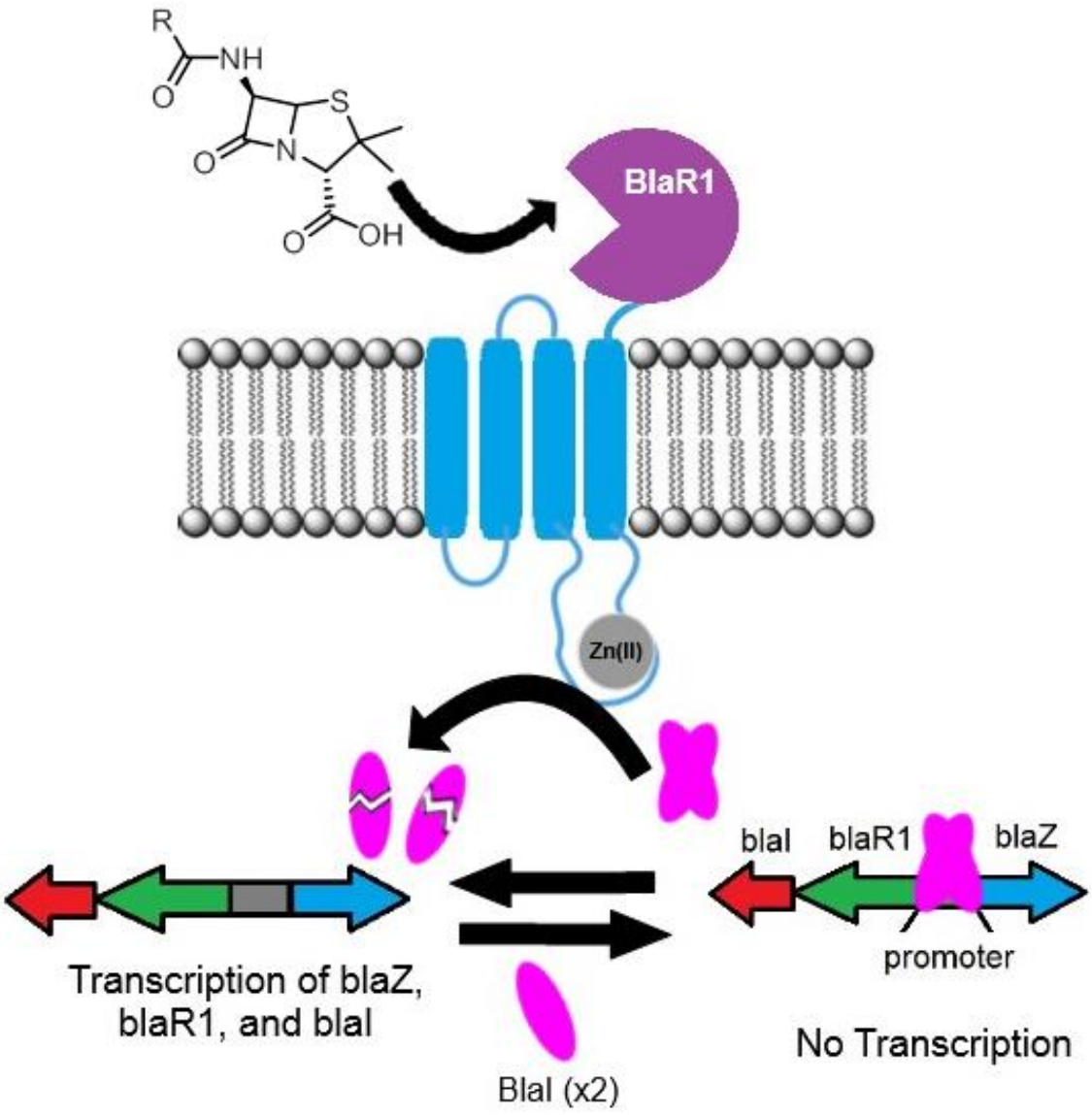

Figure 4.7: Schematic of the events involved in β-lactam induced transcription of β-lactamase and its regulatory machinery.

Recognition of β-lactam antibiotic at the cell surface by the BlaR1 sensor domain (purple) leads to activation of the cytoplasmic zinc protease (blue and gray). The protease cleaves the BlaI (pink) dimer from the promoter region of DNA allowing active transcription of β-lactamase from the *blaZ* gene as well as *blaI and blaR1*.

The structures of BlaI in its free and DNA-bound form (as a dimer) were solved in 2005 (Figure 4.8).[36] The 14.1 KD protein is 126 amino acids in length and contains an *N*-terminal winged helix-turn-helix DNA binding domain and a *C*-terminal dimerization domain. These structural features as well as the DNA binding interface are well conserved between BlaI and MecI.[37] Considerable conformational change has been observed between the free and DNA-bound forms of BlaI. BlaI exists in a 'closed' conformation when free in solution, and in an 'open' conformation when bound to DNA. This conformational change is hypothesized to maximize the BlaI-DNA interface to allow for stable binding. Additionally, the conformational change observed when BlaI is bound to DNA reveals a number of previously hidden 'cavities'. These are hypothesized to reveal the cleavage sites for BlaR1 mediated proteolysis. This scenario would thus ensure that BlaI is preferentially cleaved in its DNA-bound form.

Two elements of the BlaI DNA interaction still remained a mystery even after the initial structural investigation. The first was what initiates DNA binding and dimerization in the first place, and the second is whether BlaI forms the dimer sequentially upon DNA binding, or in solution, allowing the preformed dimer to bind DNA. A subsequent investigation revealed that BlaI is capable of binding the DNA as a monomer or as a dimer, and that both species are present unbound to DNA.[38] However, it is unfavorable for the dimer to form sequentially on the DNA (as one monomer binding at a time). So, it is more likely that BlaI binds the promoter as the monomer or as the dimer, but not as two monomers.

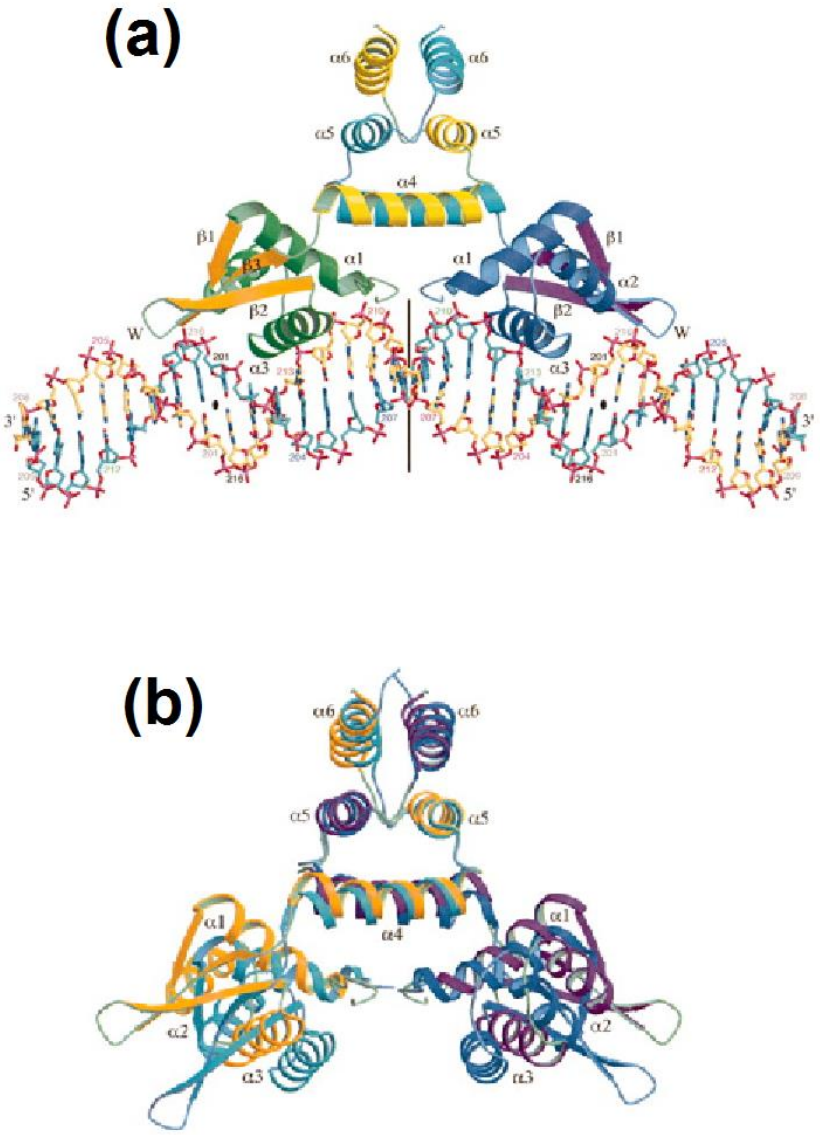

Figure 4.8: The structure of BlaI bound to the bla operator

(a) The structure of BlaI bound to DNA as a dimer. The winged helix-turn-helix DNA binding domains are coloured green and gold (left monomer) and blue and purple (right monomer), while the dimerization domains are yellow and cyan, respectively. (b) Superposition of the unbound BlaI and DNA-bound BlaI dimers. The unbound BlaI monomers are coloured cyan and blue, and the DNA-bound BlaI monomers are orange and magenta. This superposition shows that significant conformational change of BlaI takes place upon the dimer binding DNA. This image was adapted from Safo et al. (2005).[36]

Although the machinery that allows induction of PBP2a from the *mecA* gene is molecularly distinct, the high degree of homology between the regulatory proteins of the *mec* operon and those of the *bla* operon allow the *bla* regulatory machinery to control expression of PBP2a.[26,39] That is, activation of the BlaR1/BlaI signaling will induce expression of both β-lactamase and PBP2a especially in instances where the regulatory elements of the *mec* operon are non-functional. Although these induction pathways have been well studied, they have not yet been exploited as druggable targets for treatment of MRSA.

4.1.5 Attempts to develop resistance-modifying agents (RMAs) targeting β-lactam resistance determinants are ongoing.

Clavulanic acid, a potent serine β-lactamase inhibitor, was isolated from *Streptomyces clavulingerus* and characterized in 1977 (Figure 4.9).[40] Notably, clavulanic acid was reported to have very weak antibacterial activity on its own, but potentiated β-lactam antibiotics against a range of β-lactamase-producing bacteria. Clavulanic acid acts as a suicide inhibitor. It possesses a chemical core similar to that of β-lactams but does not dissociate from the β-lactamase active cite following hydrolysis, thereby inactivating the enzyme.[41] Although some analogs of clavulanic acid have been developed, these represent the only resistance-modifying agents (RMAs) for β-lactam antibiotics in clinical use today.[42] Although this class of β-lactamase inhibitor is effective against a variety of serine β-lactamases, there still exists a need for unique β-lactam RMAs, and those capable of potentiating β-lactams against strains producing PBP2a.

There have been numerous attempts to identify small molecule potentiators of antibiotics against multi-drug resistant (MDR) MRSA. Notable examples involve

identification of active components in natural product extracts (notably green tea extract) and combinatorial genetic and small molecule screening efforts.

The observation that green tea extracts seem to mitigate methicillin resistance in MRSA drove an effort to identify the active component and the mechanism whereby it exerted its effects.[43] Epicatechin gallate (ECG) was identified as the active agent, which was shown to exert its effects independently of β-lactamase inhibition or modulation of PBP2a expression.[44,45] ECG was eventually shown to alter cell wall morphology by

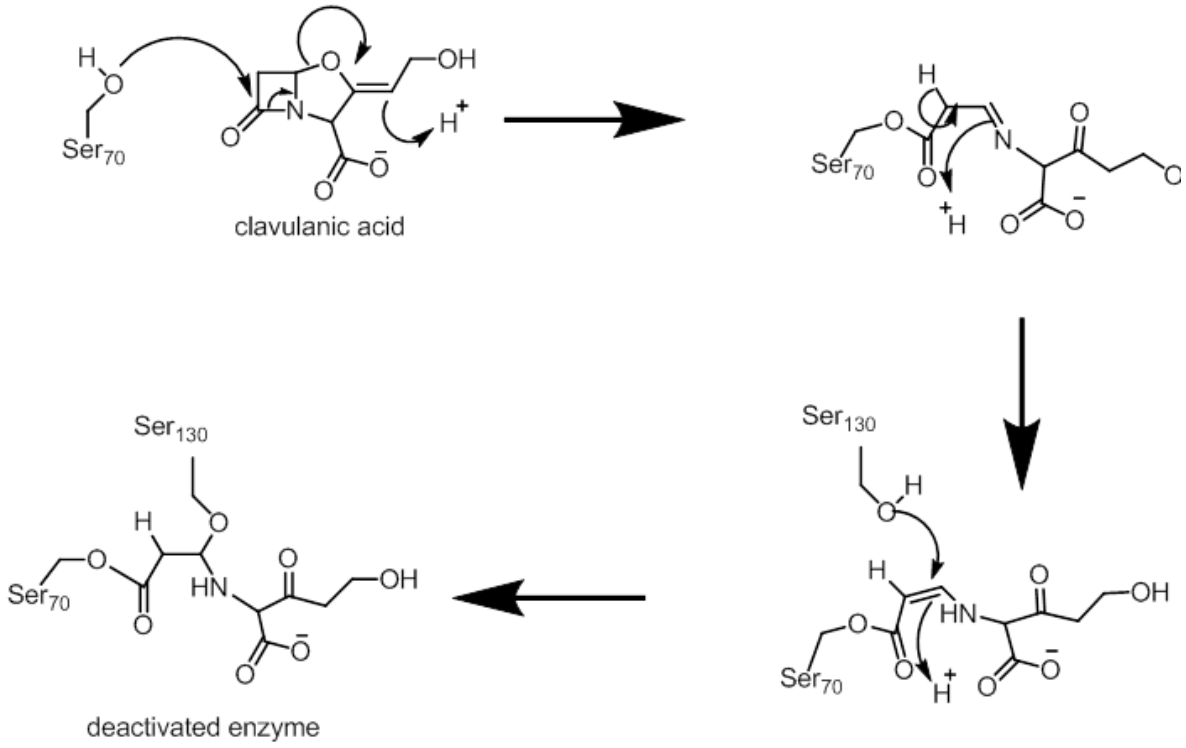

Figure 4.9: Mechanism of action of the β-lactamase inhibitor, clavulanic acid.

Following acylation of the active Ser_{70} in the β-lactamase active site, a transient imine intermediate is formed. This subsequently rearranges to form a stable enamine intermediate. This enamine can persist, or the enamine bond can undergo a crosslinking reaction with another nucleophile within the enzyme active site (commonly Ser_{130}), resulting in the permanently deactivated enzyme. Drawn based on Drawz and Bonomo (2010).[16]

inserting into the plasma membrane of *S. aureus* and delocalizing the peptidoglycan synthesis machinery[46,47]. Although this mechanism results in β-lactam potentiation, it is non-specific and also leads to cell death on its own in both resistant and non-resistant *S. aureus*.[48]

Another effort to develop β-lactam potentiating agents involved systematic identification of non-essential components involved in cell wall synthesis. This effort largely revolved around the wall teichoic acid (WTA) synthesis pathway.[49,50] WTA is a Gram-positive-specific cell wall polymer found in similar amounts to peptidoglycan. However, unlike peptidoglycan, the absence of WTA alone does not cause cell death in vitro, but does cause changes in cell morphology, growth rates, and proper orientation of cell wall proteins.[51] Through genetic screening and small molecule library screening approaches, several small molecule inhibitors of early and late stage WTA synthesis have been identified that act synergistically with β-lactam antibiotics.[52] Notably a TarO inhibitor (targocil, early stage synthesis factor) and a TarG inhibitor (tunamycin, late stage synthesis factor) have been reported. Although both of these show synergy against MRSA in combination with β-lactam antibiotics, late stage inhibition of WTA synthesis is bactericidal on its own, and so comes with a high probability of resistance development.[53] Additionally, although TarO inhibition is not lethal to cells on its own, targocil also targets essential eukaryotic machinery.

Although both these compounds (targocil and tunamycin) represent strides in the direction of developing viable RMAs against MRSA, there is still a need for more finely tuned small molecule potentiators of β-lactams, as well as those that are effective in Gram-negative as well as Gram-positive bacteria. To this end, we undertook detailed

mechanistic investigation of our previously identified β-lactam RMA (Of1). Our goals were to identify the mechanism of action (MOA) in order to assess whether or not its target may exist in Gram-negative cells, as well as to identify whether Of1 targets a formerly un-drugged pathway in MRSA.

4.1.6 The highly tuned specificity of Of1 prompted investigation of its mechanism of action.

We previously discovered a tricyclic indoline, Of1, that is capable of modulating the resistance of MRSA and *E. faecium* to β-lactam antibiotics.[54] We were highly intrigued by the specificity of Of1 for β-lactam antibiotics, a property indicating that its mechanism of action (MOA) involves a specific interaction with the β-lactam resistance machinery. During our structure-activity-relationship (SAR) studies of Of1, we discovered that its most active analog is highly synergistic with amoxicillin/clavulanic acid (FICI = 0.0315), with cefazolin (FICI=0.0156) and with meropenem (FICI = 0.0315).[55] This result indicates that Of1 targets an element of the resistance machinery that in some way influences and amplifies the MOA of β-lactam antibiotics. Intrigued by this development, we set forth to identify the pathway and molecular target of Of1. The studies described herein effectively narrowed the target pathway of Of1, and established that Of1 targets some aspect of the regulatory pathway responsible for inducible β-lactam resistance. Our most recent data indicates that Of1 acts by stabilizing the binding of BlaI to the promoter region of the *bla* operon, and likely the *mec* operon as well, thereby reducing expression of resistance determinants in MRSA. Going forward, we will validate this observation by undertaking detailed investigations of the binding mode of Of1.

4.2 Of1 acts synergistically with a known β-lactamase inhibitor, clavulanic acid.

In order to investigate the MOA of Of1, we first examined its synergistic activity with the known β-lactamase inhibitor, clavulanic acid. Clavulanic acid specifically inhibits β-lactamases that rely on an active serine residue to hydrolyze the β-lactam ring. These are the most common type of β-lactamase found in Gram-positive bacteria (Figure 4.9).[40] Clavulanic acid is a suicide inhibitor: that is, it acts by irreversibly acylating the active serine residue, thereby rendering the enzyme inactive. By assessing the degree to which Of1 has synergistic action with clavulanic acid, we could potentially gain information about its interaction with the β-lactam resistance machinery. An additive interaction between the two RMAs would indicate that Of1 either acts on the same target and at the same site as clavulanic acid (i.e. the β-lactamase catalytic site), or that it acts on a completely unrelated cellular process that also affects the β-lactam resistance phenotype. On the other hand, a synergistic interaction between the two is indicative of complementary activities upon a single pathway, or possibly action of Of1 at an allosteric site on the β-lactamase enzyme that amplifies the effects of clavulanic acid [56], or could potentially indicate that Of1 acts upstream of β-lactamase to amplify the effect of clavulanic acid.

In order to assess the synergistic action of Of1 in combination with clavulanic acid, a modified checkerboard fractional inhibitory concentration index (FICI) evaluation was performed.[57,58] Briefly, medium was supplemented with a low concentration of amoxicillin (4 µg/ml). Of1 was diluted in two-fold series down the plate, and clavulanic acid was diluted in two-fold series across the plate so that each well contained a different concentration combination of the two RMAs in combination with amoxicillin.

The FICI was calculated as previously described with the exception that only the concentration ratios of the two RMAs were taken into account since the concentration of antibiotic remained constant throughout the assay plate. [55] The result of this experiment showed that Of1 displayed synergy with clavulanic acid in two MRSA strains, ATCC BAA-44 and ATCC 33592, with FICI values of 0.25 and 0.06, respectively. Furthermore, we observed that the potentiation of clavulanic acid by Of1 was greater than the inverse.

Based on these data, we hypothesized that Of1 could exert its activity either by acting upstream of the β-lactamase enzyme, reducing its presence in the cell possibly by blocking its expression, or that Of1 could be a potential allosteric inhibitor of β-lactamase, which, when used in combination with clavulanic acid potentiates the active site inhibitor's effects, but still has β-lactamase inhibitory effect on its own. Although historically β-lactamase has not been known to have allosteric sites with effects on enzyme activity, such sites were recently identified by computational modeling.[59] In order to differentiate these hypotheses, we decided to conduct a set of β-lactamase enzyme activity assays to assess the effect of Of1 on β-lactamase activity and induction.

4.3 Of1 reduces β-lactamase activity in induced *S. aureus* cultures independently of β-lactamase inhibition.

Of1 was next assayed for its ability to inhibit the activity of naturally produced β-lactamase from MRSA and β-lactamase-producing methicillin-sensitive *Staphylococcus aureus* (MSSA) isolates. Three sequenced, representative strains were used for this

study based on their use previously in a similar investigation.[60] These were MRSA252, NRS123 (a.k.a, MW2), and NRS128 (a.k.a., NCTC8325). MRSA252 and NRS123 are both MRSA strains expressing both β-lactamase and PBP2a. Each of the two MRSA strains is known to have a fully intact and inducible *bla* operon.[61,62] NRS128 is a β-lactamase-producing MSSA strain, it has a fully intact *bla* operon, but does not produce PBP2a.[63] Of1 is capable of potentiating β-lactam antibiotics in all three strains (data not shown).

Activity of extracellular β-lactamase in the media of cultures induced with ampicillin to produce β-lactamase via the *bla* operon was monitored using the chromogenic reagent nitrocefin as described previously.[60] Nitrocefin is a cephalosporin

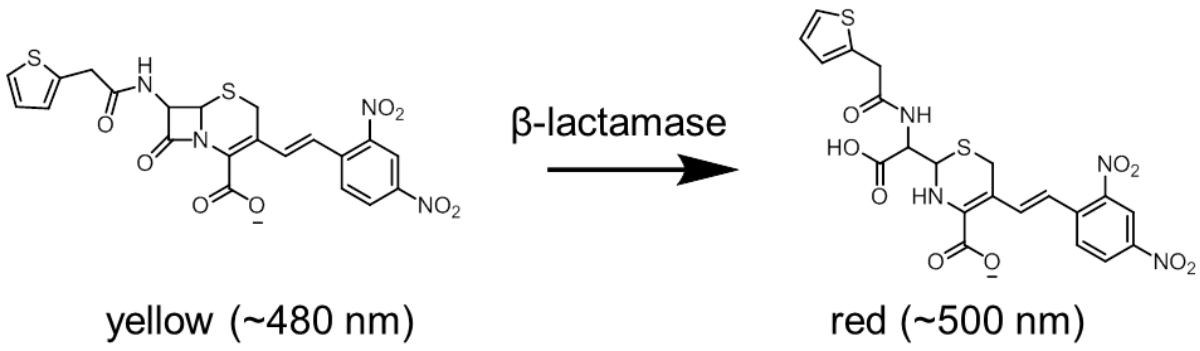

Figure 4.10: Structures of the intact and hydrolyzed colorigenic reagent, nitrocefin.

Upon hydrolysis by β-lactamase, the absorbance peak of nitrocefin shifts from ~480 nm (yellow) to ~500 nm (red). Absorbance at 500 nm can be used to track the activity of β-lactamase in real time in a saturating nitrocefin solution.

that is sensitive to all classes of β-lactamase.[64,65] The absorbance peak of intact nitrocefin is ~380 nm. However, when nitrocefin is hydrolyzed by β-lactamase, its absorbance peak shifts to ~500 nm (Figure 4.10). Real-time monitoring of absorbance as β-lactamase hydrolyzes a nitrocefin solution is thus a quantitative method to assess enzyme activity.

In order to assay the level of β-lactamase induction after β-lactam treatment, cultures were first grown to log phase and were subsequently induced to produce β-lactamase by adding ¼ MIC concentrations of ampicillin to the growth medium. Cultures were subsequently grown for one additional hour before the medium was separated from cells for β-lactamase activity analysis. The level of β-lactamase induction was estimated based on the initial rate of nitrocefin hydrolysis in media separated from induced cells as compared to un-induced cultures (baseline). OD_{600} values were assessed before cells were centrifuged. All cultures exhibited similar growth following β-lactam treatment. The level of β-lactamase induction differed between strains, but significant and consistent induction was observed for all strains tested (Figure 4.11).

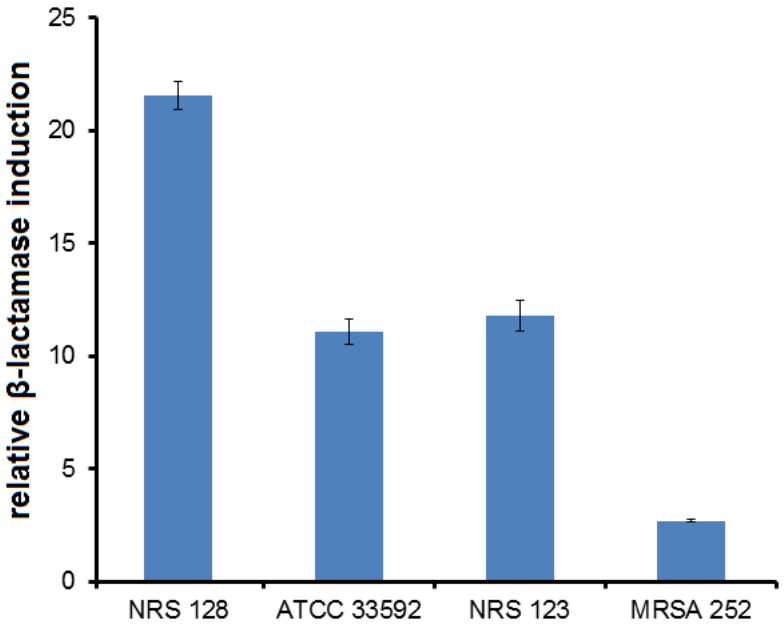

Figure 4.11: β-lactamase induction level of various S. aureus strains as measured by nitrocefin hydrolysis.

Individual *S. aureus* strains were induced to produce β-lactamase by treatment with ¼ MIC ampicillin for one hour. The rate of nitrocefin hydrolysis in induced strains was normalized to the baseline rate of hydrolysis to estimate the amount of β-lactamase induction. β-lactamase expression was inducible in all strains, but different levels of induction were observed.

Following β-lactamase induction and media collection, the effect of Of1 on induced β-lactamase activity was assayed. Media from induced cells was treated with various concentrations of Of1 or clavulanic acid. Predictably, clavulanic acid treatment reduced β-lactamase activity in a dose-dependent manner; however, treatment with Of1 had no effect on β-lactamase activity (Figure 4.12). Although this result does not give a definitive direction as to the target or target pathway of Of1, it serves to confirm that Of1 does not inhibit the catalytic site of β-lactamase, which is in agreement with the FICI

result. The lack of β-lactamase inhibition by Of1 also rules out the possibility that Of1 is acting at an allosteric site to inhibit the enzyme.

Although Of1 is not acting as an allosteric inhibitor, the FICI indicates that Of1 may be exerting its effect on a pathway involving β-lactamase. We thusly set forth to assess the effect of Of1 on β-lactam dependent β-lactamase induction in *S. aureus.* This investigation was performed by inducing β-lactamase production in cells while

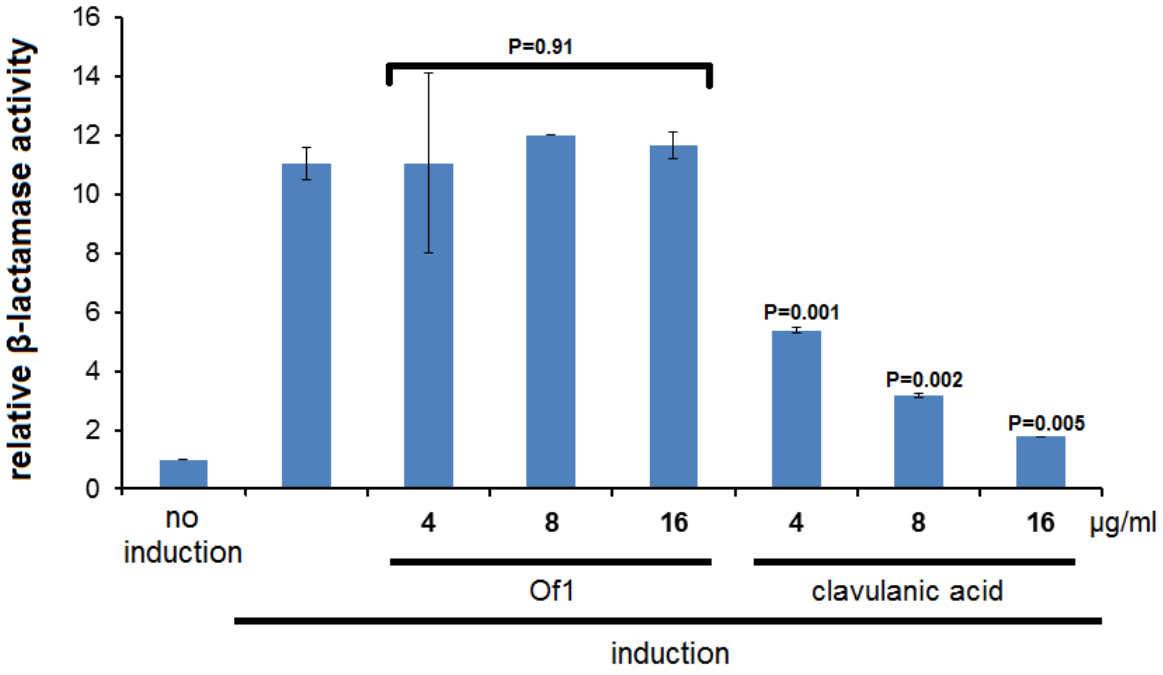

Figure 4.12: Treatment of β-lactamase preparations with Of1 does not result in reduced β-lactamase activity.

MRSA strains were treated with ¼ MIC ampicillin to induce β-lactamase production. After one hour, medium containing β-lactamase was separated and left untreated or was treated with various concentrations of Of1 or clavulanic acid. Although clavulanic acid treatment resulted in a dose-dependent reduction in β-lactamase activity, treatment with Of1 had no effect on β-lactamase activity (P=0.91). These representative data are from MRSA ATCC 33592. The experiment was performed in duplicate. ANOVA analysis of the variance of induced samples, compared with induced and treated samples was performed using Microsoft Excel. Error bars indicate standard deviation.

simultaneously treating cells with various concentrations of Of1 for one hour. Media was then separated from cells and β-lactamase activity was dose-dependent assayed in each condition using nitrocefin. Remarkably, treatment with Of1 afforded a reduction in β-lactamase activity in all MRSA strains tested (Figure 4.13). These results together indicate that while Of1 has no effect on the catalytic activity of the β-lactamase enzyme, it does exert an effect on the process leading to its production or activation in cells.

Although the end result of Of1 treatment seems to be blockage of β-lactam dependent

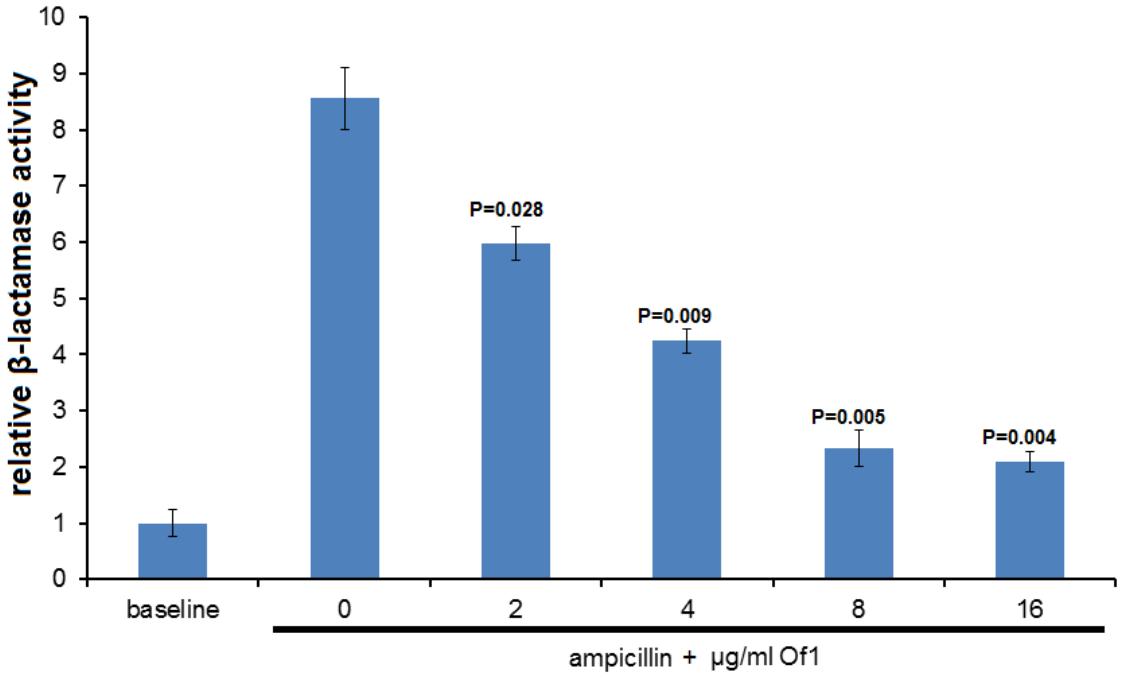

Figure 4.13: Treatment of *S. aureus* cells with Of1 blocks β-lactam dependent β-lactamase induction.

S. aureus strains were treated with vehicle, ¼ MIC ampicillin, or ampicillin and various concentrations of Of1. After one hour, medium containing β-lactamase was separated and assayed by monitoring nitrocefin hydrolysis. Treatment with Of1 in this way reduced β-lactamase activity in a dose-dependent manner, thus leading to the conclusion that Of1 blocks induction of β-lactamase. These representative data are from MRSA NRS 123. The experiment was performed in duplicate. ANOVA analysis of the variance of induced samples verses samples induced and treated with Of1 using Microsoft Excel. Error bars indicate standard deviation.

production of β-lactamase, the point of the induction pathway at which Of1 exerts its effects is still unclear. Additionally, although these results indicate a dose-dependent effect on β-lactamase production, the effect of Of1 on PBP2a, which is largely responsible for the resistance phenotype exhibited by MRSA, is as of yet unclear. In order to further our understanding of the MOA of Of1, we conducted an RT-qPCR gene expression analysis of the resistance determinants to assess the consequences of Of1 on the inducible expression of β-lactamase and PBP2a.

4.4 Of1 reduces transcription of the *mecA* and *blaZ* genes in β-lactam induced MRSA cells.

Based on the dose-dependent reduction in β-lactamase activity observed upon simultaneous treatment with Of1 under β-lactamase-inducing conditions, we hypothesized that Of1 is blocking the β-lactam-dependent induction of β-lactamase under control of the *bla* operon. Furthermore, although our β-lactamase activity assay results indicate that Of1 reduces β-lactamase activity in treated cells independently of β-lactamase inhibition, we were intrigued to assess the effect of Of1 on PBP2a induction. The possibility of Of1 targeting β-lactam-dependent induction of β-lactamase opened the possibility that it might also inhibit β-lactam-mediated induction of PBP2a as well. This hypothesis is driven by multiple lines of evidence that show cross-talk between the *mec* and *bla* induction machinery.[39,66–68] Through various investigations, it has been established that the *bla* induction machinery is capable of also regulating expression of PBP2a from the *mecA* gene. This development is crucial for regulation of PBP2a in situations where its regulatory elements (MecR1 and MecI) are mutated or deleted, but has also been shown to occur in cases where an intact *mec* operon exists. We thus

performed our gene expression studies using primers for β-lactamase (*blaZ*) and PBP2a (*mecA*).

Two representative strains were used for the RT-qPCR gene expression assay, NRS128 (which does not express PBP2a) and NRS123 (which expresses both PBP2a and β-lactamase). Cells were grown to log phase and treated with ¼ MIC concentrations of ampicillin, ampicillin and various doses of Of1, or vehicle (baseline). After treatment, cells were allowed to grow for one hour before cells were collected, lysed and their total RNA isolated. RT-qPCR was performed using previously reported primers for *blaZ* and *mecA*, and the transcript levels of these genes were normalized to 16s rRNA levels (Primers used are listed in Table 4.2, materials and methods) [69,70].

In agreement with our β-lactamase activity assay result, treatment of both *S. aureus* strains with Of1 in conjunction with ampicillin blocks transcription of the *blaZ* gene, consequently producing the enzymatic phenotype observed previously. Furthermore, the reduction of *blaZ* transcription was dose-dependent, in accordance with our hypothesis of Of1 action, and was observed in both strains tested (Figure 4.14). Extraordinarily, treatment with Of1 in this manner also produced a dose-dependent reduction in *mecA* transcription in NRS123, indicating that Of1 not only exerts its effect on β-lactamase induction and expression, but that it also reduces PBP2a expression in the same manner.

Our RT-qPCR result indicates that Of1 targets some aspect of the *bla*/*mec* induction pathway and accordingly reduces transcription of the resistance determinants. There is a high degree of homology between the two induction pathways and the mechanisms of induction are nearly identical.

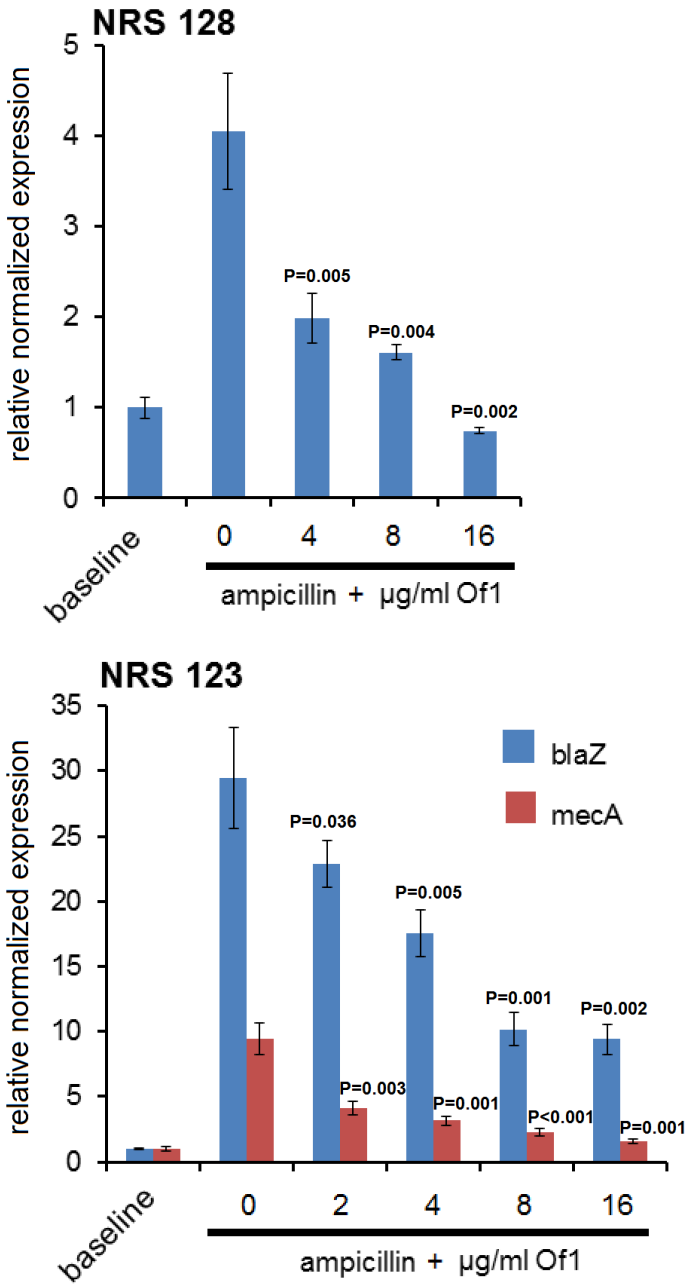

Figure 4.14: Treatment of *S. aureus* cells with Of1 blocks β-lactam dependent β-lactamase and PBP2a transcription.

S. aureus strains were treated with vehicle, ¼ MIC ampicillin, or ampicillin and various concentrations of Of1. After one hour, cells were lysed and total RNA was isolated and used for RT-qPCR. Transcript levels of *blaZ* and *mecA* were normalized to 16s rRNA. Of1 was capable of reducing *blaZ* and *mecA* transcription in cells induced with ampicillin. Error bars indicate standard error. Experiments were performed in triplicate, and all statistical analysis was performed using Bio-Rad CFX Manager software.

The prospect that Of1 targets both pathways simultaneously is possible. However, it is far more likely that Of1 primarily targets the *bla* induction machinery, since β-lactamase induction is not strongly controlled by the *mec* operon, while PBP2a induction is reported, in many cases, to be under control of the *bla* operon, which contributes to *mec* regulation even in instances where a fully intact *mec* operon is present.

Regardless of its molecular target, these results, together with Of1's specificity, indicate that its target resides within the *mec/bla* induction pathways. This development is highly noteworthy as these pathways have never been druggable specifically, not for lack of trying.[44,71] We have thus potentially discovered a new way to drug a formerly undruggable induction pathway. Our excitement over this discovery notwithstanding, the molecular target of Of1 still remains a mystery. The remainder of this investigation involved biochemical investigation of candidate targets for their response to Of1 *in vitro*, thereby defining the target of Of1, or ruling out potential mechanisms of action.

4.5 Of1 enhances the binding of the BlaI dimer to the *bla* operon.

Based on our observation that Of1 modulates expression of the MRSA resistance determinants (*blaZ* and *mecA*), we hypothesized that Of1 is somehow interrupting the two-component expression system for one or both of these genes[39,60,72]. We thus decided to assess the effect of Of1 on candidate portions of the regulatory system, starting with the effect of Of1 on DNA binding by the repressor protein BlaI. The promoter region of the *bla* operator consists of two palindromic sequences, both of which are bound by BlaI, known as the 'Z-dyad' and the 'R1-dyad', located upstream of

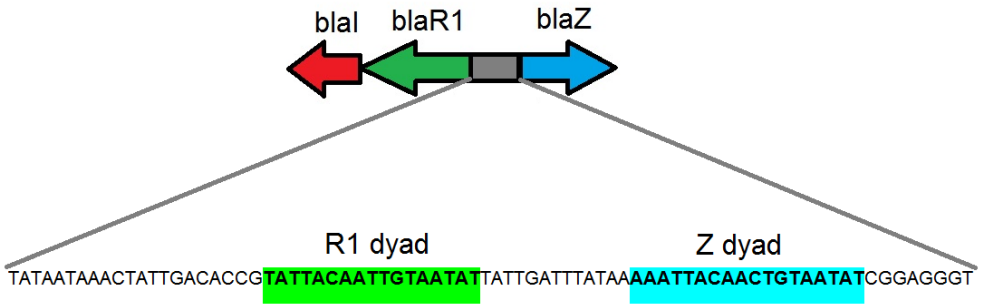

Figure 4.15: BlaI binding sequences within the bla promoter.

The promoter region of the *bla* operon contains two sequences where BlaI binds, upstream of the *blaZ* gene and the divergently transcribed *blaR1* and *blaI genes*, respectively.

the genes encoding β-lactamase and BlaR1/BlaI, respectively (Figure 4.15).[25] Cleavage of BlaI bound to the DNA by the activated BlaR1 allows expression of the resistant determinant, β-lactamase, as well as the regulatory machinery. Although expression of these is necessarily greater upon activation in the presence of β-lactam, there is a low level of basal expression from the operator, allowing for basal expression of the repressor (BlaI), the sensor/activator (BlaR1), as well as β-lactamase in the absence of β-lactam induction of the system.[73] Since expression from the *bla* operon is initiated by removal of BlaI from the DNA (either by proteolysis or by dissociation), stabilizing the interaction between the DNA and BlaI should result in reduced expression from the operon and thus reduced expression of β-lactamase. Furthermore, since BlaI is known to cross-regulate the expression of PBP2a from *mecA* (located on the *mec* operon), stabilization of BlaI bound to DNA should also result in reduced expression of PBP2a.[66] We therefore tested the ability of Of1 to stabilize binding between BlaI and the *bla* operator DNA using fluorescence polarization (FP).

The *blaI* gene was amplified by PCR from pI258 isolated from *S. aureus* NRS128 (Table 4.2). The PCR fragment was cloned into plasmid pET-28c(+) so that the protein expressed with a 6xHis tag for ease of purification. BlaI was expressed in *E. coli* BL-21 and purified using immobilized metal ion affinity chromatography (IMAC). This purification achieved approximately 70% purity of BlaI, which is sufficient for FP (Figure 4.16). We initially investigated the effect of Of1 on BlaI binding to the Z-dyad of the *bla* operator. For this investigation, a 30 bp oligonucleotide including the 18 bp palindromic sequence of the Z-dyad was obtained, as well as its reverse complement (Life Technologies, Table 4.2). One strand was 5' labeled with Alexafluor-488 to facilitate binding analysis by fluorescence polarization (FP). Oligonucleotides were annealed

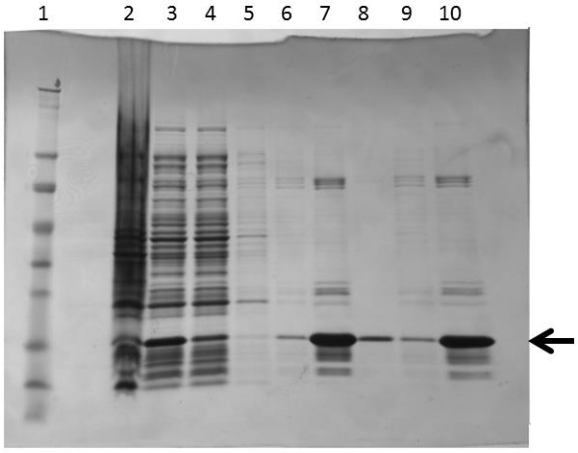

Figure 4.16: Enrichment of BlaI for FP binding experiments.

Stages of purification are illustrated by SDS-PAGE. 6x His-tagged BlaI (arrow) was purified using a Ni(II)-NTA column followed by dialysis to remove imidazole. Lane 1: marker, lane 2: cell lysate, lane 3: cleared lysate, lane 4: Ni(II) column flowthrough, lane 5: 50 mM imidazole wash, lane 6: 100 mM imidazole elution (E1), lane 7: 500 mM imidazole elution (E2), lane 8: residual BlaI on beads, lane 9: dialyzed E1, lane 10: dialyzed E2. BlaI concentration was quantified using a NanoDrop 2000, and purity determined using ImageJ.

using standard protocols.

In order to investigate the effect of Of1 on BlaI binding to dsDNA, we first assessed the binding of BlaI to the Z-dyad in the absence of Of1 using a similar method to previous reports.[38] The data do not fit to a model representing a 1:1 binding mode, or a model in which only a pre-formed dimer binds the DNA. Equation 1 was thus derived based on previous FP analyses, and well known mathematical models for binding: [74,75]

$$\Delta mP = P_f + (P_{max\cdot M} - P_f) * \left(\frac{[M]}{K_{d2} + [M]}\right) + (P_{max\cdot D} - P_f) * \left(\frac{x - [M]}{K_{d3} + (x - [M])}\right) \text{(Eq. 1)}$$

where

$$[M] = \frac{-K_{d1} \pm \sqrt{K_{d1}^2 + 8 * K_{d1} * x}}{4}$$

Equation 1 takes into account the BlaI monomer binding DNA (K_{d2}) as well as the BlaI dimer bound to DNA (K_{d3}). Using this binding model, we were also able to verify the dissociation constant for BlaI dimer formation (K_{d1}) which was consistent with previous reports.[38] The apparent K_d for the formation of the DNA-dimer complex via sequential binding of two monomers (K_{d4}) was calculated based on the following relationship:

$$K_{d4} = \frac{K_{d3} \times K_{d1}}{K_{d2}} \text{(Eq. 2)}$$

The effect of Of1 on BlaI DNA binding was assessed by conducting two simultaneous FP binding assays in the presence of a single concentration of Of1 (20 µg/ml) or vehicle (1% DMSO). We found that the presence of Of1 in the binding assay changes the mode of binding significantly (Figure 4.17).

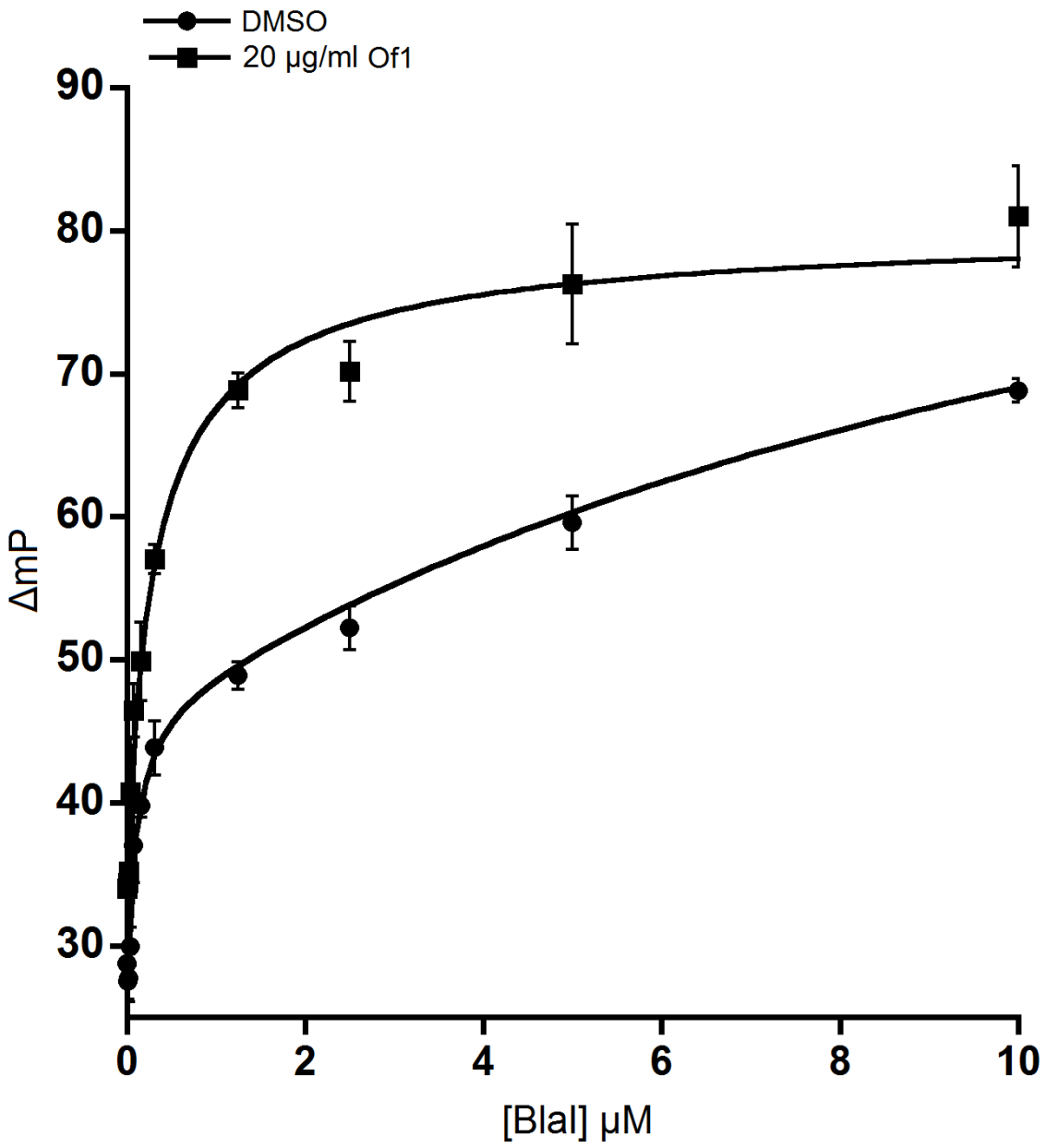

Figure 4.17: Binding of BlaI to the Z-dyad of the *bla* operator sequence in the absence and presence of Of1.

FP binding assays were conducted using labeled dsDNA corresponding to the Z-dyad sequence. Two binding assays were conducted simultaneously: BlaI binding in the presence of vehicle only (DMSO) and in the presence of 20 µg/ml Of1 in DMSO. Addition of Of1 to the system enhanced BlaI binding to the Z-dyad sequence.

Table 4.1: Binding affinities of BlaI calculated in the presence and absence of Of1.

Parameter[a]	Vehicle[a]	20 µg/ml Of1[a]
K_{d1}	1.9 ± 0.035	1.8 ± 0.064
K_{d2}	0.60 ± 0.35	0.52 ± 0.35
K_{d3}	9.3 ± 2.8	0.11 ± 0.17
K_{d4}	29.5 ± 16.7	0.38 ± 0.36

[a]All K_d values are the apparent values for the condition. [b]All K_d values are expressed in µM. K_{d1} corresponds to BlaI dimerization, K_{d2} corresponds to the BlaI monomer binding to DNA, and K_{d3} corresponds to the dimer-DNA binding interaction.

Intriguingly, although the addition of Of1 does not alter the apparent affinity of the monomer-DNA interaction, it does seem to significantly reduce the apparent K_{d3} and K_{d4} values, which both correspond to stabilization of the BlaI dimer bound to DNA (Table 4.1). In addition, K_{d1}, corresponding to the dissociation constant for the free dimer, was not significantly changed. This observation indicates that Of1 specifically interacts with the BlaI dimer bound to DNA, and stabilizes this interaction. This is very intriguing, considering that structural investigations of BlaI in its DNA-bound and free forms indicate that significant conformational changes occur upon dimer binding to DNA, which seem to result in the formation of a number of 'cavities'.[36] The authors hypothesized that these structural shifts allow access to the BlaR1 cleavage site on BlaI, allowing proteolysis and transcription from the *bla* operon. The conformational changes seen in the dimeric form of BlaI bound to DNA would thus make this form of the protein more prone to proteolytic attack by the BlaR1 protease. It therefore stands to

reason that stabilization of the BlaI dimer bound to DNA would effectively reduce expression from the *bla* operon. In addition, it is possible that Of1 could bind this complex in such a way that could potentially block proteolysis by the BlaR1 protease.

Although these data indicate a potential mechanism of action of Of1, they are still preliminary in nature. More follow-up is needed to determine the exact mode of binding of Of1, its preferred binding partner, as well as the effect of Of1 interacting with the BlaI-DNA complex on BlaI proteolysis. However, these results are extremely promising and indicate that we have identified a potential target and mechanism for Of1.

4.6 Conclusions and future directions

Based on our initial discovery of a compound, Of1, capable of re-sensitizing MRSA to β-lactam antibiotics, we decided to investigate its mechanism of action. Based on the ability of Of1 to potentiate the amoxicillin/clavulanic acid combination (Augmentin), we first assessed the degree of synergy of the Of1/clavulanic acid combination using a modified checkerboard assay and calculating the FICI. We found that Of1 displays significant synergy with clavulanic acid, indicating that the mode of action (MOA) of Of1 is related to that of clavulanic acid, but they do not share a target (i.e. β-lactamase). With this result in hand, we sought to confirm that Of1 does not inhibit β-lactamase. Based on the checkerboard assay result, we thought it unlikely that Of1 would be targeting the active site of β-lactamase, but this result does not rule out the possibility that Of1 targets an allosteric site on the β-lactamase enzyme. We investigated this possibility and found that Of1 has no inhibitory activity against β-lactamase. However, Of1 does inhibit production of β-lactamase in cells that have been

induced to produce the enzyme by addition of β-lactam to their growth medium. We discovered that this effect shows dose-dependence on Of1. To follow-up on this result, we assessed the ability of Of1 to block transcription of β-lactamase and PBP2a in β-lactam-induced cells. We found that Of1 is capable of reducing transcription of, not one, but both of these β-lactam resistance determinants. These data together indicated to us that Of1 may block some element of the two-component induction pathway responsible for inducible expression of β-lactamase and PBP2a. We hypothesized that Of1 exerted its effect on the β-lactamase induction pathway rather than targeting both pathways independently, since the *bla* regulatory machinery is known to interact with the *mec* operon, but the inverse is uncommon.[26,76]

We conducted a preliminary investigation of the effect of Of1 on BlaI promoter binding using an FP binding assay in the presence or absence of a constant concentration of Of1. To our delight, we observed that Of1 enhances the binding interaction between the DNA and the dimeric form of BlaI. We hypothesize that stabilizing this interaction increases the amount of *bla* operon DNA bound to BlaI and therefore reduces transcription from the *bla* operon. It is likely, but remains to be tested, that a similar outcome will be observed for the *mec* operator promoter region. Reduction in transcription from these sites would thus result in reduced expression of the MRSA resistance determinants and the observed re-sensitized phenotypes. Our working hypothesis is that Of1 binds the DNA-dimer complex and prevents dissociation of BlaI, thereby reducing transcription from the *bla* operon (Figure 4.18). Although this result is preliminary, we believe that this is a large step toward identifying the exact molecular target of Of1.

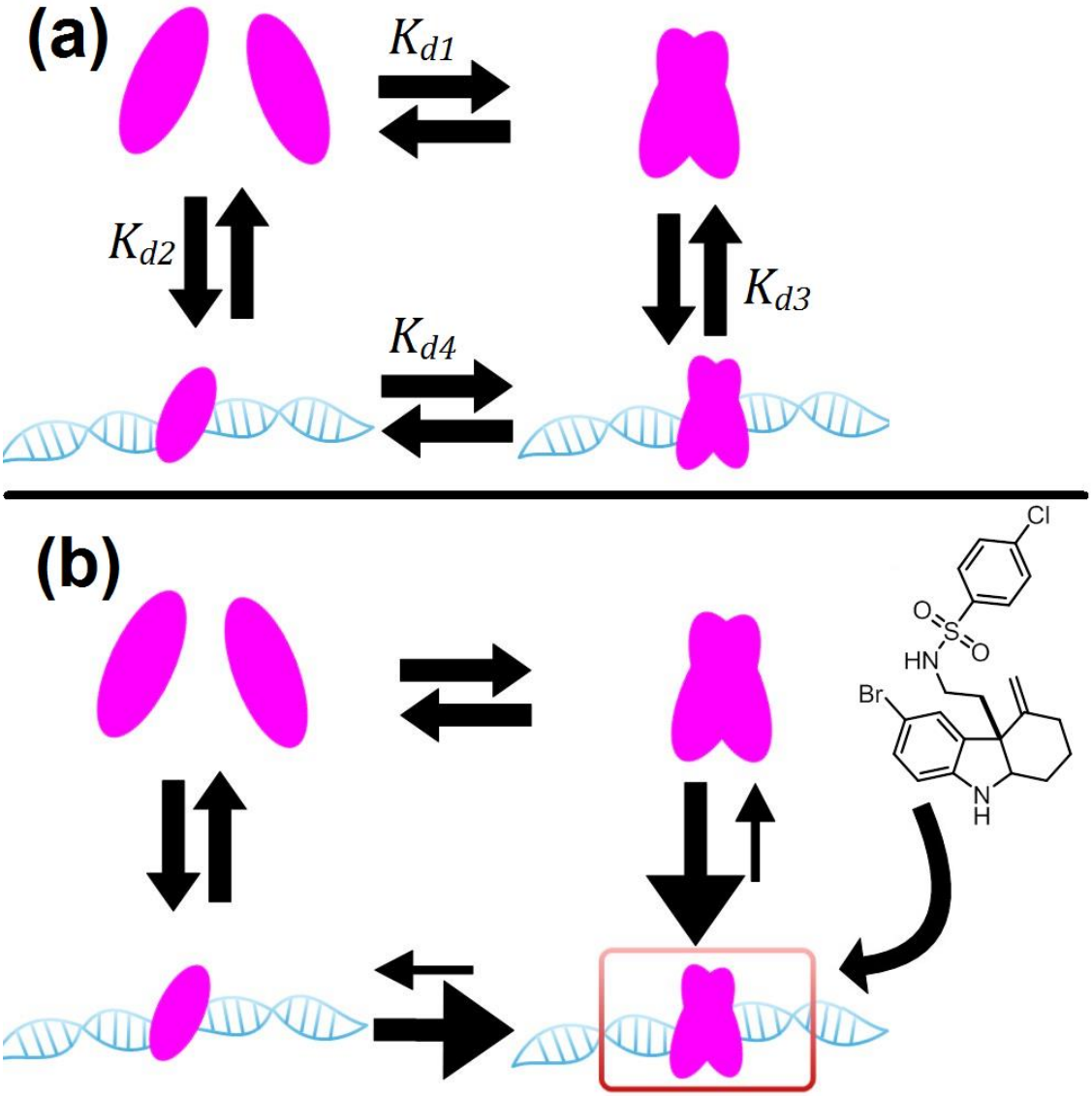

Figure 4.18: A model for the observed effects of Of1.

Models for BlaI-DNA binding equilibria are shown in the absence (a) and presence (b) of Of1. Based on the data we have established this working model for the mechanism of action of Of1. Four binding equilibria are represented. Formation of the free BlaI dimer (K_{d1}), the BlaI monomer binding to DNA (K_{d2}), formation of the DNA-BlaI-dimer complex (K_{d3}), and formation of the DNA/dimer complex as a result of two monomers binding the DNA (K_{d4}). Addition of Of1 visibly enhanced binding of BlaI to DNA, but when the data were fit, only K_{d3} showed significant reduction. We thus propose that Of1 exerts its effect by binding to and stabilizing the DNA-dimer complex.

Going forward, we will perform a series of experiments to confirm our initial observation. We have not yet tested the ability of Of1 to inhibit proteolysis of BlaI by BlaR1. Although we had intended to perform this assay in parallel with the FP binding assay, difficulties cloning BlaR1 did not allow for sufficient time to conduct the experiment. The plasmid containing inducible BlaR1 was, however, successfully constructed and we will be able to use it in experiments shortly. We will assess the ability of Of1 to inhibit BlaR1 dependent proteolysis of BlaI using a previously described method.[77] We will also assess the effect of Of1 on BlaI and MecI binding to the *mec* operator promoter region. This will give valuable insight as to the specificity of Of1. Although our working hypothesis is that Of1 preferentially targets BlaI bound to DNA as a dimer, because of the high degree of homology between MecI and BlaI, it is possible that Of1 interacts with both.

In addition to the investigations identified already, we will also use a fluorescent analog of Of1 ($Of1^{fluor}$), to confirm our hypothesized MOA, and establish the form of BlaI to which Of1 binds. FP binding experiments will be conducted using $Of1^{fluor}$ as a tracer. This will allow differentiation of Of1 binding to BlaI (as a dimer) alone, the DNA alone, or the BlaI DNA complex.

If Of1 is indeed exerting its effect by targeting the BlaI-DNA complex and stabilizing the interaction, this would represent a novel mechanism of small molecule inhibition. Although targeting two-component induction systems has recently been a sought after target, so far, only one other instance of a small molecule targeting a two-component regulatory system for resistance modulation has been reported.[78–80] Such a mechanism would not only represent the first of its kind for modulation of β-lactam

resistance, but also provides a resistance-modifying strategy against both β-lactamase and PBP2a, a feat which has not yet been realized.

Due to the stark lack of novel antibiotics on the market, there has been an increased interest in alternative antimicrobial approaches.[81,82] In addition to the obvious advantage RMAs provide by extending the usable life of known antibiotics, there has also been evidence that resistance evolution to RMA/antibiotic combinations is far less likely than resistance evolution to antibiotics targeting essential pathways. Here we have reported a mechanistic investigation of a β-lactam RMA and propose that it acts by stabilizing the BlaI repressor-DNA interaction, thereby reducing expression of resistance determinants. This represents an entirely novel mechanism for combating β-lactam resistance.

4.7 Materials and methods

4.7.1 Bacterial strains and reagents.

Strains ATCC BAA-44 (MRSA) and ATCC 25923 (MSSA) were gifts from Daniel Feldheim and Charles McHenry's laboratories, respectively. Strain ATCC 33592, and MRSA 252 were purchased from the ATCC. *S. aureus* NRS123 and NRS128 were obtained from BEI resources. All antimicrobial compounds were purchased from Sigma-Aldrich. The growth media used for all MIC experiments was Mueller Hinton Broth (MHB) purchased from HIMEDIA through VWR (cat: 95039-356).

Table 4.2: Oligonucleotides used in this study.

Primer name	Application	Sequence
RT-q_blaZ_FWD	blaZ RT-qPCR (forward primer)	5’-acttcaacacctgctgctttc-3’
RT-q_blaZ_REV	blaZ RT-qPCR (reverse primer)	5’-tgaccacttttatcagcaacc-3’
RT-q_mecA_FWD	mecA RT-qPCR (forward primer)	5′-ctcaggtactgctatccacc-3′
RT-q_mecA_REV	mecA RT-qPCR (reverse primer)	5′-ggaacttgttgagcagagg-3′
RT-q_16s_FWD	16s RT-qPCR (forward primer)	5′-ccagcagccgcggtaat-3′
RT-q_16s_REV	16s RT-qPCR (reverse primer)	5′-cgcgctttacgcccaata-3′
His/T7_BlaI_FW_BamHI	Cloning blaI into pET-28c(+), forward primer, contains BamHI restriction site	5’-cgc**ggatcc**tcatggccaataagcaagttgaa-3’
His/T7_BlaI_RV_HindIII	Cloning blaI into pET-28c(+), reverse primer, contains HindIII restriction site	5’-atgc**aagctt**acttttactaatatcatttaaaatg-3’
FP-label Z-dyad	Labeled oligo for BlaI FP binding experiment	5’-AlexaFluor488-atttataaaaattacaactgtaatatcgga-3’
Z-dyad reverse complement	unlabeled oligo (complement) for BlaI FP binding experiment	5’-tccgatattacagttgtaatttttataaat-3’

4.7.2 Checkerboard FICI determination.

Checkerboard assays were performed as described previously with the notable difference that media was supplemented with amoxicillin at a constant concentration (4 μg/mL).[55,58] Of1 diluted down the columns of a 96-well microplate, while clavulanic acid was diluted across the rows. Plates were prepared in duplicate. The inoculum was prepared by diluting a bacterial day culture (OD_{600} 0.15-0.4) to OD_{600} 0.002. This dilution was further diluted two fold when added to the prepared 96-well microplates for a final inoculum concentration of OD_{600} 0.001. All plates were incubated at 37°C with shaking for 18 hours before results were interpreted. The FICI was calculated as described previously using the parameters calculated in the presence of amoxicillin.[55,58]

4.7.3 β-lactamase activity assays.

An overnight culture of MRSA was grown in MHB and sub-cultured 1:100. Cells were grown to OD_{600} of ~0.5 prior to treatment. Cells were divided into 5-6 10 mL fractions in MHB and treated with vehicle (DMSO), ampicillin at ¼ of the MIC value, or ampicillin and various concentrations of Of1 (2-16 μg/mL). Samples were incubated with shaking at 37 ˚C for 1 hour. Cell growth was consistent regardless of treatment. Cells were placed on ice and media was separated from cells by centrifugation (3200xg, 4°C, 30 min). Detection of 3 β-lactamase activity in media from cultured cells was performed as described previously.[60] Media was equilibrated to room temperature prior to addition of the colorigenic agent, nitrocefin. 99 μL of media from each treatment was added to a UV-optical bottom 96-well plate. To each well, 1 μL of a 10 mM nitrocefin stock (in DMSO) was added (to afford a final, saturating, concentration of 100 μM). Nitrocefin hydrolysis was immediately monitored by tracking absorbance at 492 nm in

real time using the Perkin Elmer EnVision plate reader. The initial rate of hydrolysis was obtained from the slope of the time course which was linear in the first several minutes of monitoring. This initial rate was used as a proxy for the relative concentration of β-lactamase in the media. The initial rate for each treatment condition was normalized to the baseline rate of hydrolysis to establish the 'fold' of β-lactamase induction.

4.7.4 RT-qPCR gene expression analysis.

An overnight culture of MRSA was grown in MHB and sub-cultured 1:100. Cells were grown to OD_{600} of ~0.5 prior to treatment. Cells were divided into 5-6 10 mL fractions in MHB and treated with vehicle (DMSO), ampicillin at ¼ of the MIC value, or ampicillin and various concentrations of Of1 (2-16 μg/mL). Samples were incubated with shaking at 37 ˚C for 1 hour. 5 mL RNALOCK Reagent (Omega Biotech) was added to each sample cells were collected by centrifugation (4000 rpm, 4˚C, 20 min). Cells were resuspended in a 1:1 Trizol (Life technologies)/BRK-lysis buffer (Omega Biotech) solution (1 mL total). Cells were lysed by sonication using a micro-tip (output 35, 6 x 30s pulses). Total RNA was isolated using the EZNA Bacterial RNA kit according to the manufacturer's instructions (Omega Biotech). RNA concentration determined using a NanoDrop 2000 spectrophotometer (Thermo Fisher). RT-qPCR performed using qScript™ One-Step SYBR Green qRT-PCR master mix according to the manufacturer's instructions (Quanta Biosciences) and primers detecting *blaZ* and *mecA* mRNA transcripts. Transcript levels of *blaZ* and *mecA* were normalized to *S. aureus* 16s rRNA, which was detected in the same manner. RT-qPCR was performed using the CFX384 detection system from BioRad with accompanying software.

4.7.5 Cloning of blaI and blaR1.

Cloning of the *blaI* and *blaR1* genes was performed similarly to previous reports.[38,60,77] The plasmid pI258 was extracted from NRS128 and used as the source of the *blaI* and *blaR1* genes.[83] The presence of pI258 was confirmed by restriction digest with EcoRI.[18] Primers were designed using the full length sequences of *blaI* and *blaR1* and were designed for insertion into the pET-28c(+) vector (Novagen). Primers are listed in table 4.1. The *blaI* insert was designed to contain *N*-terminal T7 and 6xHis tags, and the *blaR1* insert was designed to include an *N*-terminal 6xHis tag. Primers used to amplify *blaI* contained recognition sites for BamHI and HindIII restriction endonucleases and those used amplify *blaRI* contained restriction sequences for recognition by NdeI and XhoI. SyFi high-fidelity DNA polymerase (Empirical bioscience) was used to amplify both genes. PCR products were cleaned up using Cycle-Pure PCR cleanup kit (Omega) and were subsequently digested with the appropriate restriction enzymes. Each digested fragment was run on a 1% agarose gel along with digested pET-28c(+) and purified from the gel using QIAquick Gel Extraction Kit (QAIGEN). The fragments were subsequently ligated into pET-28c(+) using T4 DNA ligase following the manufacturer's instructions (New England Biolabs). A portion of the ligation mixture was used to transform competent DH5α cells using a common heat shock protocol. Transformed cells were transferred to LB and grown for one hour at 37°C with shaking. Following the outgrowth period, cells were plated onto LB agar containing 50 µg/ml kanamycin and allowed to incubate overnight at 37°C. Following overnight incubation, Plasmid DNA from multiple transformants was isolated using the QAIprep Spin Miniprep Kit (QAIGEN), and a portion of the colony was subject to colony PCR for the insert.

Isolated plasmids were digested with the appropriate restriction endonucleases to confirm the presence of the insert. Plasmids that showed the appropriate sized insert following restriction digest were sent out for sequencing (Quintara Biosciences). The plasmids were designated pET_T7.HisBlaI and pET_HisBlaR1, respectively.

4.7.6 Expression and purification of BlaI.

Competent E. coli Bl-21 cells were transformed with pET_T7.HisBlaI using a standard heat shock protocol. Transformed cells were grown on LB agar containing 50 µg/mL kanamycin. Plates were sealed with parafilm and stored at 4°C. A single colony of transformed Bl-21 was isolated and grown overnight in LB supplemented with 50 µg/mL kanamycin. The next day, the overnight culture was subcultured 1:100 in LB with 50 µg/mL kanamycin and grown at 37°C to OD_{600} ~0.8. Cultures were then cold-shocked in an ice water bath for 30 minutes. 0.5 mM IPTG was then added and cultures were incubated at 18°C overnight to allow induction of BlaI. After induction, cells were collected by centrifugation (4000xg, 4°C, 30 min). The cell pellets were flash frozen in liquid nitrogen and stored at -80°C.

For purification, cell pellets were thawed in lysis buffer (50 mM HEPES, pH 7.6, 0.2 M NaCl, 5% glycerol, 2.5 ug/ml DNAseI, 20 mM imidazole) and lysed by sonication (output 80, 7 x 15s pulses). Lysed cells were centrifuged to separate the lysate from the insoluble fraction at 10000 rpm for 45 minutes at 4°C. The cleared lysate was passed through a column containing high density nickel-NTA beads (Gold Biotechnology) by gravity flow. The column was washed with 10 column volumes of wash buffer (50 mM HEPES, pH 7.6, 0.2 M NaCl, 5% glycerol, 100 mM imidazole) and BlaI was eluted with

a high imidazole elution buffer (50 mM HEPES, pH 7.6, 0.2 M NaCl, 5% glycerol, 500 mM imidazole). The elution was dialyzed using a Slide-A-Lyzer™ 3.5K MWCO Dialysis Cassette in 300x volume assay buffer (50 mM HEPES, pH 7.6, 0.2 M NaCl, 5% glycerol) with two three hour buffer changes and one 16 hour change. Protein concentration was determined using NanoDrop 2000 spectrophotometer, and purity determined using a coomassie stained SDS-PAGE gel.

4.7.7 Fluorescence polarization binding experiments.

Fluorescence polarization binding assays were performed similarly to previous reports.[38] The DNA sequences used in this study correspond to the Z-dyad of the *bla* operator. These were 5'Aalexa Fluor 488-atttataaaaattacaactgtaatatcgga-3' and its reverse complement, 5'-tccgatattacagttgtaatttttataaat-3'. These were annealed at a 1:1 molar ratio to afford the dsDNA FP tracer. Dilutions of BlaI (up to 35 μM) were prepared in black, low-binding, half area 96-well plates (Corning 3993). To each concentration of BlaI, labeled dsDNA was added to a final concentration of 1 nM. The reaction was incubated in the dark and FP was read using the Perkin Elmer EnVision microplate reader. Time points were taken at 10, 30, and 90 minutes. The assay was performed in triplicate in the presence of 20 μg/mL Of1 or vehicle. The final concentration of DMSO in all conditions was 1%. The data was plotted as a function of BlaI concentration and fit to equation 1 using KaleidaGraph (v4.1.1, Synergy Software).

4.7.8 Derivation of equations 1 and 2.

Derivation of equation 1 was accomplished by taking into account the two modes of BlaI binding to DNA as well as the dimerization of BlaI in solution. Overall, there were four binding interactions to consider:

The monomer/dimer equilibrium (K_{d1}): $2M \rightarrow D$; $K_{d1} = \frac{[M]^2}{[D]}$

The monomer/DNA binding equilibrium (K_{d2}): $M + DNA \rightarrow DNA \cdot M$; $K_{d2} = \frac{[M]*[DNA]}{[DNA \cdot M]}$

The dimer/DNA binding equilibrium (K_{d3}): $D + DNA \rightarrow DNA \cdot D$; $K_{d3} = \frac{[D]*[DNA]}{[DNA \cdot D]}$

The formation of the dimer/DNA complex via sequential binding of two monomers (K_{d4}): $M + DNA \cdot M \rightarrow DNA \cdot D$; $K_{d4} = \frac{[M]*[DNA \cdot M]}{[DNA \cdot D]}$

The data was plotted and fit as a function of total BlaI (x). Since [BlaI]>>DNA in this system, $[BlaI]_{total} \approx [BlaI]_{free} = x$, and since BlaI exists in solution as both a monomer and a dimer $x = M + D$,. Solving for D gives: $D = x - M$. Solving for $[M]$ in terms of K_{d1} and x gives:

$$[M] = \frac{-K_{d1} \pm \sqrt{K_{d1}^2 + 8 * K_{d1} * x}}{4}$$

Solving for the monomer DNA interaction in terms of fractional occupancy gives:

$$\frac{[DNA \cdot M]}{[DNA]_{total}} = \frac{[M]}{K_{d2} + [M]}$$

Solving for the dimer DNA interaction in terms of fractional occupancy gives:

$$\frac{[DNA \cdot D]}{[DNA]_{total}} = \frac{x - [M]}{K_{d3} + (x - [M])}$$

We considered the total polarization output to be the sum of the contributing factors: the free DNA (P_f), the DNA bound to the monomer(P_M), and the DNA bound to the dimer (P_D):

$mP = P_f + P_M + P_D$.

The contributions from $DNA \cdot M$ and $DNA \cdot D$ were multiplied by the dynamic ranges of their binding interactions, $(P_{max \cdot M} - P_f)$ and $(P_{max \cdot D} - P_f)$, respectively. The data were thus fit to the following equation (1):

$$\Delta mP = P_f + (P_{max \cdot M} - P_f) * \left(\frac{[M]}{K_{d2} + [M]}\right) + (P_{max \cdot D} - P_f) * \left(\frac{x - [M]}{K_{d3} + (x - [M])}\right) (Eq. 1)$$

where

$$[M] = \frac{-K_{d1} \pm \sqrt{K_{d1}^2 + 8 * K_{d1} * x}}{4}$$

K_{d4} is calculated by rearranging its expression in terms of K_{d1}, K_{d2} , and K_{d3} to afford:

$$K_{d4} = \frac{K_{d3} \times K_{d1}}{K_{d2}} \text{ (Eq. 2)}$$

4.8 References

1. Manring, M. M., Hawk, A., Calhoun, J. H. & Andersen, R. C. Treatment of war wounds: A historical review. *Clinical Orthopaedics and Related Research* **467,** 2168–2191 (2009).

2. Andersen, A. S. *et al.* A novel approach to the antimicrobial activity of maggot debridement therapy. *J. Antimicrob. Chemother.* **65,** 1646–1654 (2010).

3. Aminov, R. I. A brief history of the antibiotic era: lessons learned and challenges for the future. *Front. Microbiol.* **1,** 134 (2010).

4. Hare, R. New light on the history of penicillin. *Med. Hist.* **26,** 1–24 (1982).

5. Fleming, A. On the antibacterial action of cultures of a penicillium, with special reference to their use in the isolation of B. influenzæ. *Br. J. Exp. Pathol.* **10,** 226–236 (1929).

6. Chain, E. *et al.* THE CLASSIC: penicillin as a chemotherapeutic agent. 1940. *Clin. Orthop. Relat. Res.* **439,** 23–26 (2005).

7. Lowy, F. D. Antimicrobial resistance : the example of Staphylococcus aureus. **111,** 1265–1273 (2003).

8. Dalhoff, A., Janjic, N. & Echols, R. Redefining penems. *Biochem. Pharmacol.* **71,** 1085–95 (2006).

9. Rolinson, G. N. The Garrod lecture. The influence of 6-aminopenicillanic acid on antibiotic development. *J. Antimicrob. Chemother.* **22,** 5–14 (1988).

10. Ballio, A., Chain, E. B., Dentice Di Accadia, F., Rolinson, G. N. & Batchleor, F. R. Penicillin derivatives of p-aminobenzylpenicillin. *Nature* **183,** 180–181 (1959).

11. Nafsika, G. H. & Fung, L. Y. Penicillin-binding proteins in bacteria. *Antimicrob. Agents Chemother.* **18,** 148–157 (1980).

12. Vollmer, W., Blanot, D. & De Pedro, M. A. Peptidoglycan structure and architecture. *FEMS Microbiology Reviews* **32,** 149–167 (2008).

13. Koch, A. L. Bacterial Wall as Target for Attack: Past, Present, and Future Research. *Clinical Microbiology Reviews* **16,** 673–687 (2003).

14. Kirby, W. M. Extraction of a highly potent penicillin inactivator from penicillin resistant staphylococci. *Science* **99,** 452–3 (1944).

15. Nathwani, D. & Wood, M. J. Penicillins. A current review of their clinical pharmacology and therapeutic use. *Drugs* **45,** 866–94 (1993).

16. Drawz, S. M. & Bonomo, R. a. Three decades of beta-lactamase inhibitors. *Clin. Microbiol. Rev.* **23,** 160–201 (2010).

17. Malachowa, N. & DeLeo, F. R. Mobile genetic elements of Staphylococcus aureus. *Cell. Mol. Life Sci.* **67,** 3057–71 (2010).

18. Novick, R. P., Murphy, E., Gryczan, T. J., Baron, E. & Edelman, I. Penicillinase plasmids of Staphylococcus aureus: Restriction-deletion maps. *Plasmid* **2,** 109–129 (1979).

19. Chambers, H. F. & Deleo, F. R. Waves of resistance: Staphylococcus aureus in the antibiotic era. *Nat. Rev. Microbiol.* **7,** 629–41 (2009).

20. Center for Disease Control and Prevention. *Antibiotic resistance threats*. (2013).

21. Lim, D. & Strynadka, N. C. J. Structural basis for the beta lactam resistance of PBP2a from methicillin-resistant Staphylococcus aureus. *Nat. Struct. Biol.* **9,** 870–876 (2002).

22. Fuda, C., Suvorov, M., Vakulenko, S. B. & Mobashery, S. The basis for resistance to beta-lactam antibiotics by penicillin-binding protein 2a of methicillin-resistant Staphylococcus aureus. *J. Biol. Chem.* **279,** 40802–40806 (2004).

23. Ito, T., Okuma, K., Ma, X. X., Yuzawa, H. & Hiramatsu, K. Insights on antibiotic resistance of Staphylococcus aureus from its whole genome: genomic island SCC. *Drug Resist. Updat.* **6,** 41–52 (2003).

24. Hanssen, A.-M. & Ericson Sollid, J. U. SCCmec in staphylococci: genes on the move. *FEMS Immunol. Med. Microbiol.* **46,** 8–20 (2006).

25. Clarke, S. R. & Dyke, K. G. Studies of the operator region of the Staphylococcus aureus beta-lactamase operon. *J. Antimicrob. Chemother.* **47,** 377–389 (2001).

26. Arêde, P., Ministro, J. & Oliveira, D. C. Redefining the role of the β-lactamase locus in methicillin-resistant Staphylococcus aureus: β-lactamase regulators disrupt the mecimediated strong repression on mecA and optimize the phenotypic expression of resistance in strains with constitutive mecA e. *Antimicrob. Agents Chemother.* **57,** 3037–3045 (2013).

27. Hanique, S. *et al.* Evidence of an Intramolecular Interaction between the Two Domains of the BlaR1 Penicillin Receptor during the Signal Transduction. *J. Biol. Chem.* **279,** 14264–14272 (2004).

28. Zhang, H. Z., Hackbarth, C. J., Chansky, K. M. & Chambers, H. F. A proteolytic transmembrane signaling pathway and resistance to beta-lactams in staphylococci. *Science* **291,** 1962–5 (2001).

29. Chambers, H. F. Methicillin resistance in staphylococci : molecular and biochemical basis and clinical Methicillin Resistance in Staphylococci : Molecular and Biochemical Basis and Clinical Implications. *Microbiology* **10,** (1997).

30. Stapleton, P. D. & Taylor, P. W. Methicillin resistance in Staphylococcus aureus: mechanisms and modulation. *Sci. Prog.* **85,** 57–72 (2002).

31. Ubukata, K., Yamashita, N. & Konno, M. Occurrence of a beta-lactam-inducible penicillin-binding protein in methicillin-resistant staphylococci. *Antimicrob. Agents Chemother.* **27,** 851–7 (1985).

32. Archer, G. L. & Bosilevac, J. M. Signaling antibiotic resistance in staphylococci. *Science* **291,** 1915–1916 (2001).

33. Golemi-Kotra, D., Cha, J. Y., Meroueh, S. O., Vakulenko, S. B. & Mobashery, S. Resistance to beta-lactam antibiotics and its mediation by the sensor domain of the transmembrane BlaR signaling pathway in Staphylococcus aureus. *J. Biol. Chem.* **278,** 18419–25 (2003).

34. Cha, J. & Mobashery, S. Lysine N-decarboxylation in the BlaR1 protein from Staphylococcus aureus at the root of its function as an antibiotic sensor. *J. Am. Chem. Soc.* **129,** 3834–3835 (2007).

35. Borbulevych, O. *et al.* Lysine N ζ-decarboxylation switch and activation of the β-lactam sensor domain of BlaR1 protein of methicillin-resistant Staphylococcus aureus. *J. Biol. Chem.* **286,** 31466–31472 (2011).

36. Safo, M. K. *et al.* Crystal structures of the BlaI repressor from Staphylococcus aureus and its complex with DNA: Insights into transcriptional regulation of the bla and mec operons. *J. Bacteriol.* **187,** 1833–1844 (2005).

37. García-Castellanos, R. *et al.* Three-dimensional structure of MecI. Molecular basis for transcriptional regulation of staphylococcal methicillin resistance. *J. Biol. Chem.* **278,** 39897–39905 (2003).

38. Llarrull, L. I., Prorok, M. & Mobashery, S. Binding of the gene repressor BlaI to the bla operon in methicillin-resistant Staphylococcus aureus. *Biochemistry* **49,** 7975–7 (2010).

39. Hackbarth, C. J. & Chambers, H. F. blaI and blaR1 regulate beta-lactamase and PBP 2a production in methicillin-resistant Staphylococcus aureus. *Antimicrob. Agents Chemother.* **37,** 1144–1149 (1993).

40. Reading, C. & Cole, M. Clavulanic acid: a beta-lactamase-inhiting beta-lactam from Streptomyces clavuligerus. *Antimicrob. Agents Chemother.* **11,** 852–7 (1977).

41. Cole, M. Biochemistry and action of clavulanic acid. *Scott. Med. J.* **27 Spec No,** S10–6 (1982).

42. Roemer, T. & Boone, C. Systems-level antimicrobial drug and drug synergy discovery. *Nat. Chem. Biol.* **9,** 222–31 (2013).

43. Yam, T. S., Hamilton-Miller, J. M. & Shah, S. The effect of a component of tea (Camellia sinensis) on methicillin resistance, PBP2' synthesis, and beta-lactamase production in Staphylococcus aureus. *J. Antimicrob. Chemother.* **42,** 211–216 (1998).

44. Zhao, W.-H., Hu, Z.-Q., Okubo, S., Hara, Y. & Shimamura, T. Mechanism of Synergy between Epigallocatechin Gallate and Beta-Lactams against Methicillin-Resistant Staphylococcus aureus. *Antimicrob. Agents Chemother.* **45,** 1737–1742 (2001).

45. Shibata, H. *et al.* Alkyl gallates, intensifiers of beta-lactam susceptibility in methicillin-resistant Staphylococcus aureus. *Antimicrob. Agents Chemother.* **49,** 549–55 (2005).

46. Stapleton, P. D., Shah, S., Ehlert, K., Hara, Y. & Taylor, P. W. Europe PMC Funders Group The β -lactam-resistance modifier (–) -epicatechin gallate alters the architecture of the cell wall of Staphylococcus aureus. **153,** 2093–2103 (2008).

47. Bernal, P. *et al.* Insertion of epicatechin gallate into the cytoplasmic membrane of methicillin-resistant Staphylococcus aureus disrupts penicillin-binding protein (PBP) 2a-mediated beta-lactam resistance by delocalizing PBP2. *J. Biol. Chem.* **285,** 24055–65 (2010).

48. Toda, M., Okubo, S., Hiyoshi, R. & Shimamura, T. The bactericidal activity of tea and coffee. *Lett Appl Microbiol* **8,** 123–125 (1989).

49. Pasquina, L. W., Santa Maria, J. P. & Walker, S. Teichoic acid biosynthesis as an antibiotic target. *Curr. Opin. Microbiol.* **16,** 531–7 (2013).

50. Lee, S. H. *et al.* Antagonism of chemical genetic interaction networks resensitize MRSA to β-lactam antibiotics. *Chem. Biol.* **18,** 1379–89 (2011).

51. Brown, S., Santa Maria, J. P. & Walker, S. Wall teichoic acids of Gram-positive bacteria. *Annu. Rev. Microbiol.* **67,** 313–36 (2013).

52. Wang, H. *et al.* Discovery of wall teichoic acid inhibitors as potential anti-MRSA β-lactam combination agents. *Chem. Biol.* **20,** 272–84 (2013).

53. Roemer, T., Schneider, T. & Pinho, M. G. Auxiliary factors: a chink in the armor of MRSA resistance to β-lactam antibiotics. *Curr. Opin. Microbiol.* **16,** 538–48 (2013).

54. Podoll, J. D. *et al.* Bio-inspired synthesis yields a tricyclic indoline that selectively resensitizes methicillin-resistant Staphylococcus aureus (MRSA) to β-lactam antibiotics. *Proc. Natl. Acad. Sci. U. S. A.* **110,** 15573–15578 (2013).

55. Chang, L. *et al.* Structure-activity relationship studies of the tricyclic indoline resistance-modifying agent. *J. Med. Chem.* **57,** 3803–17 (2014).

56. Bennouar, K. E. *et al.* Synergy between l-DOPA and a novel positive allosteric modulator of metabotropic glutamate receptor 4: Implications for Parkinson's disease treatment and dyskinesia. *Neuropharmacology* **66,** 158–169 (2013).

57. Sopirala, M. M. *et al.* Synergy testing by Etest, microdilution checkerboard, and time-kill methods for pan-drug-resistant Acinetobacter baumannii. *Antimicrob. Agents Chemother.* **54,** 4678–83 (2010).

58. Surface, R. *et al.* Comparison of Fractional Inhibitory Concentration Index with Response Surface Modeling for Characterization of In Vitro Interaction of Antifungals against Itraconazole-Susceptible and -Resistant. *Antimicrob. Agents Chemother.* **46,** 702–707 (2002).

59. Meneksedag, D., Dogan, A., Kanlikilicer, P. & Ozkirimli, E. Communication between the active site and the allosteric site in class A beta-lactamases. *Comput. Biol. Chem.* **43,** 1–10 (2013).

60. Llarrull, L. I., Toth, M., Champion, M. M. & Mobashery, S. Activation of BlaR1 protein of methicillin-resistant Staphylococcus aureus, its proteolytic processing, and recovery from induction of resistance. *J. Biol. Chem.* **286,** 38148–58 (2011).

61. Holden, M. T. G. *et al.* Complete genomes of two clinical Staphylococcus aureus strains: Evidence for the rapid evolution of virulence and drug resistance. *Proc. Natl. Acad. Sci.* **101,** 9786–9791 (2004).

62. Baba, T. *et al.* Genome and virulence determinants of high virulence community-acquired MRSA. *Lancet* **359,** 1819–1827 (2002).

63. Berscheid, A., Sass, P., Weber-Lassalle, K., Cheung, A. L. & Bierbaum, G. Revisiting the genomes of the Staphylococcus aureus strains NCTC 8325 and RN4220. *Int. J. Med. Microbiol.* **302,** 84–87 (2012).

64. Callaghan, C. H. O., Morris, A., Kirby, M., Shingler, A. H. & Kirby, S. M. Novel Method for Detection of 3-Lactamases by Using a Chromogenic Cephalosporin Substrate. (1972). doi:10.1128/AAC.1.4.283.Updated

65. Zygmunt, D. J., Stratton, C. W. & Kernodlel, D. S. Characterization of Four Lactamases Produced by Staphylococcus aureus. *Antimicrob. Agents Chemother.* **36,** 440–445 (1992).

66. Arêde, P., Ministro, J. & Oliveira, D. C. Redefining the role of the β-lactamase locus in methicillin-resistant Staphylococcus aureus: β-lactamase regulators disrupt the MecI-mediated strong repression on mecA and optimize the

phenotypic expression of resistance in strains with constitutive mecA . *Antimicrob. Agents Chemother.* **57,** 3037–45 (2013).

67. Arêde, P., Milheiriço, C., de Lencastre, H. & Oliveira, D. C. The anti-repressor MecR2 promotes the proteolysis of the mecA repressor and enables optimal expression of β-lactam resistance in MRSA. *PLoS Pathog.* **8,** e1002816 (2012).

68. Oliveira, D. C. & de Lencastre, H. Methicillin-resistance in Staphylococcus aureus is not affected by the overexpression in trans of the mecA gene repressor: a surprising observation. *PLoS One* **6,** e23287 (2011).

69. Martineau, F. *et al.* Multiplex PCR assays for the detection of clinically relevant antibiotic resistance genes in staphylococci isolated from patients infected after cardiac surgery. *J. Antimicrob. Chemother.* **46,** 527–534 (2000).

70. Shang, W., Davies, T. a, Flamm, R. K. & Bush, K. Effects of ceftobiprole and oxacillin on mecA expression in methicillin-resistant Staphylococcus aureus clinical isolates. *Antimicrob. Agents Chemother.* **54,** 956–9 (2010).

71. Nicolson, K., Evans, G. & O'Toole, P. W. Potentiation of methicillin activity against methicillin-resistant Staphylococcus aureus by diterpenes. *FEMS Microbiol. Lett.* **179,** 233–9 (1999).

72. Thumanu, K. *et al.* Discrete steps in sensing of beta-lactam antibiotics by the BlaR1 protein of the methicillin-resistant Staphylococcus aureus bacterium. *Proc. Natl. Acad. Sci. U. S. A.* **103,** 10630–10635 (2006).

73. Clarke, S. R. & Dyke, K. G. The signal transducer (BlaRI) and the repressor (BlaI) of the Staphylococcus aureus beta-lactamase operon are inducible. *Microbiology* **147,** 803–810 (2001).

74. Goodrich, J. A. & Kugel, J. F. *Binding and Kinetics for Molecular Biologists*. (Cold Spring Harbor, 2007).

75. Rossi, A. M. & Taylor, C. W. Analysis of protein-ligand interactions by fluorescence polarization. *Nat. Protoc.* **6,** 365–87 (2011).

76. Rosato, A. E. *et al.* mecA-blaZ Corepressors in Clinical Staphylococcus aureus Isolates. *Antimicrob. Agents Chemother.* **47,** 1460–1463 (2003).

77. Llarrull, L. I. & Mobashery, S. Dissection of events in the resistance to β-lactam antibiotics mediated by the protein BlaR1 from Staphylococcus aureus. *Biochemistry* **51,** 4642–9 (2012).

78. Stephenson, K. & Hoch, J. A. Virulence- and antibiotic resistance-associated two-component signal transduction systems of Gram-positive pathogenic bacteria as

targets for antimicrobial therapy. in *Pharmacology and Therapeutics* **93,** 293–305 (2002).

79. Francis, S., Wilke, K. E., Brown, D. E. & Carlson, E. E. Mechanistic insight into inhibition of two-component system signaling. *Medchemcomm* **4,** 269–277 (2013).

80. Harris, T. L. *et al.* Small molecule downregulation of PmrAB reverses lipid a modification and breaks colistin resistance. *ACS Chem. Biol.* **9,** 122–127 (2014).

81. Ruer, S., Pinotsis, N., Steadman, D., Waksman, G. & Remaut, H. Virulence-targeted Antibacterials: Concept, Promise, and Susceptibility to Resistance Mechanisms. *Chem. Biol. Drug Des.* n/a–n/a (2015). doi:10.1111/cbdd.12517

82. Abreu, A. C., McBain, A. J. & Simões, M. Plants as sources of new antimicrobials and resistance-modifying agents.Abreu, A. C., McBain, A. J., & Simões, M. (2012). Plants as sources of new antimicrobials and resistance-modifying agents. Natural Product Reports, 29(9), 1007–21. doi:10.1039/c2np200. *Nat. Prod. Rep.* **29,** 1007–21 (2012).

83. Wang, P., Projan, S. J. & Novick, R. P. Nucleotide sequence of β-lactamase regulatory genes from staphylococcal plasmid p1258. *Nucleic Acids Res.* **19,** 4000–4000 (1991).

BIBLIOGRAPHY

Abreu, Ana Cristina, Andrew J. McBain, and Manuel Simões. 2012. “Plants as Sources of New Antimicrobials and Resistance-Modifying agents.Abreu, A. C., McBain, A. J., & Simões, M. (2012). Plants as Sources of New Antimicrobials and Resistance-Modifying Agents. Natural Product Reports, 29(9), 1007–21. doi:10.1039/c2np200.” *Natural product reports* 29(9):1007–21.

Allis, C. D., J. K. Bowen, G. N. Abraham, C. V Glover, and M. a Gorovsky. 1980. “Proteolytic Processing of Histone H3 in Chromatin: A Physiologically Regulated Event in Tetrahymena Micronuclei.” *Cell* 20(1):55–64.

Aminov, Rustam I. 2010. “A Brief History of the Antibiotic Era: Lessons Learned and Challenges for the Future.” *Frontiers in microbiology* 1:134.

Anand, Ruchi, and Ronen Marmorstein. 2007. “Structure and Mechanism of Lysine-Specific Demethylase Enzymes.” *The Journal of biological chemistry* 282(49):35425–29.

Andersen, Anders S. et al. 2010. “A Novel Approach to the Antimicrobial Activity of Maggot Debridement Therapy.” *Journal of Antimicrobial Chemotherapy* 65:1646–54.

Archer, G. L., and J. M. Bosilevac. 2001. “Signaling Antibiotic Resistance in Staphylococci.” *Science (New York, N.Y.)* 291:1915–16.

Arêde, Pedro, Catarina Milheiriço, Hermínia de Lencastre, and Duarte C. Oliveira. 2012. “The Anti-Repressor MecR2 Promotes the Proteolysis of the mecA Repressor and Enables Optimal Expression of B-Lactam Resistance in MRSA.” *PLoS pathogens* 8(7):e1002816.

Arêde, Pedro, Joana Ministro, and Duarte C. Oliveira. 2013. “Redefining the Role of the B-Lactamase Locus in Methicillin-Resistant Staphylococcus Aureus: B-Lactamase Regulators Disrupt the MecI-Mediated Strong Repression on mecA and Optimize the Phenotypic Expression of Resistance in Strains with Constitutive mecA .” *Antimicrobial agents and chemotherapy* 57(7):3037–45.

Arêde, Pedro, Joana Ministro, and Duarte C. Oliveira. 2013. “Redefining the Role of the B-Lactamase Locus in Methicillin-Resistant Staphylococcus Aureus: B-Lactamase Regulators Disrupt the Mecimediated Strong Repression on mecA and Optimize the Phenotypic Expression of Resistance in Strains with Constitutive mecA E.” *Antimicrobial Agents and Chemotherapy* 57:3037–45.

Austin, Michael B., Paul E. O’Maille, and Joseph P. Noel. 2008. “Evolving Biosynthetic Tangos Negotiate Mechanistic Landscapes.” *Nature chemical biology* 4:217–22.

Baba, Tadashi et al. 2002. “Genome and Virulence Determinants of High Virulence Community-Acquired MRSA.” *Lancet* 359:1819–27.

Bal, a. M. et al. 2013. “Vancomycin in the Treatment of Meticillin-Resistant Staphylococcus Aureus (MRSA) Infection: End of an Era?” *Journal of Global Antimicrobial Resistance* 1(1):23–30.

Ballio, A., E. B. Chain, F. Dentice Di Accadia, G. N. Rolinson, and F. R. Batchleor. 1959. “Penicillin Derivatives of P-Aminobenzylpenicillin.” *Nature* 183:180–81.

Ban, Y., Y. Murakami, Y. Iwasawa, M. Tsuchiya, and N. Takano. n.d. “Indole Alkaloids in Medicine.” *Medicinal research reviews* 8:231–308.

Bennouar, Khaled Ezaheir et al. 2013. “Synergy between L-DOPA and a Novel Positive Allosteric Modulator of Metabotropic Glutamate Receptor 4: Implications for Parkinson’s Disease Treatment and Dyskinesia.” *Neuropharmacology* 66:158–69.

Bernal, Patricia et al. 2010. “Insertion of Epicatechin Gallate into the Cytoplasmic Membrane of Methicillin-Resistant Staphylococcus Aureus Disrupts Penicillin-Binding Protein (PBP) 2a-Mediated Beta-Lactam Resistance by Delocalizing PBP2.” *The Journal of biological chemistry* 285(31):24055–65.

Bernstein, Bradley E., Alexander Meissner, and Eric S. Lander. 2007. “The Mammalian Epigenome.” *Cell* 128(4):669–81.

Berscheid, Anne, Peter Sass, Konstantin Weber-Lassalle, Ambrose L. Cheung, and Gabriele Bierbaum. 2012. “Revisiting the Genomes of the Staphylococcus Aureus Strains NCTC 8325 and RN4220.” *International Journal of Medical Microbiology* 302:84–87.

Biel, Markus, Veit Wascholowski, and Athanassios Giannis. 2005. “Epigenetics--an Epicenter of Gene Regulation: Histones and Histone-Modifying Enzymes.” *Angewandte Chemie (International ed. in English)* 44(21):3186–3216.

Blair, Jessica M. a., Mark a. Webber, Alison J. Baylay, David O. Ogbolu, and Laura J. V. Piddock. 2014. “Molecular Mechanisms of Antibiotic Resistance.” *Nature Reviews Microbiology* 13(1):42–51.

Borbulevych, Oleg et al. 2011. “Lysine N Z-Decarboxylation Switch and Activation of the B-Lactam Sensor Domain of BlaR1 Protein of Methicillin-Resistant Staphylococcus Aureus.” *Journal of Biological Chemistry* 286(36):31466–72.

Brown, Dean G., Tricia L. May-dracka, Moriah M. Gagnon, and Ruben Tommasi. 2014. “Trends and Exceptions of Physical Properties on Antibacterial Activity for Gram-Positive and Gram-Negative Pathogens.”

Brown, Stephanie, John P. Santa Maria, and Suzanne Walker. 2013. “Wall Teichoic Acids of Gram-Positive Bacteria.” *Annual review of microbiology* 67(6):313–36.

Callaghan, Cynthia H. O., A. Morris, M. Kirby, A. H. Shingler, and Susan M. Kirby. 1972. “Novel Method for Detection of 3-Lactamases by Using a Chromogenic Cephalosporin Substrate.”

Center for Disease Control and Prevention. 2013. *Antibiotic Resistance Threats*.

Cha, Jooyoung, and Shahriar Mobashery. 2007. “Lysine N-Decarboxylation in the BlaR1 Protein from Staphylococcus Aureus at the Root of Its Function as an Antibiotic Sensor.” *Journal of the American Chemical Society* 129:3834–35.

Chain, E. et al. 2005. “THE CLASSIC: Penicillin as a Chemotherapeutic Agent. 1940.” *Clinical Orthopaedics and Related Research* 439:23–26.

Chambers, Henry F. 1997. “Methicillin Resistance in Staphylococci : Molecular and Biochemical Basis and Clinical Methicillin Resistance in Staphylococci : Molecular and Biochemical Basis and Clinical Implications.” *Microbiology* 10(4).

Chambers, Henry F., and Frank R. Deleo. 2009. “Waves of Resistance: Staphylococcus Aureus in the Antibiotic Era.” *Nature reviews. Microbiology* 7(9):629–41.

Chang, Le et al. 2014. “Structure-Activity Relationship Studies of the Tricyclic Indoline Resistance-Modifying Agent.” *Journal of medicinal chemistry* 57(9):3803–17.

Chang, Yanqi et al. 2009. “Structural Basis for G9a-like Protein Lysine Methyltransferase Inhibition by BIX-01294.” *Nature structural & molecular biology* 16(3):312–17.

Chen, Zhongzhou et al. 2006. “Structural Insights into Histone Demethylation by JMJD2 Family Members.” *Cell* 125(4):691–702.

Cho, Yumi et al. 2014. “A Histone Demethylase Inhibitor, Methylstat, Inhibits Angiogenesis in Vitro and in Vivo.” *RSC Advances* 4(72):38230.

Clarke, S. R., and K. G. Dyke. 2001. “The Signal Transducer (BlaRI) and the Repressor (BlaI) of the Staphylococcus Aureus Beta-Lactamase Operon Are Inducible.” *Microbiology* 147:803–10.

Clarke, Simon R., and K. G. Dyke. 2001. “Studies of the Operator Region of the Staphylococcus Aureus Beta-Lactamase Operon.” *The Journal of antimicrobial chemotherapy* 47:377–89.

Clatworthy, Anne E., Emily Pierson, and Deborah T. Hung. 2007. “Targeting Virulence: A New Paradigm for Antimicrobial Therapy.” *Nature chemical biology* 3(9):541–48.

Cloos, Paul a C. et al. 2006. “The Putative Oncogene GASC1 Demethylates Tri- and Dimethylated Lysine 9 on Histone H3.” *Nature* 442(7100):307–11.

Cloos, Paul a C., Jesper Christensen, Karl Agger, and Kristian Helin. 2008. “Erasing the Methyl Mark: Histone Demethylases at the Center of Cellular Differentiation and Disease.” *Genes & development* 22(9):1115–40.

CLSI. 2007. *Performance Standards for Antimicrobial Susceptibility Testing ; Seventeenth Informational Supplement*. Wayne.

CLSI. 2009. *Methods for Dilution Antimicrobial Susceptibility Tests for Bacteria That Grow Aerobically ; Approved Standard — Eighth Edition*. 8th ed. Wayne.

Coates, Anthony R. M., Gerry Halls, and Yanmin Hu. 2011. “Novel Classes of Antibiotics or More of the Same?” *British journal of pharmacology* 163(1):184–94.

Cohen, M. L. 1992. “Epidemiology of Drug Resistance: Implications for a Post-Antimicrobial Era.” *Science (New York, N.Y.)* 257(5073):1050–55.

Cole, M. 1982. “Biochemistry and Action of Clavulanic Acid.” *Scottish medical journal* 27 Spec No:S10–6.

Cole, Philip a. 2008a. “Chemical Probes for Histone-Modifying Enzymes.” *Nature chemical biology* 4(10):590–97.

Cole, Philip a. 2008b. “Chemical Probes for Histone-Modifying Enzymes.” *Nature chemical biology* 4(10):590–97.

Couture, Jean-françois, Evys Collazo, Patricia A. Ortiz-Tello, Joseph S. Brunzelle, and Raymond C. Trievel. 2007. “Specificity and Mechanism of JMJD2A, a Trimethyllysine-Specific Histone Demethylase.” *Nature structural & molecular biology* 14(8):689–95.

Dalhoff, Axel, Nebojsa Janjic, and Roger Echols. 2006. “Redefining Penems.” *Biochemical pharmacology* 71(7):1085–95.

Davies, Julian, and Dorothy Davies. 2010. “Origins and Evolution of Antibiotic Resistance.” *Microbiology and molecular biology reviews : MMBR* 74(3):417–33.

DeLuca, V. et al. 1986. “Biosynthesis of Indole Alkaloids: Developmental Regulation of the Biosynthetic Pathway from Tabersonine to Vindoline in Catharanthus Roseus.” *Journal of Plant Physiology* 125:147–56.

Dias, Daniel a., Sylvia Urban, and Ute Roessner. 2012. “A Historical Overview of Natural Products in Drug Discovery.” *Metabolites* 2:303–36.

Dobson, Christopher M. 2004. “Chemical Space and Biology.” *Nature* 432:824–28.

Drawz, Sarah M., and Robert a Bonomo. 2010. “Three Decades of Beta-Lactamase Inhibitors.” *Clinical microbiology reviews* 23(1):160–201.

Duncan, Elizabeth M., and C. David Allis. 2011. *Epigenetics and Disease*. edited by Susan M. Gasser and En Li. Basel: Springer Basel.

Fang, Xueliang, and Renxiao Wang. 2004. “The Ki Calculator For Fluorescence-Based Competitive Binding Assays.” Retrieved (sw16.im.med.umich.edu/software/calc_ki).

Felsenfeld, Gary, and Mark Groudine. 2003. “Controlling the Double Helix.” *Nature* 421(6921):448–53.

Fischle, Wolfgang, Yanming Wang, and C. David Allis. 2003. “Histone and Chromatin Cross-Talk.” *Current Opinion in Cell Biology* 15:172–83.

Fleming, A. 1929. “On the Antibacterial Action of Cultures of a Penicillium, with Special Reference to Their Use in the Isolation of B. Influenzæ.” *British journal of experimental pathology* 10(3):226–36.

Francis, Samson, Kaelyn E. Wilke, Douglas E. Brown, and Erin E. Carlson. 2013. “Mechanistic Insight into Inhibition of Two-Component System Signaling.” *MedChemComm* 4(1):269–77.

Fuda, Cosimo, Maxim Suvorov, Sergei B. Vakulenko, and Shahriar Mobashery. 2004. “The Basis for Resistance to Beta-Lactam Antibiotics by Penicillin-Binding Protein 2a of Methicillin-Resistant Staphylococcus Aureus.” *The Journal of biological chemistry* 279:40802–6.

García-Castellanos, Raquel et al. 2003. “Three-Dimensional Structure of MecI. Molecular Basis for Transcriptional Regulation of Staphylococcal Methicillin Resistance.” *Journal of Biological Chemistry* 278:39897–905.

Goldberg, Aaron D., C. David Allis, and Emily Bernstein. 2007. “Epigenetics: A Landscape Takes Shape.” *Cell* 128(4):635–38.

Golemi-Kotra, Dasantila, Joo Young Cha, Samy O. Meroueh, Sergei B. Vakulenko, and Shahriar Mobashery. 2003. “Resistance to Beta-Lactam Antibiotics and Its Mediation by the Sensor Domain of the Transmembrane BlaR Signaling Pathway in Staphylococcus Aureus.” *The Journal of biological chemistry* 278(20):18419–25.

Goodrich, James. A., and Jennifer. F. Kugel. 2007. *Binding and Kinetics for Molecular Biologists*. New York: Cold Spring Harbor.

Hackbarth, C. J., and H. F. Chambers. 1993. “blaI and blaR1 Regulate Beta-Lactamase and PBP 2a Production in Methicillin-Resistant Staphylococcus Aureus.” *Antimicrobial agents and chemotherapy* 37(5):1144–49.

Halberstadt, Adam L., and Mark A. Geyer. 2011. “Multiple Receptors Contribute to the Behavioral Effects of Indoleamine Hallucinogens.” *Neuropharmacology* 61:364–81.

Hanique, Sophie et al. 2004. “Evidence of an Intramolecular Interaction between the Two Domains of the BlaR1 Penicillin Receptor during the Signal Transduction.” *Journal of Biological Chemistry* 279(14):14264–72.

Hanssen, Anne-Merethe, and Johanna U. Ericson Sollid. 2006. “SCCmec in Staphylococci: Genes on the Move.” *FEMS immunology and medical microbiology* 46(1):8–20.

Hare, Ronald. 1982. “New Light on the History of Penicillin.” *Medical History* 26:1–24.

Harris, Tyler L. et al. 2014. “Small Molecule Downregulation of PmrAB Reverses Lipid a Modification and Breaks Colistin Resistance.” *ACS Chemical Biology* 9:122–27.

Hausinger, Robert P. 2004. *FeII/alpha-Ketoglutarate-Dependent Hydroxylases and Related Enzymes.*

He, Jin, Anh Tram Nguyen, and Yi Zhang. 2011. “KDM2b/JHDM1b, an H3K36me2-Specific Demethylase, Is Required for Initiation and Maintenance of Acute Myeloid Leukemia.” *Blood* 117(14):3869–80.

Højfeldt, Jonas W., Karl Agger, and Kristian Helin. 2013. “Histone Lysine Demethylases as Targets for Anticancer Therapy.” *Nature reviews. Drug discovery* 12(12):917–30.

Holden, M. T. G. et al. 2004. “Complete Genomes of Two Clinical Staphylococcus Aureus Strains: Evidence for the Rapid Evolution of Virulence and Drug Resistance.” *Proceedings of the National Academy of Sciences* 101(26):9786–91.

Horton, John R. et al. 2010. “Enzymatic and Structural Insights for Substrate Specificity of a Family of Jumonji Histone Lysine Demethylases.” *Nature structural & molecular biology* 17(1):38–43.

Horwitz, S. B. et al. 1986. “Taxol: Mechanisms of Action and Resistance.” *Annals of the New York Academy of Sciences* 466:733–44.

Huang, Xinyi. 2003. “Fluorescence Polarization Competition Assay: The Range of Resolvable Inhibitor Potency Is Limited by the Affinity of the Fluorescent Ligand.” *Journal of biomolecular screening* 8(1):34–38.

Ishimura, Akihiko et al. 2009. “Jmjd2c Histone Demethylase Enhances the Expression of Mdm2 Oncogene.” *Biochemical and biophysical research communications* 389(2):366–71.

Ito, Teruyo, Keiko Okuma, Xiao Xue Ma, Harumi Yuzawa, and Keiichi Hiramatsu. 2003. “Insights on Antibiotic Resistance of Staphylococcus Aureus from Its Whole Genome: Genomic Island SCC.” *Drug Resistance Updates* 6(1):41–52.

Jordan, Mary Ann, Douglas Thrower, and Leslie Wilson. 1991. “Mechanism of Inhibition of Cell Proliferation by Vinca Alkaloids.” *Cancer Research* 51:2212–22.

Kawazu, Masahito et al. 2011. “Histone Demethylase JMJD2B Functions as a Co-Factor of Estrogen Receptor in Breast Cancer Proliferation and Mammary Gland Development.” *PloS one* 6(3):e17830.

Khalil, Ahmad M., and John L. Rinn. 2011. “RNA-Protein Interactions in Human Health and Disease.” *Seminars in Cell and Developmental Biology* 22(4):359–65.

Kirby, W. M. 1944. “Extraction of a Highly Potent Penicillin Inactivator from Penicillin Resistant Staphylococci.” *Science (New York, N.Y.)* 99(2579):452–53.

Klose, Robert J., and Yi Zhang. 2007. “Regulation of Histone Methylation by Demethylimination and Demethylation.” *Nature reviews. Molecular cell biology* 8(4):307–18.

Koch, Arthur L. 2003. “Bacterial Wall as Target for Attack: Past, Present, and Future Research.” *Clinical Microbiology Reviews* 16:673–87.

Kouzarides, Tony. 2007. “Chromatin Modifications and Their Function.” *Cell* 128(4):693–705.

Krishnan, Swathi, Evys Collazo, Patricia a Ortiz-Tello, and Raymond C. Trievel. 2011. “Purification and Assay Protocols for Obtaining Highly Active Jumonji C Demethylases.” *Analytical biochemistry* 420(1):48–53.

Krohn, Kenneth A., and Jeanne M. Link. 2003. “Interpreting Enzyme and Receptor Kinetics: Keeping It Simple, but Not Too Simple.” *Nuclear Medicine and Biology* 30(8):819–26.

Kutchan, Tm. 1995. “Alkaloid Biosynthesis -- The Basis for Metabolic Engineering of Medicinal Plants.” *The Plant cell* 7(July):1059–70.

Lee, Jung Shin, Edwin Smith, and Ali Shilatifard. 2010. “The Language of Histone Crosstalk.” *Cell* 142:682–85.

Lee, Sang Ho et al. 2011. “Antagonism of Chemical Genetic Interaction Networks Resensitize MRSA to B-Lactam Antibiotics.” *Chemistry & biology* 18(11):1379–89.

Leeds, Jennifer A., Esther K. Schmitt, and Philipp Krastel. 2006. “Recent Developments in Antibacterial Drug Discovery: Microbe-Derived Natural Products--from Collection to the Clinic.” *Expert opinion on investigational drugs* 15:211–26.

Lewis, Kim. 2013. “Platforms for Antibiotic Discovery.” *Nature reviews. Drug discovery* 12(5):371–87.

Lim, Daniel, and Natalie C. J. Strynadka. 2002. “Structural Basis for the Beta Lactam Resistance of PBP2a from Methicillin-Resistant Staphylococcus Aureus.” *Nature structural biology* 9:870–76.

Lipinski, Christopher A., Franco Lombardo, Beryl W. Dominy, and Paul J. Feeney. 2001. “Experimental and Computational Approaches to Estimate Solubility and Permeability in Drug Discovery and Development Settings.” 46:3–26.

Littleton, John, Trent Rogers, and Deane Falcone. 2005. “Novel Approaches to Plant Drug Discovery Based on High Throughput Pharmacological Screening and Genetic Manipulation.” *Life sciences* 78(5):467–75.

Liu, Yongxiang, Wenqing Xu, and Xiang Wang. 2010. “Gold(I)-Catalyzed Tandem Cyclization Approach to Tetracyclic Indolines.” *Organic letters* 12(7):1448–51.

Llarrull, Leticia I., and Shahriar Mobashery. 2012. “Dissection of Events in the Resistance to B-Lactam Antibiotics Mediated by the Protein BlaR1 from Staphylococcus Aureus.” *Biochemistry* 51(23):4642–49.

Llarrull, Leticia I., Mary Prorok, and Shahriar Mobashery. 2010. “Binding of the Gene Repressor BlaI to the Bla Operon in Methicillin-Resistant Staphylococcus Aureus.” *Biochemistry* 49(37):7975–77.

Llarrull, Leticia I., Marta Toth, Matthew M. Champion, and Shahriar Mobashery. 2011. “Activation of BlaR1 Protein of Methicillin-Resistant Staphylococcus Aureus, Its Proteolytic Processing, and Recovery from Induction of Resistance.” *The Journal of biological chemistry* 286(44):38148–58.

Lo, Michael M. C., Christopher S. Neumann, Satoshi Nagayama, Ethan O. Perlstein, and Stuart L. Schreiber. 2004. “A Library of Spirooxindoles Based on a Stereoselective Three-Component Coupling Reaction.” *Journal of the American Chemical Society* 126:16077–86.

Lowy, Franklin D. 2003. “Antimicrobial Resistance : The Example of Staphylococcus Aureus.” 111(9):1265–73.

Luo, Xuelai et al. 2011. “A Selective Inhibitor and Probe of the Cellular Functions of Jumonji C Domain-Containing Histone Demethylases.” *Journal of the American Chemical Society* 133(24):9451–56.

Malachowa, Natalia, and Frank R. DeLeo. 2010. “Mobile Genetic Elements of Staphylococcus Aureus.” *Cellular and molecular life sciences : CMLS* 67(18):3057–71.

Manring, M. M., Alan Hawk, Jason H. Calhoun, and Romney C. Andersen. 2009. “Treatment of War Wounds: A Historical Review.” *Clinical Orthopaedics and Related Research* 467:2168–91.

Mantri, Monica, Zhihong Zhang, Michael a McDonough, and Christopher J. Schofield. 2012. “Autocatalysed Oxidative Modifications to 2-Oxoglutarate Dependent Oxygenases.” *The FEBS journal* 279(9):1563–75.

Martineau, Francis et al. 2000. “Multiplex PCR Assays for the Detection of Clinically Relevant Antibiotic Resistance Genes in Staphylococci Isolated from Patients Infected after Cardiac Surgery.” *Journal of Antimicrobial Chemotherapy* 46(4):527–34.

Meneksedag, Deniz, Asligul Dogan, Pinar Kanlikilicer, and Elif Ozkirimli. 2013. “Communication between the Active Site and the Allosteric Site in Class A Beta-Lactamases.” *Computational Biology and Chemistry* 43:1–10.

Meng, He, and Krishna Kumar. 2007. “Antimicrobial Activity and Protease Stability of Peptides Containing Fluorinated Amino Acids.” *Journal of the American Chemical Society* 129(50):15615–22.

Meseguer, B., D. Alonso-Díaz, N. Griebenow, T. Herget, and H. Waldmann. 1999. “Natural Product Synthesis on Polymeric Supports-Synthesis and Biological Evaluation of an Indolactam Library.” *Angewandte Chemie (International ed. in English)* 38:2902–6.

Michael Barbour, P., Jessica D. Podoll, Laura J. Marholz, and Xiang Wang. 2014. “Discovery and Initial Structure–activity Relationships of N-Benzyl Tricyclic Indolines as Antibacterials for Methicillin-Resistant Staphylococcus Aureus.” *Bioorganic & Medicinal Chemistry Letters* 24:5602–5.

Mosammaparast, Nima, and Yang Shi. 2010. “Reversal of Histone Methylation: Biochemical and Molecular Mechanisms of Histone Demethylases.” *Annual review of biochemistry* 79:155–79.

Nafsika, Georgopapadakou H., and Liu Y. Fung. 1980. “Penicillin-Binding Proteins in Bacteria.” *Antimicrobial Agents and Chemotherapy* 18(1):148–57.

Nakamura, Satoki et al. 2011. “JmjC-Domain Containing Histone Demethylase 1B-Mediated p15(Ink4b) Suppression Promotes the Proliferation of Leukemic Progenitor Cells through Modulation of Cell Cycle Progression in Acute Myeloid Leukemia.” *Molecular carcinogenesis* (May):1–13.

Nathwani, D., and M. J. Wood. 1993. “Penicillins. A Current Review of Their Clinical Pharmacology and Therapeutic Use.” *Drugs* 45(6):866–94.

Ng, Stanley S. et al. 2007. “Crystal Structures of Histone Demethylase JMJD2A Reveal Basis for Substrate Specificity.” *Nature* 448(7149):87–91.

Nicolson, K., G. Evans, and P. W. O’Toole. 1999. “Potentiation of Methicillin Activity against Methicillin-Resistant Staphylococcus Aureus by Diterpenes.” *FEMS microbiology letters* 179(2):233–39.

Nielsen, Thomas E., and Stuart L. Schreiber. 2008. “Towards the Optimal Screening Collection: A Synthesis Strategy.” *Angewandte Chemie - International Edition* 47:48–56.

Nikolovska-Coleska, Zaneta et al. 2004. “Development and Optimization of a Binding Assay for the XIAP BIR3 Domain Using Fluorescence Polarization.” *Analytical biochemistry* 332(2):261–73.

Novick, R. P., E. Murphy, T. J. Gryczan, E. Baron, and I. Edelman. 1979. “Penicillinase Plasmids of Staphylococcus Aureus: Restriction-Deletion Maps.” *Plasmid* 2(1):109–29.

O’Shea, Rosemarie, and Heinz E. Moser. 2008. “Physicochemical Properties of Antibacterial Compounds: Implications for Drug Discovery.” *Journal of Medicinal Chemistry* 51:2871–78.

Oliveira, Duarte C., and Hermínia de Lencastre. 2011. “Methicillin-Resistance in Staphylococcus Aureus Is Not Affected by the Overexpression in Trans of the mecA Gene Repressor: A Surprising Observation.” *PloS one* 6(8):e23287.

Overington, John P., Bissan Al-Lazikani, and Andrew L. Hopkins. 2006. “How Many Drug Targets Are There?” *Nature reviews. Drug discovery* 5:993–96.

Ozer, Abdullah, and Richard K. Bruick. 2007. “Non-Heme Dioxygenases: Cellular Sensors and Regulators Jelly Rolled into One?” *Nature chemical biology* 3(3):144–53.

Pasquina, Lincoln W., John P. Santa Maria, and Suzanne Walker. 2013. “Teichoic Acid Biosynthesis as an Antibiotic Target.” *Current opinion in microbiology* 16(5):531–37.

Payne, David J. 2008. “Microbiology. Desperately Seeking New Antibiotics.” *Science (New York, N.Y.)* 321(5896):1644–45.

Payne, David J., Michael N. Gwynn, David J. Holmes, and David L. Pompliano. 2007. “Drugs for Bad Bugs: Confronting the Challenges of Antibacterial Discovery.” *Nature reviews. Drug discovery* 6(1):29–40.

Peng, Wei et al. 2015. “Areca Catechu L. (Arecaceae): A Review of Its Traditional Uses, Botany, Phytochemistry, Pharmacology and Toxicology.” *Journal of Ethnopharmacology*.

Périchon, Bruno, and Patrice Courvalin. 2009. “VanA-Type Vancomycin-Resistant Staphylococcus Aureus.” *Antimicrobial Agents and Chemotherapy* 53:4580–87.

Podoll, Jessica D. et al. 2013. “Bio-Inspired Synthesis Yields a Tricyclic Indoline That Selectively Resensitizes Methicillin-Resistant Staphylococcus Aureus (MRSA) to B-Lactam Antibiotics.” *Proceedings of the National Academy of Sciences of the United States of America* 110(39):15573–78.

Qiu, Jihui et al. 2010. “The X-Linked Mental Retardation Gene PHF8 Is a Histone Demethylase Involved in Neuronal Differentiation.” *Cell research* 20(8):908–18.

Reading, C., and M. Cole. 1977. “Clavulanic Acid: A Beta-Lactamase-Inhiting Beta-Lactam from Streptomyces Clavuligerus.” *Antimicrobial agents and chemotherapy* 11(5):852–57.

Rodriguez, Raphaël. 2012. “Target-Oriented and Diversity-Oriented Organic Synthesis.” Pp. 513–18 in *Modern Tools for the Synthesis of Complex Bioactive Molecules*.

Roemer, Terry, and Charles Boone. 2013. “Systems-Level Antimicrobial Drug and Drug Synergy Discovery.” *Nature chemical biology* 9(4):222–31.

Roemer, Terry, Tanja Schneider, and Mariana G. Pinho. 2013. “Auxiliary Factors: A Chink in the Armor of MRSA Resistance to B-Lactam Antibiotics.” *Current opinion in microbiology* 16(5):538–48.

Rolinson, G. N. 1988. “The Garrod Lecture. The Influence of 6-Aminopenicillanic Acid on Antibiotic Development.” *The Journal of antimicrobial chemotherapy* 22(1):5–14.

Rosato, Adriana E. et al. 2003. “mecA-blaZ Corepressors in Clinical Staphylococcus Aureus Isolates.” *Antimicrobial Agents and Chemotherapy* 47(4):1460–63.

Rose, Nathan R., Michael A. McDonough, Oliver N. F. King, Akane Kawamura, and Christopher J. Schofield. 2011. “Inhibition of 2-Oxoglutarate Dependent Oxygenases.” *Chemical Society reviews* 40(8):4364–97.

Rossi, Ana M., and Colin W. Taylor. 2011. “Analysis of Protein-Ligand Interactions by Fluorescence Polarization.” *Nature protocols* 6(3):365–87.

Rossolini, Gian Maria. 2005. “Acquired Metallo-Beta-Lactamases: An Increasing Clinical Threat.” *Clinical infectious diseases : an official publication of the Infectious Diseases Society of America* 41(11):1557–58.

Ruer, Ségolène, Nikos Pinotsis, David Steadman, Gabriel Waksman, and Han Remaut. 2015. “Virulence-Targeted Antibacterials: Concept, Promise, and Susceptibility to Resistance Mechanisms.” *Chemical Biology & Drug Design* n/a–n/a.

Safo, Martin K. et al. 2005. “Crystal Structures of the BlaI Repressor from Staphylococcus Aureus and Its Complex with DNA: Insights into Transcriptional Regulation of the Bla and Mec Operons.” *Journal of Bacteriology* 187:1833–44.

De Santa, Francesca et al. 2007. “The Histone H3 Lysine-27 Demethylase Jmjd3 Links Inflammation to Inhibition of Polycomb-Mediated Gene Silencing.” *Cell* 130(6):1083–94.

Schatz, A., E. Bugle, and S. A. Waksman. 1944. “Streptomycin, a Substance Exhibiting Antibiotic Activity Against Gram-Positive and Gram-Negative Bacteria.*.” *Experimental Biology and Medicine* 55(1):66–69.

Seenundun, Shayesta et al. 2010. “UTX Mediates Demethylation of H3K27me3 at Muscle-Specific Genes during Myogenesis.” *The EMBO journal* 29(8):1401–11.

Sekirnik, Rok, Nathan R. Rose, Jasmin Mecinović, and Christopher J. Schofield. 2010. “2-Oxoglutarate Oxygenases Are Inhibited by a Range of Transition Metals.” *Metallomics : integrated biometal science* 2(6):397–99.

Sengoku, Toru, and Shigeyuki Yokoyama. 2011. “Structural Basis for Histone H3 Lys 27 Demethylation by UTX / KDM6A.” 2266–77.

Shackleton, Mark, Elsa Quintana, Eric R. Fearon, and Sean J. Morrison. 2009. “Heterogeneity in Cancer: Cancer Stem Cells versus Clonal Evolution.” *Cell* 138(5):822–29.

Shang, Wenchi, Todd a Davies, Robert K. Flamm, and Karen Bush. 2010. “Effects of Ceftobiprole and Oxacillin on mecA Expression in Methicillin-Resistant Staphylococcus Aureus Clinical Isolates.” *Antimicrobial agents and chemotherapy* 54(2):956–59.

Shi, J. et al. 2012. “The Polycomb Complex PRC2 Supports Aberrant Self-Renewal in a Mouse Model of MLL-AF9;NrasG12D Acute Myeloid Leukemia.” *Oncogene* 32(7):930–38.

Shi, Yang, and Johnathan R. Whetstine. 2007. “Dynamic Regulation of Histone Lysine Methylation by Demethylases.” *Molecular cell* 25(1):1–14.

Shi, Yujiang et al. 2004. “Histone Demethylation Mediated by the Nuclear Amine Oxidase Homolog LSD1.” *Cell* 119(7):941–53.

Shibata, Hirofumi et al. 2005. “Alkyl Gallates, Intensifiers of Beta-Lactam Susceptibility in Methicillin-Resistant Staphylococcus Aureus.” *Antimicrobial agents and chemotherapy* 49(2):549–55.

Shilatifard, Ali. 2006. “Chromatin Modifications by Methylation and Ubiquitination: Implications in the Regulation of Gene Expression.” *Annual review of biochemistry* 75:243–69.

Simonini, M. V et al. 2006. “The Benzamide MS-275 Is a Potent, Long-Lasting Brain Region-Selective Inhibitor of Histone Deacetylases.” *Proceedings of the National Academy of Sciences of the United States of America* 103(5):1587–92.

Sopirala, Madhuri M. et al. 2010. “Synergy Testing by Etest, Microdilution Checkerboard, and Time-Kill Methods for Pan-Drug-Resistant Acinetobacter Baumannii.” *Antimicrobial agents and chemotherapy* 54(11):4678–83.

Spring, David R. 2005. “Chemical Genetics to Chemical Genomics: Small Molecules Offer Big Insights.” *Chemical Society Reviews* 34(6):472.

Stapleton, Paul D., Saroj Shah, Kerstin Ehlert, Yukihiko Hara, and Peter W. Taylor. 2008. “Europe PMC Funders Group The B -Lactam-Resistance Modifier (–) -Epicatechin Gallate Alters the Architecture of the Cell Wall of Staphylococcus Aureus.” 153(Pt 7):2093–2103.

Stapleton, Paul D., and Peter W. Taylor. 2002. “Methicillin Resistance in Staphylococcus Aureus: Mechanisms and Modulation.” *Science progress* 85(Pt 1):57–72.

Stephenson, Keith, and James A. Hoch. 2002. “Virulence- and Antibiotic Resistance-Associated Two-Component Signal Transduction Systems of Gram-Positive Pathogenic Bacteria as Targets for Antimicrobial Therapy.” Pp. 293–305 in *Pharmacology and Therapeutics*, vol. 93.

Stockwell, B. R. 2000. “Chemical Genetics: Ligand-Based Discovery of Gene Function.” *Nature reviews. Genetics* 1(November):116–25.

Strahl, Brian D., and C. David Allis. 2000. “The Language of Covalent Histone Modifications.” *Nature* 403(6765):41–45.

Stryjewski, Martin E., and G. Ralph Corey. 2014. “Methicillin-Resistant Staphylococcus Aureus: An Evolving Pathogen.” *Clinical infectious diseases : an official publication of the Infectious Diseases Society of America* 58 Suppl 1(Suppl 1):S10–9.

Suganuma, Tamaki, and Jerry L. Workman. 2008. “Crosstalk among Histone Modifications.” *Cell* 135:604–7.

Sumranjit, Jitapa, and Sang J. Chung. 2013. “Recent Advances in Target Characterization and Identification by Photoaffinity Probes.” *Molecules (Basel, Switzerland)* 18(9):10425–51.

Surface, Response et al. 2002. “Comparison of Fractional Inhibitory Concentration Index with Response Surface Modeling for Characterization of In Vitro Interaction of Antifungals against Itraconazole-Susceptible and -Resistant.” *Antimicrobial agents and chemotherapy* 46(3):702–7.

Tanaka, J. C. A., C. C. da Silva, A. J. B. de Oliveira, C. V. Nakamura, and B. P. Dias Filho. 2006. “Antibacterial Activity of Indole Alkaloids from Aspidosperma Ramiflorum.” *Brazilian Journal of Medical and Biological Research* 39:387–91.

Thumanu, Kanjana et al. 2006. “Discrete Steps in Sensing of Beta-Lactam Antibiotics by the BlaR1 Protein of the Methicillin-Resistant Staphylococcus Aureus Bacterium.” *Proceedings of the National Academy of Sciences of the United States of America* 103(Track II):10630–35.

Toda, Masako, Sachie Okubo, Reiko Hiyoshi, and Tadakatsu Shimamura. 1989. “The Bactericidal Activity of Tea and Coffee.” *Lett Appl Microbiol* 8:123–25.

Tsukada, Yu-ichi et al. 2006. “Histone Demethylation by a Family of JmjC Domain-Containing Proteins.” *Nature* 439(7078):811–16.

Ubukata, K., N. Yamashita, and M. Konno. 1985. “Occurrence of a Beta-Lactam-Inducible Penicillin-Binding Protein in Methicillin-Resistant Staphylococci.” *Antimicrobial agents and chemotherapy* 27(5):851–57.

Upadhyay, Anup K., and Xiaodong Cheng. 2011. “Dynamics of Histone Lysine Methylation: Structures of Methyl Writers and Erasers.” Pp. 107–24 in *Epigenetics and Disease*, vol. 3, edited by Susan M. Gasser and En Li. Basel: Springer Basel.

Verpoorte, Rob. 1998. “Exploration of Nature’s Chemodiversity: The Role of Secondary Metabolites as Leads in Drug Development.” *Drug Discovery Today* 3(5):232–38.

Vincent, Audrey, and Isabelle Van Seuningen. 2012. “On the Epigenetic Origin of Cancer Stem Cells.” *Biochimica et biophysica acta* 1826(1):83–88.

Vollmer, Waldemar, Didier Blanot, and Miguel A. De Pedro. 2008. “Peptidoglycan Structure and Architecture.” *FEMS Microbiology Reviews* 32:149–67.

Wang, Fang et al. 2012. “Solubilized Gramicidin A as Potential Systemic Antibiotics.” *Chembiochem : a European journal of chemical biology* 13(1):51–55.

Wang, Hao et al. 2013. “Discovery of Wall Teichoic Acid Inhibitors as Potential Anti-MRSA B-Lactam Combination Agents.” *Chemistry & biology* 20(2):272–84.

Wang, Pei-zhi, Steven J. Projan, and Richard P. Novick. 1991. “Nucleotide Sequence of B-Lactamase Regulatory Genes from Staphylococcal Plasmid p1258.” *Nucleic Acids Research* 19(14):4000–4000.

Worthington, Roberta J., and Christian Melander. 2013. “Overcoming Resistance to B-Lactam Antibiotics.” *The Journal of organic chemistry* 78(9):4207–13.

Worthington, Roberta J., Justin J. Richards, and Christian Melander. 2012. “Small Molecule Control of Bacterial Biofilms.” *Organic & biomolecular chemistry* 10(37):7457–74.

Wright, Gerard D. 2007. “The Antibiotic Resistome: The Nexus of Chemical and Genetic Diversity.” *Nature reviews. Microbiology* 5(3):175–86.

Xiang, Yang et al. 2007. “JARID1B Is a Histone H3 Lysine 4 Demethylase up-Regulated in Prostate Cancer.” *Proceedings of the National Academy of Sciences of the United States of America* 104(49):19226–31.

Xu, Wenqing et al. 2013. “Quantitative Analysis of Histone Demethylase Probes Using Fluorescence Polarization.” *Journal of medicinal chemistry* 56(12):5198–5202.

Yam, T. S., J. M. Hamilton-Miller, and S. Shah. 1998. “The Effect of a Component of Tea (Camellia Sinensis) on Methicillin Resistance, PBP2’ Synthesis, and Beta-Lactamase Production in Staphylococcus Aureus.” *The Journal of antimicrobial chemotherapy* 42:211–16.

Yeo, Se Jeong, Yongxiang Liu, and Xiang Wang. 2012. “A One-Pot Three-Component Reaction for the Preparation of Highly Functionalized Tryptamines.” *Tetrahedron* 68(3):813–18.

Yvette Fofie, N′GuessanBra, Rokia Sanogo, Kiyinlma Coulibaly, and Diénéba Kone Bamba. 2015. “Minerals Salt Composition and Secondary Metabolites of Euphorbia Hirta Linn., an Antihyperglycemic Plant.” *Pharmacognosy Research* 7:7.

Zhang, H. Z., C. J. Hackbarth, K. M. Chansky, and H. F. Chambers. 2001. “A Proteolytic Transmembrane Signaling Pathway and Resistance to Beta-Lactams in Staphylococci.” *Science (New York, N.Y.)* 291(5510):1962–65.

Zhang, J. H. 1999. “A Simple Statistical Parameter for Use in Evaluation and Validation of High Throughput Screening Assays.” *Journal of Biomolecular Screening* 4(2):67–73.

Zhao, W. H., Z. Q. Hu, Sachie Okubo, Yukihiko Hara, and T. Shimamura. 2001. “Mechanism of Synergy between Epigallocatechin Gallate and Beta-Lactams against Methicillin-Resistant Staphylococcus Aureus.” *Antimicrobial Agents and Chemotherapy* 45(6):1737–42.

Zygmunt, Deborah J., Charles W. Stratton, and Douglas S. Kernodlel. 1992. “Characterization of Four Lactamases Produced by Staphylococcus Aureus.” *Antimicrobial agents and chemotherapy* 36(2):440–45.